

**A Condensed Matter Model of Fundamental Particle Genesis  
as a Function  
of an Accelerating Cosmic Spacetime Expansion**

Fundamental Rest Mass Quanta as  
Simple Harmonic Rotational Oscillations of  
the Spacetime Continuum,  
Driven by Cosmic Expansion  
with  
Application of the Analysis to the  
Experimental Field of Cold Fusion

By Martin Gibson

August 6, 2019, with Addendum September 6, 2021

Martin Gibson  
P.O. Box 2358  
Southern Pines, NC 28388  
910-585-1234  
[martin@uniservent.org](mailto:martin@uniservent.org)



# **A Condensed Matter Model of Fundamental Particle Genesis as a Function of an Accelerating Cosmic Spacetime Expansion**

Martin Gibson

## **Abstract**

The intention of this monograph is to present a foundational model of quantum physical processes as a function of an accelerating, isotropic cosmic expansion. It represents a modification of general relativity as a solution to the gravitational field equation in an initial condition of flat spacetime in which the Einstein curvature tensor vanishes and the stress-energy tensor consists of the dynamic properties of an individual fundamental baryonic particle, the neutron, first as a potential and then as an emergent adiabatic process due to isotropic stress and strain. This fundamental form is developed as an emergent function of the product of the cosmological constant of GR quantified as the Hubble rate with a bi-directional quantum metric, defined herein on a unit cube centered on one of an indefinite number of such centers of isotropic expansion. The isotropic stress is shown to create a torsion strain at the femtometer scale, from which the restorative force initiates a well-defined characteristic rotational oscillation according to the principles of classical wave mechanics.

While the speed of light is held to be invariant in this model, the principle gauge of time is the expansion rate, the source of which operates orthogonal to three-dimensional space. Quantum spin energy, spin angular momentum, and charge are generated by the antisymmetric components and quantum gravity is generated by the symmetric components of the quantum stress-energy double matrix.

Ongoing expansion causes a differential change in inertial density per time unit which is equal to the differential change in mechanical impedance per length unit according to the Hubble rate. These differential drops over time result in a discontinuity at the nodes of the neutron waveform which results in the transmission of a small fraction of the neutron wave energy as the rest mass of the electron and a transfer of the neutron wave momentum as elementary charge, so that beta decay is shown to be tuned to the Hubble rate. With the emission of the electron in a condensed matter state absent ionization, atomic interactions result from the nodal/wave phase interactions of the emitted electron waveform.

This non-stochastic model is developed using dimensional analysis without the addition of extraneous parameters and validated based on the observable invariant properties of the neutron and electron mass and the related reduced Compton wavelengths, the value of  $\hbar$  and the speed of light. Newton's gravitational constant is derived and found to be  $6.67319 \times 10^{-11} \text{ m}^3 \text{ kg}^{-1} \text{ s}^{-2}$ , close to the 2018 CODATA value of  $6.67430(15) \times 10^{-11}$ . The Hubble rate is derived and found to have a lower threshold of  $73.08 \text{ km/Mpc /s}$ , which is interpreted as a dimensionless, compounding strain of  $2.36839 \times 10^{-18} \text{ s}^{-1}$ . This is within the uncertainty of a recent referenced study by Riess et al, which reports the most precisely defined figure to date at  $H_0 = 74.03 \pm 1.42 \text{ km s}^{-1} \text{ Mpc}^{-1}$ , validating this approach. It addresses the concerns in that study of the  $4.4\sigma$  between their figure and the results of the LCDM Planck study at  $67.74 \text{ km} \pm 0.46 \text{ km s}^{-1} \text{ Mpc}^{-1}$ .

The model provides an intuitive grasp of such quantum phenomena and concepts as electron orbitals, tunneling, and nuclear and molecular bonding in the context of condensed matter physical phenomena such as the continued reported experimental results of positive correlations of anomalous heat and helium production in support of cold fusion. This model provides an understanding of physical phenomena that can, among other things, help explicate and expedite the safe development and utilization of palladium catalyzed deuterium nuclear fusion.

## Table of Contents

0 — Notes Concerning Dimensional Analysis and Wave Formalism	1
0a — Classical Wave Dynamics	5
1 — A Heuristic Example of a Classical Basis for Quantum Phenomena	8
2 — The Classical Basis for Quantum Phenomena	12
2a — Symmetric Components of the Wave Tensor and Quantum Gravity	13
2b — Anti-Symmetric Components of the Wave Tensor and Spin & Charge	16
2c — Geometric Considerations of Rotational Oscillation and Beta Decay	26
2d — Derivation of Beta Decay as a Function of the Hubble Rate	29
2e — The Missing Mass of Beta Decay	36
2f — Evaluation of Elementary Charge	40
2g — Special Relativity and Muon & Tau Families	43
3 — Condensed Matter Application of this Model	44
4 — Conclusions	53
Bibliography, Citations, and Other Resources	57
Addendum — Isotropic Expansion Stress on a Unit Space (IESUS)	59
to Section 2g — Muon & Tau Families	
— Detail of the effects of IESUS	77

## Figures, Diagrams, Tables, and Charts

Figure 0	Wave Kinematic Functions	5
Figure 1	Isotropic Expansion Stress over Time	9
Figure 2	Expansion Stress < Inertia, $r_0 = t / m_0$	9
Figure 3	Expansion Stress => Inertia, $r_0$	9
Figure 4	Expansion Stress in Maximally Dense Space	10
Figure 5	Expansion Stress w/ Differential Vectors	10
Figure 6	Expansion Stress in 3D Manifold	10
Figure 7	Graphic of Emergent Cuboctahedral Lattice Cell	10
Figure 8	Graphic of one half of an Inversphere	11
Diagram 0	Femto Scale Torsion	16
Diagram 1	Rotational Oscillation	17
Diagram 2	Neutron Oscillation	19
Diagram 3	Proton Oscillation	20

Diagram 4	Electron Oscillation	21
Diagram 5	Anti-Proton Oscillation	22
Diagram 6	Positron Oscillation	23
Table 1	Charge and Spin Table for Ordinary Matter for C & L = 1	24
Table 2	Charge and Spin Table for Anti Matter for C & L = 1	25
Figure 9	Superposition of equal area cube and sphere	26
Figure 10	Cross-section of equal area cube and sphere	27
Table 3	Relationship of Hubble rate and particle mass/energy	33
Figure 11	Graph of exponent bases $e_n$	37
Table 4	Exponential Functions of $e_n$ for $n = 0$ to 3	37
Table 5	Natural log functions of $e_n$ for $n = 1$ to 6	38
Figure 12	Condensed Matter Graphic for N, P, and E spatial relationship	45
Figure 13	Graphic representing covalent bonding	46
Figure 14	Graphic representing electron-positron annihilation	46
Figure 15	Palladium Valence Electron Orbitals $4d^{10}$	46
Table 6	Lattice and Element Parameters for Palladium and Nickel	47
Chart 1	FCC Lattice Properties	49
Chart 2	Cuboctahedral Lattice Configuration	50
Chart 3	Hydrogen Diffusion	51
Chart 4	Fusion Path 1 in the Tetrahedral chamber	52
Chart 5	Fusion Path 2 in the Tetrahedral aperture	52
Addenda:		
Chart 6	Chart of torques of inductive and capacitive moments on fermion particle-wave nodal structure	68
Table 7	Table of IESUS Inflection Points	70
Figure 16	Cubic Expansion	77



## 0 — Notes Concerning Dimensional Analysis and Wave Formalism

An extended note about dimensional analysis as used herein is in order. In theoretical discussion, such analysis makes use of a natural unit of measurement, herein represented by a subscript nought, for any qualitative property where the existence or applicability of the units is understood and supported by observational data. To be verifiable, the natural units of that analysis must then be convertible to a standard system of measurement such as the SI. If a dimensional property such as time or distance is deemed to be fundamentally continuous, as in most interpretations of the nature of spacetime of general relativity, there may be no “natural” unit other than an observed relationship to some familiar observation about the natural world; 1/60 of 1/60 of 1/24 of one solar day of the earth for one second as a unit of time and the distance light travels in one second in a vacuum divided by 299,792,458 for one meter as a unit of distance.

The presumed scale invariant speed of light,  $c$ , thereby couples the empirically derived measures of the two fundamental properties of physical kinematic analysis. Analysis is helped in some instances by the normalization of fundamental quantities. In the case of certain derivatives in which a rate of change in a dependent variable as numerator, dividend or antecedent is expressed as a function of a change in the independent variable as denominator, divisor or consequent and in which the dependent change has been evaluated in some system of accounting or calculation, the independent change is generally expressed as a unit of that property, i.e. as 299,792,458 meters per 1 second for the speed of light. For invariants or characteristic modes of a system, analysis can be facilitated by normalization, that is, by rendering the antecedent as a unit value as well; by changing 299,792,458 meters to 1 nouveau-meter, or 3.33... nano-seconds to 1 nouveau-second. The terms here are illustrative only and not intended for use. Such normalization notationally changes  $c$  to  $c_0$ , though in computation the transition back to standard units such as SI may be made.

This is in fact what happens in what is perhaps the most famous equation of physics,  $E = mc^2$ , and related wave equations involving use of the speed of light, as will be shown in this development. It is a source of much unnecessary mystification concerning mass and energy, at least to the public. When writers speak of “converting” a small amount of mass into a tremendous amount of energy, they are tacitly and generally unwittingly acknowledging the fact that the speed of light,  $c$ , is not normalized. If it was, a unit of mass would simply equal a unit of energy, though the context might indicate a unit of potential energy (mass) equals a unit of kinetic energy, thereby pointing to the fundamental concept of the conservation of energy.

The observations of dynamic analysis, that matter appears to be inherently comprised of discrete and invariant fundamental units of the properties of mass-energy, spin and charge, gives credence to the notion that these properties support ontologically natural units for their qualitative dimensions; either mass or energy that can be converted one to the other as a function of the square of the speed of light, fundamental particle spin angular momentum that arises apparently (but not necessarily in fact) apart from any geometric, dynamic basis for its dimensional property of action or angular momentum, and charge with the fundamental dimensional transformation of potential energy in its static, capacitive state and kinetic energy as current in its inductive, electromotive state.

Despite the energetic connotation of the word, a study of dynamics is grounded in the concept of inertia. It is against the backdrop of stationary objects that energetic ones are measured. Speed can only be measured with respect to an assumed stationary inertial reference frame, be that frame a configuration of fixed objects moving at a constant velocity through space or an abstraction of space itself, so a quantifiable explanation of the interaction between objects requires the concept of mass as a measure of that inertia. Mass can be thought of as a measure of 1) a resistance to change, 2) a delay or retardation factor in the process of a system, 3) a deflection agent to a moving element from an initial path, 4) a concentration of factors governing any such effects, 5) with respect to quantum particles, as a wave number, an inverse measure of a wave length, and perhaps other inertial phenomena. None of these properties can be quantified from experimental data without some reference to space and time, although they may be gauge invariant with

respect to a specific location in space and time, and yet the coupling of quantum phenomena with a spacetime continuum remains elusive for conceptual reasons.

In the case of a wave analysis, the coupling of spacetime and quanta is straight-forward, as theoretical models of mechanical, inertial, wave bearing continua are known to support the emergence of characteristic natural and resonant frequencies and wavelengths in response to a driving energy source, once some threshold input level of that energy is reached. A characteristic fundamental frequency and wavelength can then form the basis of a natural time and distance scale, and we might anticipate that a natural unit of mass as derived from the inertial density of such a continuum is indirectly related to that of the time period and the displacement distance of any wave action or oscillation defined by such a characteristic emergence.

Using the angular representations for frequency,  $\omega_0$ , and wavenumber,  $\kappa_0$ , or the number of periodic wavelengths times  $2\pi$  per standard unit of length, and inverting for  $\theta=1$ , gives a unit length of time,  $t_0$ , for one radian of wave activity at fundamental frequency and the corresponding distance unit length,  $r_0$ , or fundamental angular wavelength,  $\lambda_0$ , for one radian. The following quotient of frequency over wave number for wave form  $q$  gives the following

$$c_0 = \frac{\omega_{0q}}{\kappa_{0q}} = \frac{\cancel{\theta}/t_{0q}}{\cancel{\theta}/r_{0q}} = \frac{r_{0q}}{t_{0q}} = \left( \frac{dr}{dt_0} \right). \quad (1.1)$$

The bracketed last term is stated with the sub-nought to emphasize that while the wave speed can be stated in terms of differentials, as with most derivatives, the dependent variable is virtually always evaluated as a function of a change in one unit of the independent variable, in this case whether it is expressed as one second or one radian of motion of a theoretical clock. In the first instance,  $dr_{SI}$  is 299,792,458 meters in the SI system and in the second instance it is equal to the length of a subtending arc of 1 radian,  $dr_0$ , in the natural units used here.

It is well known that the square of the speed of wave motion, transverse and longitudinal, is a function of the stress,  $f_0$ , and the inertial density,  $\rho_0$ , of a wave bearing medium as follows, where the stress is further defined as a force,  $\tau_0$ , either shearing,  $\tau_s$ , or tension,  $\tau_t$ , per cross-sectional area,  $A_0$ , of the medium, and inertial density is defined as mass,  $m_0$ , per unit volume,  $r_0^3$ . In the final term of this equation,  $A_0$  and two of the volume length components are canceled from the term before to leave a statement for a linear component of stress, such as a tension force on a stretched string, over a linear inertial density,  $\lambda_0$ , since the cross section defining the tension stress and also the volume density of the string are the same, so that

$$c_0^2 = \frac{f_0}{\rho_0} = \frac{\tau_0}{A_0} \Big/ \frac{m_0}{r_0^3} = \frac{\tau_{t0}}{\lambda_0}. \quad (1.2)$$

Note that the string tension component, despite the cross-sectional canceling in the final term, still has the capacity for shearing stress and therefore transverse wave motion as with a sinusoidal wave. Combining (1.1) into (1.2) gives the following

$$c_0^2 = \frac{\omega_0^2}{\kappa_0^2} = \frac{\tau_{t0}}{\lambda_0} \quad (1.3)$$

Quantum mechanics uses the results of scattering experiments of photons on rest mass particles initially performed by Arthur Compton in 1922 to relate the energy-equivalent of a particle's rest mass to the change in energy of a photon scattered from the particle based on the change in wavelength of that photon and the angle of scattering, where  $h$  is Planck's constant and  $m$  is the mass of the quantum or



$$\Delta\lambda = \frac{h}{cm_q}(1 - \cos\theta)$$

$$\lambda_C = \frac{h}{cm_q}$$
(1.4)

The Compton wavelength,  $\lambda_{C,q}$ , is therefore an accepted statistically derived parameter of rest mass particles which we will use in the context of dimensional modeling to gauge the natural unit scale. In doing so in the context of the following discussion of fundamental baryonic particles, neutron and proton, as examples of rotational oscillation, we will use the Compton convention as a statistically based physical measure of those quanta's radius of rotation,  $r_q$ , but using the reduced Compton or angular measure of the wavelength,  $\tilde{\lambda}_{C,q}$  lambda-bar, and the corresponding reduced Planck's constant,  $\tilde{h}$ , h-bar,

$$\tilde{\lambda}_{C,q} = r_q = \frac{\tilde{h}}{cm_q}$$
(1.5)

It is assumed in this modeling that the product of the angular velocity of a particle wave phases,  $\omega_q$ , times a radian-arc of motion that is equal to the reduced Compton and the radius of maximum shear stress of the waveform, is at the speed of light, so that

$$c = \theta\omega = \tilde{\lambda}_{C,q}\omega_q = r_q\omega_q$$
(1.6)

and for a fundamental rotational oscillation as derived for this model,

$$c_0 = r_0\omega_0$$
(1.7)

From quantum analysis, we know the dimensional makeup of Planck's reduced quantum of action for use with angular frequency and wave number, which we can express with (1.1) as

$$\tilde{h} = m_0 r_0 c_0$$
(1.8)

Since the length dimension in the last term of (1.1) and in (1.8) can be the same in natural units, and in light of the fact that both h-bar and  $c_0$  are deemed to be invariant, we can rearrange (1.8) in terms of natural units and arrive at the following constant of inertia,  $\varkappa$  (tav), which has the value of being a time-independent fundamental gauge of length to mass, showing their essential inverse relationship.

$$\frac{\tilde{h}}{c_0} = m_0 r_0 = \varkappa$$
(1.9)

From quantum analysis we have the following condensed matter identity of a rest mass particle, either baryon or lepton, as

$$m_{0q}c_0^2 = \tilde{h}\omega_{0q} = \varkappa c_0\omega_{0q}$$
(1.10)

which with rearrangement shows that in quantum terms mass is simply a proxy for wave number as

$$m_{0q} = \frac{\varkappa}{c_0}\omega_{0q} = \varkappa\kappa_{0q} = \frac{\varkappa}{r_{0q}}$$
(1.11)

While we could continue to use the familiar quotient of h-bar over the speed of light in this discussion, and will do so where it is deemed appropriate for clarity in relating this material to the established dicta of physics, the inertial constant points directly to a physical wave nature of fundamental quanta by virtue of its conversion of angular wavenumber to mass for a particle constrained over time to a discrete location in space, whether that mass is conceived of as a derived property of an inertial substance or substrate or simply as a computational conversion of characteristic inherent energy as determined by a characteristic angular frequency determined from experiment.

It follows for a quantum particle that

$$r_{0q} = \frac{\hbar}{m_{0q}} . \quad (1.12)$$

Thus, for an inertial wave bearing medium of a given inertial density,  $\lambda_0$ , given the inertial constant, the mass of a fundamental particle oscillation,  $m_0$ , actually a form of self-oscillation, at an effective natural angular frequency,  $\omega_0$ , is a direct function of the angular wave number,  $\kappa_0$ , and therefore indirectly of the angular wavelength,  $\lambda_0 = r_0$ .

Clearly then, just as the linear wave equation contains two tacit cross-sectional area dimensions that cancel, (1.3) contains two tacit terms for the inertial constant in each side of the quotient and is in fact the dimensionally correct

$$c_0^2 = \frac{\hbar \omega_0^2}{\hbar \kappa_0^2} = \frac{\tau_{r0}}{\lambda_0} . \quad (1.13)$$

This can be rearranged in a standard form of a wave equation, where the differentials are made explicit and perhaps more recognizable in the middle two terms, as

$$\lambda_0 \equiv \hbar \kappa_0^2 \equiv \hbar \frac{\partial^2 \theta}{\partial x^2} = \frac{1}{c_0^2} \hbar \frac{\partial^2 \theta}{\partial t^2} \equiv \frac{1}{c_0^2} \hbar \omega_0^2 \equiv \frac{1}{c_0^2} \tau_0 . \quad (1.14)$$

A further rearrangement states the important relationship of the mechanical impedance,  $Z_0$ , of the continuum or wave bearing medium which is dimensionally the quotient of the fundamental stress force and the wave speed as

$$\lambda_0 c_0 = \frac{\tau_0}{c_0} \equiv Z_0 . \quad (1.15)$$

In keeping with a premise of this development, that of ongoing spacetime isotropic expansion, we state that such expansion inherently leads to a decrease in inertial density of the continuum over time, and assuming an invariant speed of wave motion, to a decrease in the stress force and impedance, so that implicit differentiation by decoupling the wave speed components and rearranging equates the change in density over time to the change in impedance over a displacement

$$\frac{d\lambda_0}{dt} = \frac{d\tau_0}{c_0 dr} = \frac{dZ_0}{dr} . \quad (1.16)$$

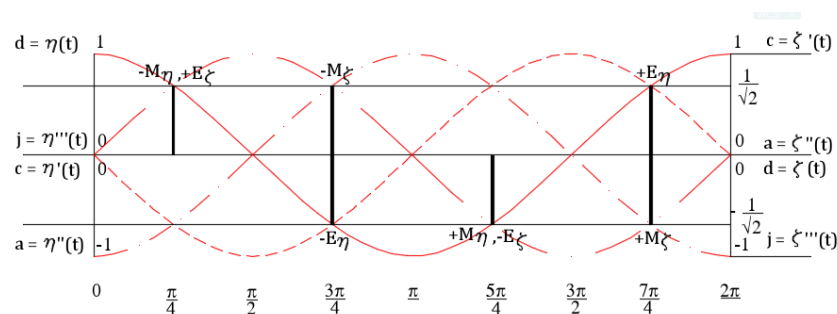
This is of principal importance in understanding the Coulomb force and the generation of the electron as it applies to condensed matter.

## 0a — Classical Wave Dynamics

Various wave properties can then be stated using this ideal analysis and the Euler formalism for the various derivative properties of a complex fundamental torsion wave, where  $\phi$  in this case is a rotating torsional displacement of the wave phase  $\eta$  and  $\zeta$  in the  $y$ - $z$  strain cross-section, where the imaginary sense,  $i$ , indicates an initial torsion strain at  $\pm y$  about  $Y$  of  $\frac{1}{2} \pi$  from  $z$  into  $+X$  as developed below, and the amplitude,  $A$ , is assumed to be equal to the angular wave length,  $r_0$ .

$$\phi = \eta + \zeta = A(\cos\theta \pm i \sin\theta) = Ae^{i\theta} = Ae^{i(\kappa x \pm \omega t)} \quad (1.17)$$

A physical example of this wave will be developed herein. Obviously the  $\zeta$  component lags the  $\eta$  component by  $\frac{1}{2} \pi$ . In the following sinusoidal plotting of the wave phases and the kinematic functions of the two points, the instances of maximum power in both the direction of storage of potential energy,  $E$ , and of release of that energy as kinetic or mechanical energy,  $M$ , for each point,  $\eta$  and  $\zeta$ , of either sense,  $\pm$ , are shown. The senses indicate the direction of displacement change for  $\eta$  and  $\zeta$ , toward  $+1$  or  $-1$  on the ordinate at the given point in the cycle. These designations will also stand for electrical potential energy or charge,  $E$ , and for magnetic energy of electrical current,  $M$ . In this development it will be seen that such wave generated mechanical power moments are sustained over time for the oscillation and serve an essential function in the generation of charge and the electron.



*Wave Kinematic Functions*

Figure 0

In the Euler formalism, each  $\frac{1}{2} \pi$  rotation in time and in space is represented by an incremental unit power of  $\omega$  and  $\kappa$  respectively as a result of each derivation. Orders of integration are represented by negative unit powers, where in cyclic terms one order of integration,  $\omega^{-1}$  or  $\kappa^{-1}$ , equates to three orders of derivation,  $\omega^3$  or  $\kappa^3$ . Represented as natural unit values, the following creates a calculus of dynamic invariants for a fundamental rotational oscillation, where we can introduce a compact and convenient notation for each invariant, using the inertial constant as the system gauge or scale factor, where subscripts indicate complex differentiation and super scripts indicate complex integration, with time to the right and space to the left.

### Wave Kinematic Time Functions

Displacement,  $r$

$$\phi(t) = Ae^{i\omega t} = r_0$$

Velocity,  $c$

$$\phi'(t) = i\omega_0 Ae^{i\omega t} = ir_0\omega_0$$

Acceleration,  $a$

$$\phi''(t) = -\omega_0^2 Ae^{i\omega t} = -r_0\omega_0^2$$

Jerk,  $j$

$$\phi'''(t) = -i\omega_0^3 Ae^{i\omega t} = -ir_0\omega_0^3$$

### Wave Dynamic Time Functions

Inertial constant,  $\tau$

$${}^0_0\tau_0 \quad m_0\phi(t) = m_0 Ae^{i\omega t} = \tau$$

Transverse Wave Momentum,  $p_0$   
(equals raw fundamental charge)

$$\tau_1 \quad m_0\phi'(t) = m_0(i\omega_0 Ae^{i\omega t}) = i\tau\omega_0$$

Transverse Wave Force,  $\tau$

$$\tau_2 \quad m_0\phi''(t) = m_0(-\omega_0^2 Ae^{i\omega t}) = -\tau\omega_0^2$$

Transverse Wave Yank,  $Y_0$

$$\tau_3 = \tau^1 \quad m_0\phi'''(t) = m_0(-i\omega_0^3 Ae^{i\omega t}) = -i\tau\omega_0^3$$

### Wave Dynamic Space Functions

Inertial constant,  $\tau$

$${}^0_0\tau_0 \quad m_0\phi(x) = \frac{\tau}{Ae^{i\kappa x}} Ae^{i\kappa x} = \tau$$

Mass,  $m_0$

$${}^1_1\tau \quad m_0\phi'(x) = \frac{\tau}{Ae^{i\kappa x}} i\kappa_0 Ae^{i\kappa x} = i\tau\kappa_0$$

Linear Density,  $\lambda_0$

$${}^2_2\tau \quad m_0\phi''(x) = \frac{\tau}{Ae^{i\kappa x}} (-\kappa_0^2 Ae^{i\kappa x}) = -\tau\kappa_0^2$$

Moment of Inertia,  $I_0$

$${}^3_3\tau = \tau^1 \quad m_0\phi'''(x) = \frac{\tau}{Ae^{i\kappa x}} (-i\kappa_0^3 Ae^{i\kappa x}) = -i\tau\kappa_0^3 = -i\tau\kappa_0^{-1}$$

## Remaining Wave Dynamic Space-Time Functions

Mechanical Impedance, $Z_0$ (of the spacetime manifold)	${}^1\mathfrak{T}_1$	$-{}^1\mathfrak{T}\kappa_0\omega_0$
Transverse Momentum Surface Density, $p_2$	${}^2\mathfrak{T}_1$	$-i{}^1\mathfrak{T}\kappa_0^2\omega_0$
Planck's Quantum of Action, $\hbar$ (Spin Angular Momentum)	${}^1\mathfrak{T}_1$	${}^1\mathfrak{T}\kappa_0^{-1}\omega_0 = {}^1\mathfrak{T}c_0$
Linear Transverse Force Density, $\tau$	${}^1\mathfrak{T}_2$	$-i{}^1\mathfrak{T}\kappa_0\omega_0^2$
Wave Stress, $f_0$	${}^2\mathfrak{T}_2 = {}^2\mathfrak{T}^2$	${}^1\mathfrak{T}\kappa_0^2\omega_0^2$
Spin Energy, $E_0$	${}^1\mathfrak{T}_2$	$i{}^1\mathfrak{T}\kappa_0^{-1}\omega_0^2$
Mass Frequency Ratio, $m_0/\omega$	${}^1\mathfrak{T}^1$	${}^1\mathfrak{T}\kappa_0\omega_0^{-1} = \frac{{}^1\mathfrak{T}}{c_0}$
Yank Surface Density, $Y_2$	${}^2\mathfrak{T}_3$	$i{}^1\mathfrak{T}\kappa_0^2\omega_0^3$
Wave Power, $P_0$ (Yank Volume Density, $Y_3$ )	${}^1\mathfrak{T}_3 = {}^3\mathfrak{T}_3$	$-{}^1\mathfrak{T}\kappa_0^{-1}\omega_0^3 = -{}^1\mathfrak{T}\kappa_0^3\omega_0^3$

## 1 — A Heuristic Example of a Classical Basis for Quantum Phenomena

We can analyze the local effects of an isotropic expansion of an ideal extended 3-D manifold by considering the heuristic example of the surface of a spherical balloon under expansion. We treat that surface as a two-dimensional manifold without boundary, a 2-sphere. The stress of expansion is directed radially from the center of the balloon from which it is transferred as transverse stress across the surface. Beyond an energy input threshold, the balloon expands with resulting strain, and the stress spreads out radially and equally from each point on the surface. Note that logically, in an elastic medium, strain always implies stress, but stress may not involve strain, just as a force pushing against and moving an object does work, but it does no work without that movement. Strain implies the energy of work.

If we select two points in very close proximity and represent only those stress vectors radiating from the two points, which necessarily incorporate those of the intervening space, we get the situation shown in Figure 1. It is important to emphasize that a point, in fact any  $n$  minus 1 reference on an  $n$ -manifold, marks a reference location on that manifold but is not itself an element of that manifold, which for a 2-sphere is an area. The two circles shown, two “1-spheres” in topological language, represent reference boundaries of equal stress for the two points chosen, of equal strain potential, and of equal time elapse for a change in stress at the boundaries to be registered at each point and vice versa. Obviously, the further the points are from each other the longer the time required for any such stress, and attendant strain to register.

Figure 1 is a snapshot in time and assumes that the process is ongoing, so that momentum efficiently allows all differential strain of expansion to flow into the continued expansion of the balloon surface. Note that if the vectors represent the stress of expansion, they do not represent the strain, even the accumulated strain, which cannot radiate from a point, a singularity, but can only radiate from an initial condition of an element of the 2-manifold, i.e. a smaller circle, as with the lighter vectors of Figure 3 radiating from the circle out.

Note also in Figure 1 that there is interaction between five stress vectors from each of the two points. The central vector of each radiates to the other point, indicating that with strain the distance between the two points will increase and without strain the pressure, or negative tension stress, between the two will intensify. The vectors to either side of this first common radial vector are tangential to the equipotential circle of the other point, indicating a shear or rotational stress and potential strain at those locations on the reference boundaries, including the areas exterior to the circles from the point of tangency up to their points of crossing. The outer most of the five interacting vectors for each point indicate a region of converging stress and potential strain. This configuration of stress and strain potential represented by the five vectors for each point indicates a potential for simple harmonic oscillation given the necessary and sufficient additional condition for wave mechanics of inertial density.

Not unlike the process of blowing up a real rubber balloon that has an initial physical configuration and does not start from a single point, we might anticipate that initiation of the process requires a threshold level of internal radial stress to be achieved before expansion of the surface as a result of transferred radial-to-surface strain. Figure 2 shows the condition prior to initiation of the process, in which the inertia of a given region of radius  $r_0$  is greater than the transverse stress represented by the radiating vectors inside the circle, and before any expansion strain has occurred. Note that  $r_0$  represents a potential for wave activity based on the properties of the inertial constant as in (1.12).

Figure 3 transposes the inertial vectors and expansion stress vectors from Figure 2 and shows the condition at one of the points on the manifold at the point in time when the inertial force is equal to the expansion force and immediately thereafter. Continued increase in the expansion stress will result in an expansion strain in the value of  $r_0$  or, if the area outside the circle is of less inertial density than that of the inside, in a strain of the area outside the periphery.

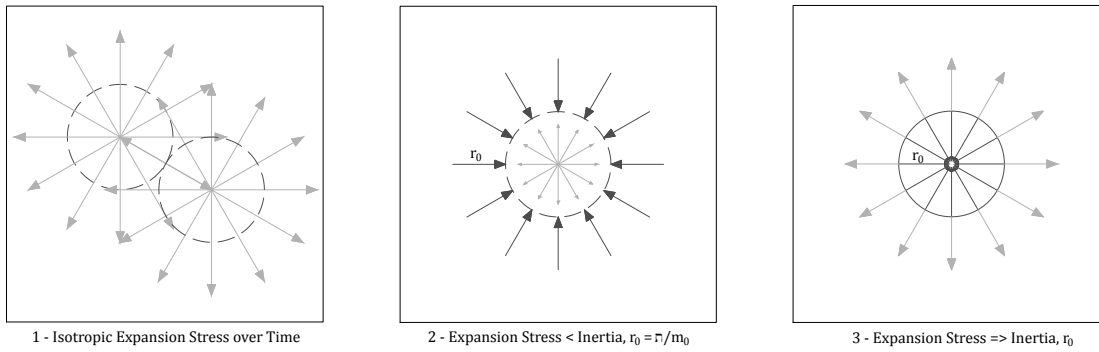


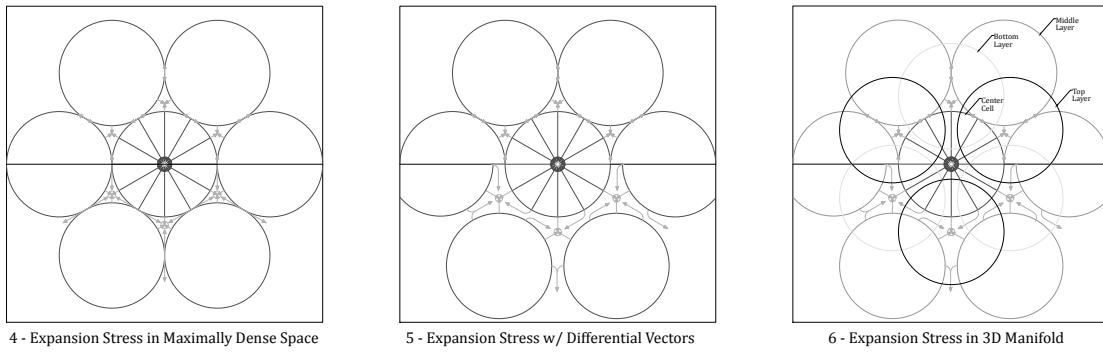
Figure 4 shows the general condition of Figure 1 in an area of initial, maximum inertial density of the 2-manifold as indicated by the maximum packing of six identical circles around each other circle, one of which is highlighted here. Under such conditions of density, the triangular interstitial areas become the focus of stress in excess of that required for equilibrium condition of the inflated manifold as in Figure 3. The upper half of the divided figure shows the state when the stress vectors from the adjoining inertial circles converge and concentrate the stress in the center of the interstitial areas. Those vectors that were originally radially in common with an adjacent cell as in Figure 1 are redirected as rotational potential to their common points of tangency. The bottom half of the figure shows the condition a moment later as the stresses increase in the interstitial regions of the manifold. Such accumulation of energy will lead to rotational and oscillatory stress and potential strain of the circle peripheries and a potential for and eventually effective continued expansion of the 2-manifold counter-centripetally in what will be registered in the interstitial regions as curvature. It will also lead to an expansion of these areas as in Figure 5.

Note there is nothing predetermined about the location of such lattice configuration which is an emergent phenomenon similar to the observed phenomena of Rayleigh-Benard convection which the reader is encouraged to investigate on the internet. In that phenomena, the function of expansion stress is replaced with a heat gradient and the anti-parallel function of inertia is replaced with gravity.

The lower half of Figure 5 shows the eventual expansion strain of the regions between the circular cells in the flat plane of the balloon surface, as well as the emergence of rotational, shear strain in that flat surface about the various cells peripheries, and finally the continued stress and strain in the interstitial areas resulting in curvature which we can see as normal to the flat surface.

To this point, our discussion has focused on the effects of expansion stress on a postulated 2-manifold, the 2-sphere cover of a 3-ball. We now extrapolate that treatment to that of a 3-manifold under expansion, a 3-sphere cover, due to a change in stress over time, which is itself normal to the “surface” of that 3-sphere; this means that the expansion operates as the symmetric components of a 4-stress . This is depicted in Figure 6, which at maximum density takes the configuration of a cuboctahedral lattice (COL). A COL is the same as a face centered cubic (FCC) structure but centered on one of the spherical cells instead of the octahedral central space of the FCC. The COL perspective is achieved by shifting the FCC perspective one half the edge length of a cube to include the four center nodes of the adjacent surfaces, twisting  $\frac{1}{4} \pi$  CCW about the top face of the cube, then tilting the top toward the viewer to look along a diagonal axis through the triangular aperture to the central sphere. The circles in this figure represent the diameters of the 2-spheres of each of three representative layers.

In Figure 6, the 3 spheres of the designated top layer center on two edges and one vertex of a defined FCC, so that the view shown is looking along one of four diagonal axes of the configuration at the center sphere. Beyond that are the six 2-sphere cells of the middle layer represent by the six surrounding circular cells of Figures 4 & 5, with the stress dynamics of those figures shown here. The bottom layer with 3 spheres represents the next layer of the 3-manifold, once again represented as four dimensional with respect to the four diagonal axes of the space. The indicators of interstitial curvature and expansion in Figure 5 represent rotational and torsion stress and strain about the center inertial spherical cell in Figure 6.



The configuration is shown as three dimensional and without the stress vectors in the following graphic.

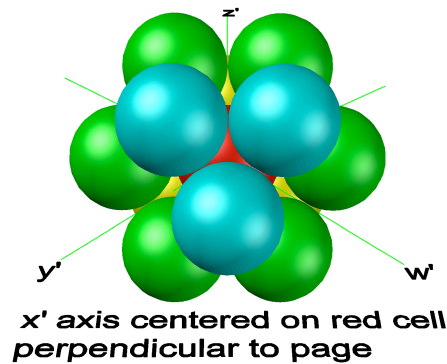


Figure 7 — Graphic of Emergent Cuboctahedral Lattice Cell

The stress of isotropic expansion on a compact 3-manifold (the three dimensional analogy of the surface of a ball) results in an emergent, initial cuboctahedral lattice of rotational stress and strain components from the uniform density in the manifold prior to that expansion. The inertial continuity and local elasticity of the manifold prevents these shear components from rupturing or creating a local internal extrusion strain, resulting instead in oscillation about each inertial center with an expansion and reduced density of the manifold in the interstitial regions. This oscillation can be represented in a couple of ways, which avoid the co-ordinate entanglement problem (not to be confused with quantum entanglement). Instead of such entanglement, rotational strain results in a recoil of the rotational displacement, which is torsional and has less torsional resistance about the diagonal axes, along a path of least action in keeping with (1.17)

A heuristic representation of this rotational oscillation is a sequence of  $4, 2/3 \pi$  CCW rotations, facing the cell center, about each of the four diagonal axes extending from the vertices of a face of the represented cube, say the upper face here, a CCW sequence of CCW rotations being equal to a CW sequence of CW  $2/3 \pi$  rotations on the opposite ends of the axes on the opposite cubic face. This can be further refined by making the diagonal rotations differential, followed sequentially by a differential rotation of the axis normal to the chosen face, proportionally so as to return all elements of the configuration to their original positions after a full rotation of the surface normal axis.

In this regard, we offer the following 4-dimensional interpretation of a 2-sphere in the context of the above development. Each of the four axes of the cubic diagonals can be defined as the central axis of a pair of pseudo-spheres, one on each side of the central 2-sphere, so that they intersect each other orthogonally at their rims as seen in Figure 8, which shows the top half of such an arrangement.



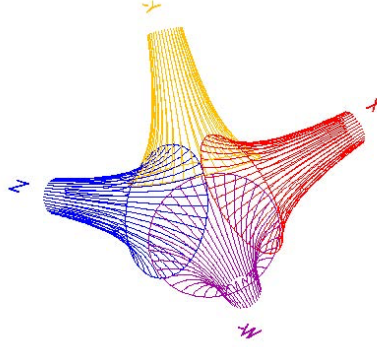


Figure 8 — Graphic of one half of an Inversphere

A pseudo-sphere has constant negative curvature, and the rim intersections will be found to coincide with the intersections of the corresponding three cubic surface axes and the surface of a sphere of curvature related to the positive of the pseudo-spheres; if the pseudo-sphere curvatures are -1, that of the sphere is  $+\frac{\sqrt{3}}{2}$ . I am calling this contraction of eight pseudo-spheres an inversphere as it inverts the positive curvature of the sphere proportionally to the negative curvatures of the concentric pseudo-spheres. Sequential oscillatory twists of the four axes as described in the development of the cuboctahedral lattice produces the rotation of the center 2-sphere, while straining the adjacent pseudo-spherical surfaces.

From this treatment it becomes apparent that the gravitational components of the resulting wave action are the symmetric components of a matrix defined on the oscillation as in the following section and form the basis of a de Sitter spacetime within the context of general relativity. The electromagnetic, weak and strong forces of quantum modeling are the function of the anti-symmetric components of that matrix and in the manner of an inversphere form the basis of an anti de Sitter quantum spacetime as developed in that section. The de Sitter and anti de Sitter geometries are inherent or curvature potentials of spacetime in this model that emerge as actual quantum effects from the inertia of spacetime in response to expansion tension as defined by the Hubble rate.

## 2 — The Classical Basis for Quantum Phenomena

The primary physical discipline for an analysis of space and time is general relativity, generally practiced as a classical field theory. The basic field equation for the theory is presented here

$$G_{\mu\nu} + g_{\mu\nu}\Lambda = \left(\frac{4\pi G}{c^4}\right)2T_{\mu\nu} \quad (1.18)$$

The first term on the left is the Einstein curvature tensor,  $G_{\mu\nu}$ , (often stated in further detail as the sum of the Ricci tensor and the Ricci scalar) which is a function of the energy per volume represented by the stress tensor,  $T_{\mu\nu}$ , on the right. As generally stated the accumulation of mass-energy defined on the right tells spacetime as  $G_{\mu\nu}$  how to curve and that curvature in turn responds to tells mass-energy how to move within it. In particular, however, it says that the right side of the equation predominates in curving spacetime if  $T_{\mu\nu}$  is great and the left side predominates in controlling the movement of matter/energy if  $G_{\mu\nu}$  is great. If both are small at some point in the manifold, we are left with a generally flat spacetime, so that  $G_{\mu\nu}$  essentially vanishes and the cosmological constant term,  $g_{\mu\nu}\Lambda$ , governing spacetime expansion is the predominant feature at that point. The metric,  $g_{\mu\nu}$ , isotropically distributes the effects of  $\Lambda$  according to the double matrix of (1.20), and their product is effectively a spacetime, oscillating strain. If  $\Lambda$  is small it means that any change is relatively slow, which appears to be the case from our perspective.

The bracketed term on the right represents the isotropic distribution of the effects of the stress-energy tensor according to the constraints of Newton's gravitational constant,  $G$ , and at the speed of light. What appears to be generally overlooked or disregarded is that the accumulated effects of  $\Lambda$  can be very great where concentrated locally at a very small scale, even for flat spacetime. At such scale and under such conditions this strain can result in curvature fluctuations as might be associated with oscillation. In any event it would be responsible for the generation of virtual particles and quantum foam of current cosmological thinking.

In this case (1.18) is reduced and transposed to show the space only components of the tensor,  $T_{ij}$ , as a function of the expansion strain as

$$T(\Lambda) = 2T_{ij} = g_{ij}\Lambda \quad (1.19)$$

The oscillating force components,  $\tau_{ij}$ , of the expression  $2T_{ij}$  can be represented by a double matrix as face centered and for the two opposing sides of a unit cube under isotropic stress and strain, where the negative sense of the second equals the addition of the opposite sense or

$$\tau_{ij} = \begin{bmatrix} -d\tau_0 & \tau_0 \cos \omega t & \tau_0 \sin \omega t \\ -\tau_0 \cos \omega t & -d\tau_0 & \tau_0 \\ -\tau_0 \sin \omega t & -\tau_0 & -d\tau_0 \end{bmatrix} - \begin{bmatrix} d\tau_0 & -\tau_0 \cos \omega t & -\tau_0 \sin \omega t \\ \tau_0 \cos \omega t & d\tau_0 & -\tau_0 \\ \tau_0 \sin \omega t & \tau_0 & d\tau_0 \end{bmatrix} \quad (1.20)$$

## 2a — Symmetric Components of the Wave Tensor and Quantum Gravity

The six symmetric differential components represent the quantum gravitational components of the system as demonstrated in the following. The matrix has been configured so that the symmetric differentials are all of the same sense, here centripetal with respect to polar coordinates and the center of a unit cube.

A scalar form of the stress-energy relationship, where  $T_0$  as a 4-dimensional spacetime stress is

$$\frac{1}{6\sqrt{3}}T_0 = f_0 = \frac{\tau_0}{A_0} \quad (1.21)$$

The inverse square root of 3 relates the orthogonality of a fourth dimension of time to the three spatial dimensions and the 6 indicates the six faces of the unit cube. If we think of the time related expansion as operating along one of the four diagonal axes of the cube at any instant of time, its relationship to the cubic faces should be clear. We next want to take the total derivative of the stress on one cubic face as

$$\begin{aligned} df &= \frac{\partial f}{\partial \tau} d\tau + \frac{\partial f}{\partial A} dA \\ df &= \frac{1}{A} d\tau - \frac{\tau}{A^2} dA \end{aligned} \quad (1.22)$$

Assuming for convenience an invariant stress so that  $df$  is zero, in natural units gives

$$\frac{\tau_0 + d\tau_0}{A_0 + dA_0} = \frac{\tau_0}{A_0} = f_0 \quad (1.23)$$

confirming the co-equal variance of the units of force and of cross-section in natural units.

Separating the total derivative (1.22) and solving for the differentials in terms of  $T_0$  gives us

$$\begin{aligned} d\tau_0 &= \frac{A_0}{6\sqrt{3}} dT_0 \\ dA_0 &= -\frac{A_0}{T_0} dT_0 \end{aligned} \quad (1.24)$$

Note that as stress expressed as a unit or as a derivative mathematically reduces to a force per UNIT of area in any system, natural or otherwise, the derivatives of stress force and of area are expressed with respect to a unit of stress, so that if we can determine the value of  $A_0$  in the first of these differentials, we can quantify the differential stress force.

The dimensional properties of  $G$  found in (1.18) are mass,  $m$ , length,  $r$ , and time,  $t$ , of some unknown natural units, though generally stated in terms of the Planck scale, and as required to produce the force of gravity when used in the equation of Newton's gravitational law. While it does not appear to be customarily acknowledged, these units can be understood to be a dimensional reduction as follows, from a fundamental expression of Newton's Law in natural units, where a unit of gravitational stress force is indicated by  $\tau_{0G}$ , and the two units of mass and square of the separation of massive bodies is converted to natural units by the quotient in the last term,

$$G = \frac{r_0^3}{m_0 t_0^2} = \frac{r_0^2}{m_0^2} \left( \frac{m_0 r_0}{t_0^2} \right) = \frac{r_0^4}{\left( \frac{\hbar}{c} \right)^2} \tau_{0G} = \frac{r_0^4}{\Gamma^2} \tau_{0G} \quad (1.25)$$

In the final term we have made use of the development of the inertial constant to convert the units of fundamental mass to length, consistent with the conventions of quantum analysis. If we can convert the force term in the final term to a length scale as well, knowing the observed value of  $G$  and the inertial constant as  $\hbar$  over the speed of light, we can solve the equation and arrive at a value for a fundamental unit of length, and thereby of mass and time as well.

First, Newton's Law can be expressed in terms of these fundamental units as the product of the number of fundamental quanta,  $n_M$ , in two gravitational bodies of mass,  $M_N$ , divided by the square of their distance of separation,  $n_r$ , in terms of fundamental units of length, times a fundamental unit of gravitational stress force

$$F_G = \frac{M_1 M_2}{d^2} G = \frac{n_{M1} m_0 n_{M2} m_0}{n_r^2 r_0^2} \left( \frac{r_0^2}{m_0^2} \tau_{0G} \right) = \frac{n_{M01} n_{M02}}{n_r^2} \tau_{0G} \quad (1.26)$$

so that the value of  $G$  unmediated by any displacement in spacetime from the source, which is presumably quantum, and between two fundamental quantum generators of gravity is simply  $\tau_{0G}$  which equals each of the 6 differentials of the symmetric components of the above matrix or

$$\tau_{0G} = d\tau_0 = \frac{A_0}{6\sqrt{3}} dT_0 \quad (1.27)$$

and we can substitute the differential here into (1.25) to get the following value for  $G$ , in which it is understood that the differential stress equals 1,

$$G = \frac{r_0^4}{\Gamma^2} A_0 df_0 = \frac{r_0^6}{6\sqrt{3}\Gamma^2} dT_0 = \frac{r_0^6}{6\sqrt{3}(\hbar/c)^2} dT = 6.67319...x10^{-11} m^3 kg^{-1} s^{-2} \quad (1.28)$$

The current 2018 CODATA value for  $G$  is  $6.67430(15) \times 10^{-11}$  with standard uncertainty for the last two digits expressed. Solving for  $r_0$ , we get a value for a fundamental natural length of  $2.1002... \times 10^{-16}$  meters, extremely close to the value of the reduced Compton wavelength of the neutron at  $2.1001... \times 10^{-16}$  meters and within the standard uncertainty given the standard uncertainty of Newton's constant. This states that Newton's constant and gravitational law are a function of expansion stress,  $T_0$ , of the spacetime manifold.

As indicated in the following development of baryonic wave mechanics, the value of (1.28) would be expected to vary slightly due to the mix of neutrons and protons in any given congregation of baryonic matter and in light of the structural nature of Newton's constant as shown in (1.26).

Thus, from (1.24) we get the following value for the differential stress force responsible for gravity as

$$d\tau_0 = \frac{r_0^2}{6\sqrt{3}} dT_0 = 4.24430...x10^{-33} \text{ Newton} \quad (1.29)$$

where the wave stress force itself, responsible for the nuclear strong force, is

$$\tau_0 = \Gamma \omega_0^2 = \Gamma \frac{c^2}{r_0^2} = \frac{\hbar c}{r_0^2} = 7.16766...x10^5 \text{ Newton} \quad (1.30)$$

and the ratio between the two is

$$\frac{\tau_0}{d\tau_0} = 1.68877\dots \times 10^{38} \quad (1.31)$$

This ratio should be the same as it is for the change in cross-section given (1.23), maintaining an invariant stress. Thus, we have the following, where it is apparent that the differential area is in fact the Planck area

$$\begin{aligned} dA_0 &= A_0 \frac{d\tau_0}{\tau_0} = r_0^2 \frac{\frac{r_0^2}{6\sqrt{3}} dT_0}{\hbar c / r_0^2} = \frac{r_0^6 dT_0}{6\sqrt{3}\hbar c} \\ &= \frac{r_0^6 dT_0}{6\sqrt{3}(\hbar/c)^2} \left( \frac{\hbar}{c^3} \right) = \frac{G\hbar}{c^3} \\ &= A_{Planck} = 2.61185\dots \times 10^{-70} \text{ meter}^2 \end{aligned} \quad (1.32)$$

This development indicates that the Planck scale, which is deemed in current theoretical thinking to be an absolute fundamental quantum scale, is in fact a classical differential related to the quantum stress tensor responsible for gravity and the strong and electromagnetic forces, applicable to the fundamental oscillation of the neutron. Thus, expansion of the cosmic manifold along the rotating diagonal axes of oscillation results in a surface differential,  $dA_0$ , and a centripetally directed differential stress force responsible for gravity,  $d\tau_0$ , which matches the wave stress of the quantum  $\tau_0/A_0$ . The square root of the inverted differential of the natural log of stress is related to the square root of the linear change of expansion as a dimensionless ratio

$$\frac{r_0}{l_{Pl}} = \sqrt{\frac{A_0}{A_{Pl}}} = \sqrt{\frac{T_0}{dT_0}} = \sqrt{(d \ln T_0)^{-1}} = 1.29952\dots \times 10^{19} \quad (1.33)$$

## 2b — Anti-Symmetric Components of the Wave Tensor and Spin & Charge

We next consider the anti-symmetric components of the matrices in light of the previous description of the emergent rotating torsional oscillation of a quantum system. As indicated by this matrix and developed below, the system generates spin angular momentum and the magnetic dipole field of each of the particles, through the oriented rotation of an inductive moment,  $L_{\mu\nu}$ , of each. This explains why there are no magnetic monopoles, as the field source is an axial vector which has inherent polarity.

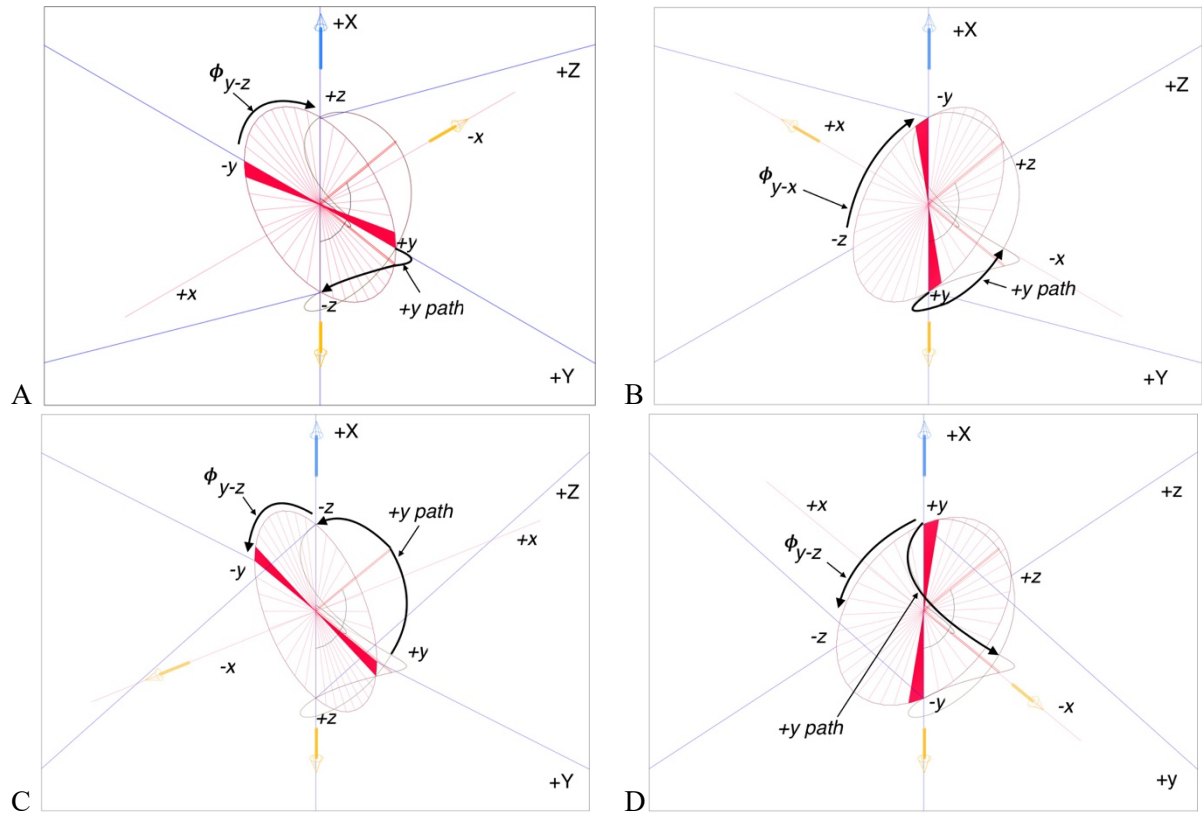


Diagram 0 — Femto Scale Torsion

Initially in X-Z plane (A), recoil under additional torsion stress in X-Y and Y-Z planes results in sustained rotation of  $\phi$  around X axis with  $y-z$  oscillation of maximum stress. Path integral of  $+y$  point on  $\phi_{x-y}$  is shown for four  $\frac{1}{2} \pi$  phases.

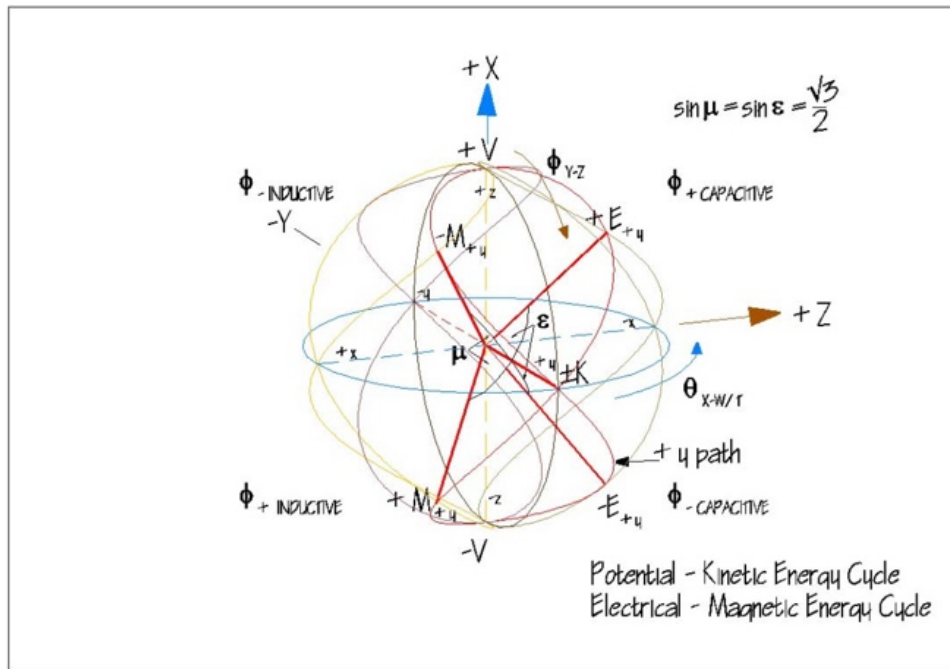


Diagram 1 — Rotational Oscillation

Rotation of  $\phi_{x-y}$  is shown with path integral of  $+y$  point scribing a figure 8 as it oscillates, always crossing the equator to the right to create the spin vector at  $+X$ . There are a continuous set of such points defined by the  $\phi_{x-y}$  circle making such a path to fill the 2-sphere. They each reach two points of maximum differential potential and kinetic energy/wave momentum, or capacitance ( $E$ ) and inductance ( $M$ ), along the path which create a capacitive and inductive moment that circulate as  $\theta$ , as shown in the following Diagrams 2-6. This results in an invariant inherent Hamiltonian and Lagrangian for the particle and is responsible for all the fundamental quantum properties.

As shown in Diagrams 0 & 1, fixed orthogonal axes are referenced in upper case and the corresponding positions labeled in lower case on the 2-sphere represent the central cell previously discussed after initial torsion strain. It is understood in the following description that any designation of a property being spatially fixed or stationary over time is relative to the dynamics of the system under discussion and is held to move with any translation or rotation of the overall system over multiple cycles of oscillation, which in terms of condensed matter is in the range of  $10^{24}$  hertz. It is not indicative of a fixed spacetime lattice substrate.

As an initial condition, the 2-sphere with central  $y-z$  disk, 1D, rotated about an arbitrary  $Y$  axis so that the initial  $+z$  aligns with the  $+X$  axis as shown and that initial  $+x$  is rotated anti-parallel to the  $Z$  axis. This results in torsion strain in the  $X-Z$  plane about the  $Y$  axis as shown as a result of the ongoing isotropic stress. Recoil stress acts to reduce the stress and strain by rotation in the  $Y-Z$  plane, normal to the twisted disk (disk selection and  $X-Z$  axis designation is arbitrary, for illustrative purpose, and could have been any great circle through the 2-sphere with the  $Y$  axis as a diameter), where  $+z$  and  $-z$  represent the points of maximum strain from the  $Z$  axis, the locus of torsion equilibrium. Such rotation of 1D,  $\phi$ , has a degree of freedom of rotation about  $+Z$ , and we have here shown it to be CCW (when facing the interior of the sphere from  $+Z$ .) This rotation initiates a spin,  $\theta$ , of 2S on the 1D edge CCW about  $+X$  at the same angular frequency as  $\phi$ , so that with each rotation of  $\phi$  and  $\theta$ , every point,  $d$ , on the circumference of 1D passes through the  $+/- V$  points on the  $X$  axis at maximum displacement and through the points of initial equilibrium,  $+/- K_d$ , at the points of maximum velocity and recoil wave momentum of the developed rotating torsion wave. Each and every  $d$  etches a distinct figure 8 strain path through the theoretical stationary space just above the “surface” of the rotationally oscillating 2S.

The points  $+/- V$  are the concentrated, sustained points of maximum potential electro-mechanical energy and the distributed, recurrent collection of  $+/- K_d$  points are the sustained loci of maximum kinetic electro-mechanical energy. They are also the loci of maximum and sustained charge at  $+/- V$  and of maximum

sustained current at  $\Sigma$ +/-  $K$ . The points +/-  $E$  and +/-  $M$  are points on the path of each  $d$  of maximum rate of capacitance or charge of potential energy in the direction of +/-  $V$  and of maximum rate of inductance or release of kinetic energy in the direction of +/-  $K$  respectively. Thus, this configuration constitutes a microscopic LC current, with inertia of the cell as the resistance component of the cycle.

As shown in Diagram 2 for the generated neutron, crossing the two points of equilibrium at +/-  $K$  for a given instant of the cycle into their corresponding instant +/-  $E$  produces an instant capacitive torque moment  $C_\varepsilon$  and crossing the two instant points of +/-  $M$  into their corresponding equilibrium +/-  $K$  produces an instant inductive torque moment  $L\mu$ . While each of the points  $E$  and  $M$  are fixed over short-range cycles of the system for each point  $d$ ,  $C_\varepsilon$  and  $L\mu$  rotate with  $\theta$  at the recoil wave speed,  $c$ . This rotational system creates a spin vector for the action of the system at  $S_L$  along with an anti-parallel magnetic moment,  $\mu$ , which is the result of the sustained rotation of  $\theta$ . This configuration explains the relationship between elemental charge at +/-  $V$  as a result of  $C_\varepsilon$  and the quantum magnetic field as a function of the rotating torque  $L\mu$ . The reason that there are no magnetic monopoles is immediately clear. In the presence of an external magnetic field  $B$ , the moment  $\mu$  aligns with  $B$  and the spin vector  $S_L$  precesses.

These torques in turn interact with the nodes and antinodes of the rotating oscillation as shown in the inset of the Neutron C-L Torques at the lower left of the figure. Note that the condition of all the torques is to advance the rotation of both  $\phi$  and  $\theta$ , making for an inherently unstable condition, given expansion of the manifold which drives the rotation. Over time in response to expansion, the condition in the middle two figures at  $K$  results in a transmission of a small portion of the energy of the oscillation as the electron wave and a flip of the  $S_L$  spin generally anti-parallel to the  $L\mu$  torque occurs, as seen in Diagram 3. The lower left inset of this figure shows the new condition at  $K$  which explains the stability of the proton, as the induction torque  $L\mu$  is anti-parallel to and retards the rotation of  $\theta$  and the torque  $C_\varepsilon$  is anti-parallel to and retards the rotation of  $\phi$ , both effects giving stability to the system. Interestingly, for the anti-proton, Diagram 5, these same influences are both parallel, leading to the instability of the system.

For the electron, shown in Diagram 4, the induction torque  $L\mu$  is parallel to both rotations and the capacitive torque  $C_\varepsilon$  is anti-parallel to both, indicative of the charge and the fact that under expansion, the cosmos is in the process of converting the concentrated elastic potential energy density of the manifold to the distributed kinetic energy of elemental and molecular interaction on both a plasma stellar and condensed matter terrestrial level. Analysis of this modeling produces observables for particle mass, spin, charge, moment, ordinary and anti-matter configurations that are consistent with observed data without the addition of extraneous free parameters. A hint at the nature of the quark phenomenology of baryons can be found, especially in conjunction with the spin and charge tables. Note that the filled and open dots preceding the values of columns 4 through 7 of those tables indicate a centripetal and counter-centripetal sense for the cross-products on each of the listed points as defined at the top of each column.

We will next analyze this stress and strain configuration and how it connects with established thinking about space and time, to show that it naturally and necessarily includes quantum gravity, giving us a complete picture for theoretical physical understanding and its relevance for an understanding of cold fusion.



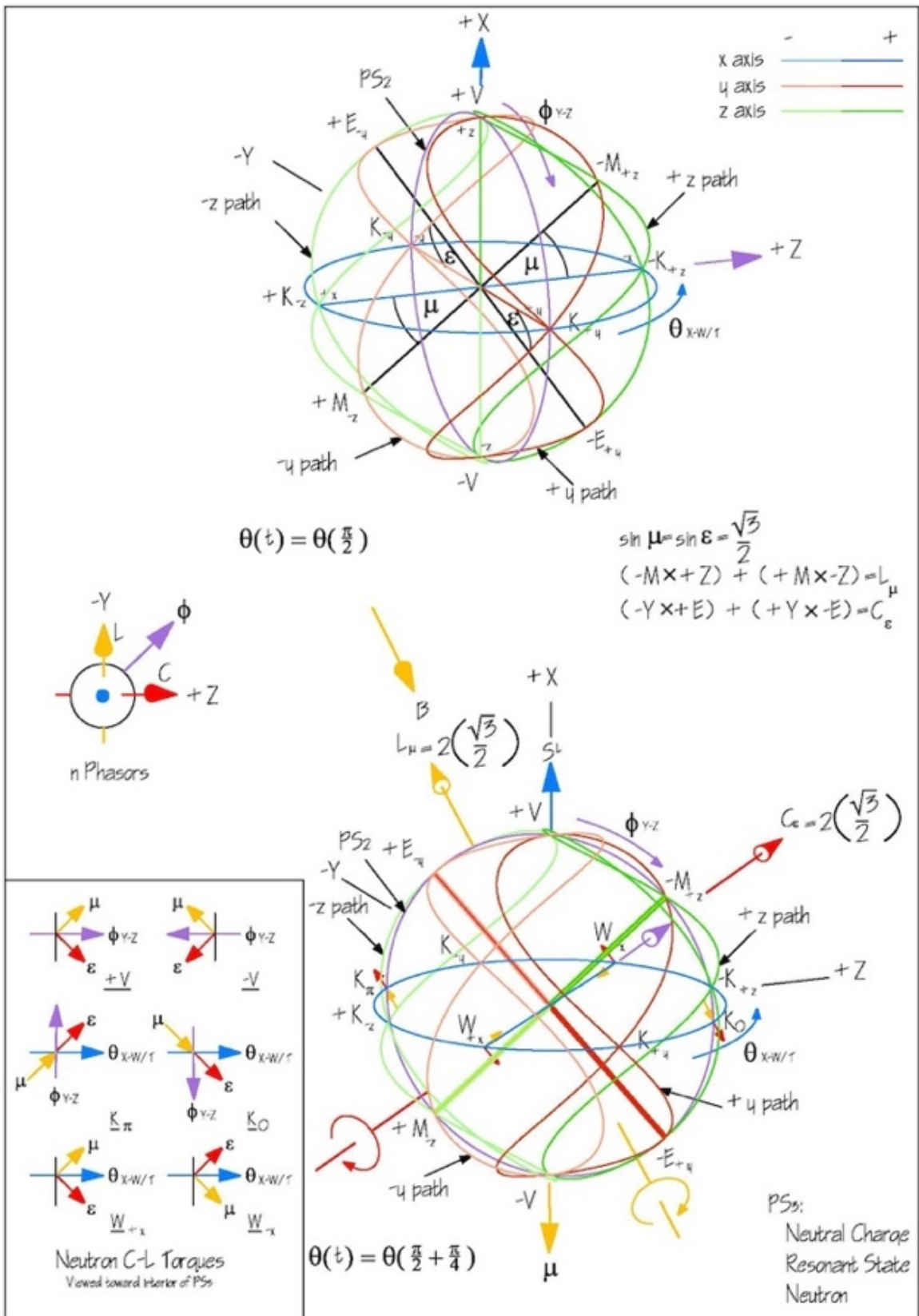


Diagram 2 - Neutron Oscillation

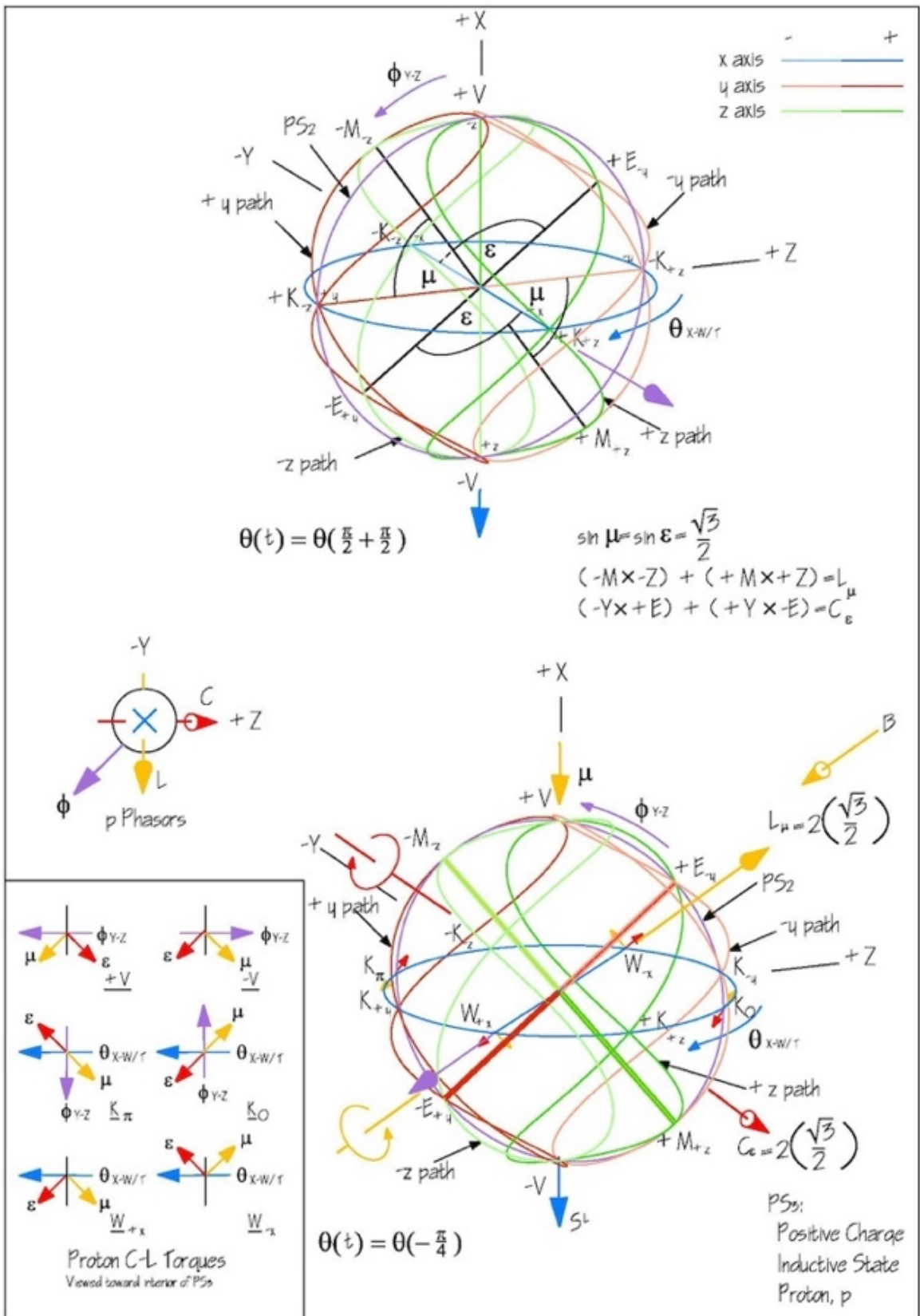


Diagram 3 - Proton Oscillation

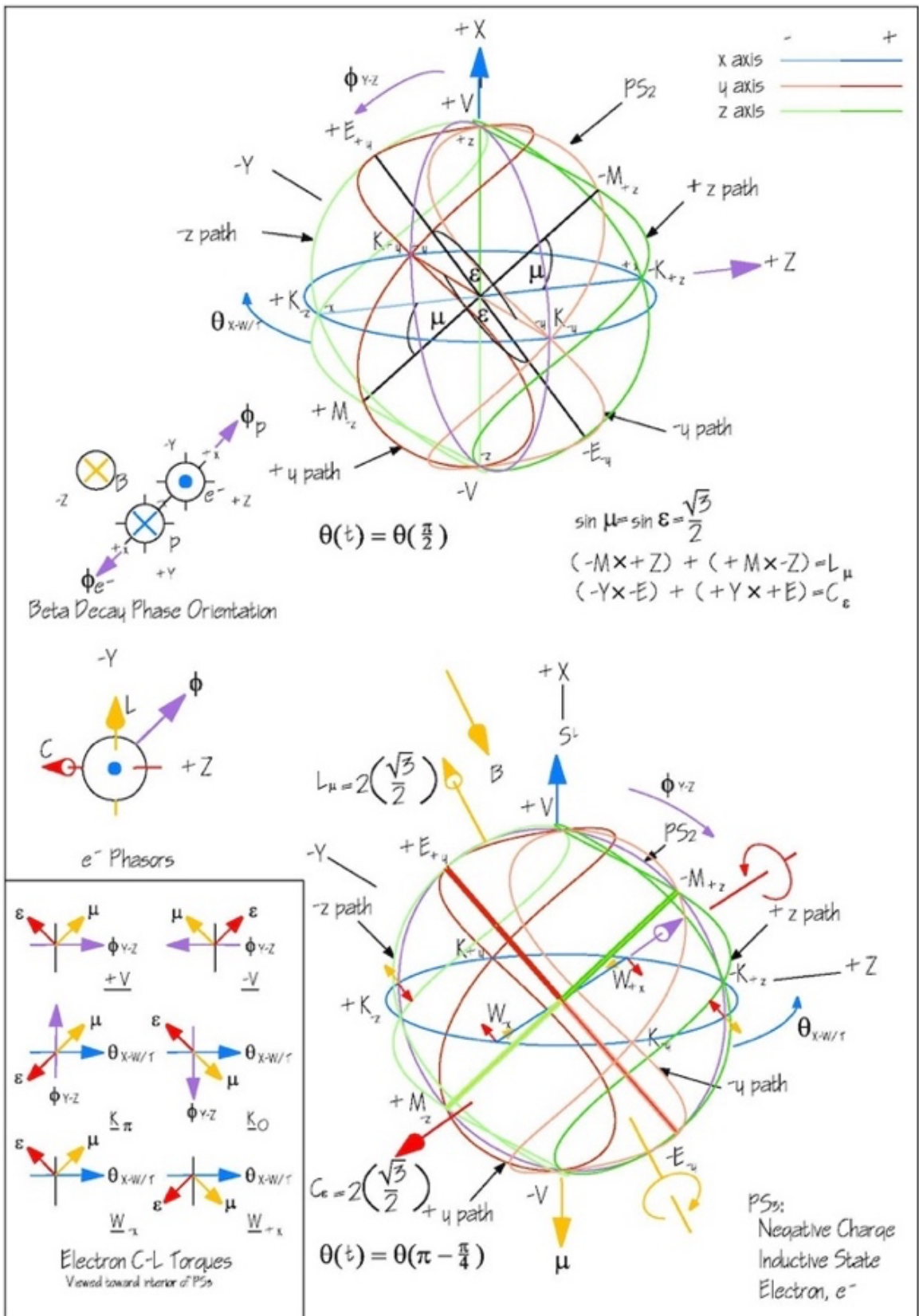


Diagram 4 - Electron Oscillation

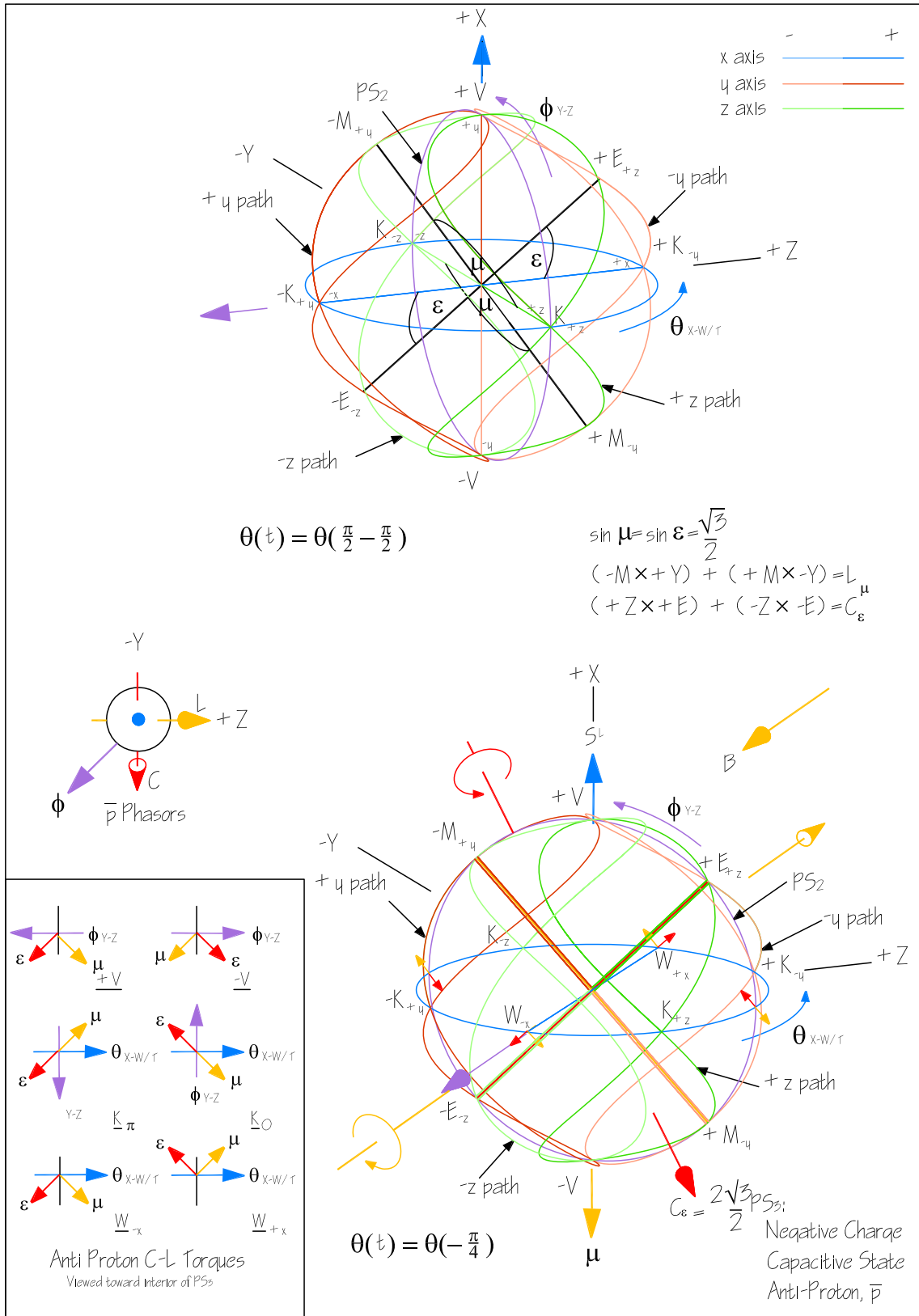


Diagram 5 – Anti-Proton Oscillation

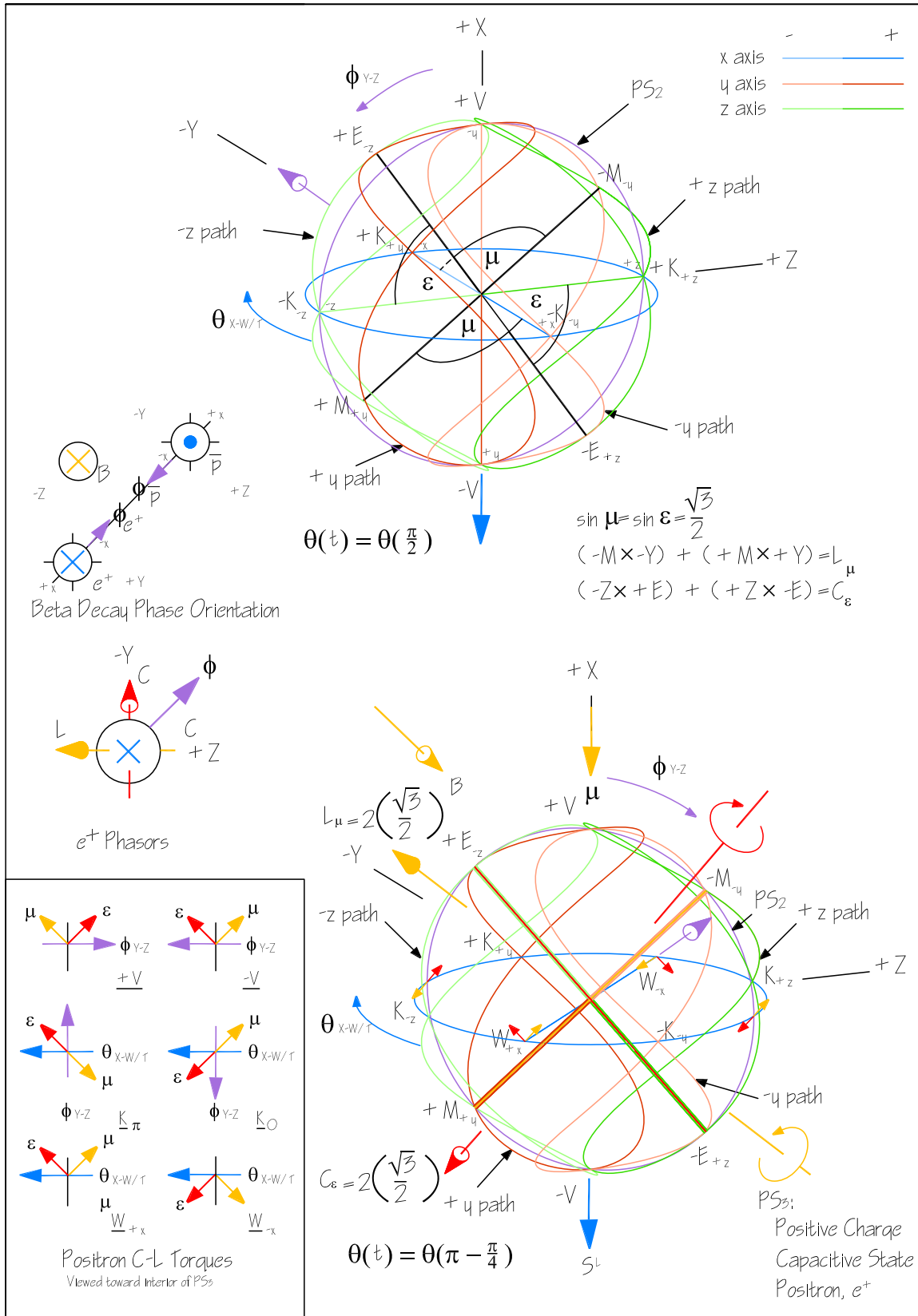


Diagram 6 – Positron Oscillation

	1	2	3	4	5	6	7	8	
Diagram, Node/Antinode, Rotation	$\mu \cdot \mathcal{E}$ $\mu, \mathcal{E} = \sqrt{\frac{2}{3}}$	$\mu \cdot$ Into $\theta, \phi$	$\mathcal{E} \cdot$ Into $\theta, \phi$	$S = \mu \times \mathcal{E}$ $\mu, \mathcal{E} = \sqrt{\frac{2}{3}}$	$\mu \times$ Into $\theta, \phi$	$\mathcal{E} \times$ Into $\theta, \phi$	$q = \frac{S}{ S } [T(\mu \times + \mathcal{E} \times)]$ $T = \frac{\sqrt{3}}{2}$	Total Charge $q_{W-}, q_{W+}$ $q_{V\pm}, q_{V\mp}$	
<b>Diagram 2 – Neutron</b>	$W_{+x} \square \theta$	0	$+\frac{1}{\sqrt{3}}$	$+\frac{1}{\sqrt{3}}$	$\bullet \frac{2}{3}$	$\bullet \frac{1}{\sqrt{3}}$	$\circ \frac{1}{\sqrt{3}}$	$\bullet 1 \left( \bullet \frac{1}{2} + \circ \frac{1}{2} \right) = 0$	
	$W_{-x} - \theta$	0	$+\frac{1}{\sqrt{3}}$	$+\frac{1}{\sqrt{3}}$	$\circ \frac{2}{3}$	$\circ \frac{1}{\sqrt{3}}$	$\bullet \frac{1}{\sqrt{3}}$	$\circ 1 \left( \circ \frac{1}{2} + \bullet \frac{1}{2} \right) = 0$	0
	$K_o - \theta$	$+\frac{2}{3}$	$+\frac{1}{\sqrt{3}}$	$+\frac{1}{\sqrt{3}}$	0	$\circ \frac{1}{\sqrt{3}}$	$\circ \frac{1}{\sqrt{3}}$	0	
	$K_\pi - \theta$	$+\frac{2}{3}$	$+\frac{1}{\sqrt{3}}$	$+\frac{1}{\sqrt{3}}$	0	$\bullet \frac{1}{\sqrt{3}}$	$\bullet \frac{1}{\sqrt{3}}$	0	
	$K_o - \phi$	$+\frac{2}{3}$	$+\frac{1}{\sqrt{3}}$	$+\frac{1}{\sqrt{3}}$	0	$\bullet \frac{1}{\sqrt{3}}$	$\bullet \frac{1}{\sqrt{3}}$	0	
	$K_\pi - \phi$	$+\frac{2}{3}$	$+\frac{1}{\sqrt{3}}$	$+\frac{1}{\sqrt{3}}$	0	$\circ \frac{1}{\sqrt{3}}$	$\circ \frac{1}{\sqrt{3}}$	0	
	$+V - \phi$	0	$+\frac{1}{\sqrt{3}}$	$+\frac{1}{\sqrt{3}}$	$\bullet \frac{2}{3}$	$\bullet \frac{1}{\sqrt{3}}$	$\circ \frac{1}{\sqrt{3}}$	$\bullet 1 \left( \bullet \frac{1}{2} + \circ \frac{1}{2} \right) = 0$	
	$-V - \phi$	0	$+\frac{1}{\sqrt{3}}$	$+\frac{1}{\sqrt{3}}$	$\circ \frac{2}{3}$	$\circ \frac{1}{\sqrt{3}}$	$\bullet \frac{1}{\sqrt{3}}$	$\circ 1 \left( \circ \frac{1}{2} + \bullet \frac{1}{2} \right) = 0$	[0]
<b>Diagram 3 – Proton</b>	$W_{+x} - \theta$	0	$-\frac{1}{\sqrt{3}}$	$+\frac{1}{\sqrt{3}}$	$\bullet \frac{2}{3}$	$\bullet \frac{1}{\sqrt{3}}$	$\bullet \frac{1}{\sqrt{3}}$	$\bullet 1 \left( \bullet \frac{1}{2} + \bullet \frac{1}{2} \right) = +1$	
	$W_{-x} - \theta$	0	$-\frac{1}{\sqrt{3}}$	$+\frac{1}{\sqrt{3}}$	$\circ \frac{2}{3}$	$\circ \frac{1}{\sqrt{3}}$	$\circ \frac{1}{\sqrt{3}}$	$\circ 1 \left( \circ \frac{1}{2} + \circ \frac{1}{2} \right) = +1$	+1
	$K_o - \theta$	$-\frac{2}{3}$	$-\frac{1}{\sqrt{3}}$	$+\frac{1}{\sqrt{3}}$	0	$\circ \frac{1}{\sqrt{3}}$	$\bullet \frac{1}{\sqrt{3}}$	0	
	$K_\pi - \theta$	$-\frac{2}{3}$	$-\frac{1}{\sqrt{3}}$	$+\frac{1}{\sqrt{3}}$	0	$\bullet \frac{1}{\sqrt{3}}$	$\circ \frac{1}{\sqrt{3}}$	0	
	$K_o - \phi$	$-\frac{2}{3}$	$+\frac{1}{\sqrt{3}}$	$-\frac{1}{\sqrt{3}}$	0	$\circ \frac{1}{\sqrt{3}}$	$\bullet \frac{1}{\sqrt{3}}$	0	
	$K_\pi - \phi$	$-\frac{2}{3}$	$+\frac{1}{\sqrt{3}}$	$-\frac{1}{\sqrt{3}}$	0	$\bullet \frac{1}{\sqrt{3}}$	$\circ \frac{1}{\sqrt{3}}$	0	
	$+V - \phi$	0	$+\frac{1}{\sqrt{3}}$	$-\frac{1}{\sqrt{3}}$	$\circ \frac{2}{3}$	$\bullet \frac{1}{\sqrt{3}}$	$\bullet \frac{1}{\sqrt{3}}$	$\circ 1 \left( \bullet \frac{1}{2} + \bullet \frac{1}{2} \right) = -1$	
	$-V - \phi$	0	$+\frac{1}{\sqrt{3}}$	$-\frac{1}{\sqrt{3}}$	$\bullet \frac{2}{3}$	$\circ \frac{1}{\sqrt{3}}$	$\circ \frac{1}{\sqrt{3}}$	$\bullet 1 \left( \circ \frac{1}{2} + \circ \frac{1}{2} \right) = -1$	$[-1] = -i1$
<b>Diagram 4 – Electron</b>	$W_{+x} - \theta$	0	$+\frac{1}{\sqrt{3}}$	$-\frac{1}{\sqrt{3}}$	$\bullet \frac{2}{3}$	$\circ \frac{1}{\sqrt{3}}$	$\circ \frac{1}{\sqrt{3}}$	$\bullet 1 \left( \circ \frac{1}{2} + \circ \frac{1}{2} \right) = -1$	
	$W_{-x} - \theta$	0	$+\frac{1}{\sqrt{3}}$	$-\frac{1}{\sqrt{3}}$	$\circ \frac{2}{3}$	$\bullet \frac{1}{\sqrt{3}}$	$\bullet \frac{1}{\sqrt{3}}$	$\circ 1 \left( \bullet \frac{1}{2} + \bullet \frac{1}{2} \right) = -1$	-1
	$K_o - \theta$	$-\frac{2}{3}$	$+\frac{1}{\sqrt{3}}$	$-\frac{1}{\sqrt{3}}$	0	$\circ \frac{1}{\sqrt{3}}$	$\bullet \frac{1}{\sqrt{3}}$	0	
	$K_\pi - \theta$	$-\frac{2}{3}$	$+\frac{1}{\sqrt{3}}$	$-\frac{1}{\sqrt{3}}$	0	$\bullet \frac{1}{\sqrt{3}}$	$\circ \frac{1}{\sqrt{3}}$	0	
	$K_o - \phi$	$-\frac{2}{3}$	$+\frac{1}{\sqrt{3}}$	$-\frac{1}{\sqrt{3}}$	0	$\bullet \frac{1}{\sqrt{3}}$	$\circ \frac{1}{\sqrt{3}}$	0	
	$K_\pi - \phi$	$-\frac{2}{3}$	$+\frac{1}{\sqrt{3}}$	$-\frac{1}{\sqrt{3}}$	0	$\circ \frac{1}{\sqrt{3}}$	$\bullet \frac{1}{\sqrt{3}}$	0	
	$+V - \phi$	0	$+\frac{1}{\sqrt{3}}$	$-\frac{1}{\sqrt{3}}$	$\circ \frac{2}{3}$	$\bullet \frac{1}{\sqrt{3}}$	$\bullet \frac{1}{\sqrt{3}}$	$\circ 1 \left( \bullet \frac{1}{2} + \bullet \frac{1}{2} \right) = -1$	$[-1] = -i1$

$-V - \phi$	0	$+\frac{1}{\sqrt{3}}$	$-\frac{1}{\sqrt{3}}$	$\bullet\frac{2}{3}$	$\circ\frac{1}{\sqrt{3}}$	$\circ\frac{1}{\sqrt{3}}$	$\bullet\left(\frac{1}{2}+\circ\frac{1}{2}\right) = -1$	
-------------	---	-----------------------	-----------------------	----------------------	---------------------------	---------------------------	---	--

Table 1 – Charge and Spin Table for Ordinary Matter for C & L = 1

	1	2	3	4	5	6	7	8	
Diagram, Node/Antinode, Rotation	$\mu \cdot \mathcal{E}$ $\mu, \mathcal{E} = \sqrt{\frac{2}{3}}$	$\mu \cdot$ Into $\theta, \phi$	$\mathcal{E} \cdot$ Into $\theta, \phi$	$S = \mu \times \mathcal{E}$ $\mu, \mathcal{E} = \sqrt{\frac{2}{3}}$	$\mu \times$ Into $\theta, \phi$	$\mathcal{E} \times$ Into $\theta, \phi$	$q = \frac{S}{ \mathcal{E} } (\mu \times + \mathcal{E} \times)$ $T = \frac{\sqrt{3}}{2}$	Total Charge $q_{W-}, q_{W+}$ $q_{V\pm}, q_{V\mp}$	
<b>Diagram 2 – Neutron</b>	$W_{+x} \square \theta$	0	$+\frac{1}{\sqrt{3}}$	$+\frac{1}{\sqrt{3}}$	$\bullet\frac{2}{3}$	$\bullet\frac{1}{\sqrt{3}}$	$\circ\frac{1}{\sqrt{3}}$	$\bullet\left(\frac{1}{2}+\circ\frac{1}{2}\right) = 0$	
	$W_{-x} - \theta$	0	$+\frac{1}{\sqrt{3}}$	$+\frac{1}{\sqrt{3}}$	$\circ\frac{2}{3}$	$\circ\frac{1}{\sqrt{3}}$	$\bullet\frac{1}{\sqrt{3}}$	$\circ\left(\frac{1}{2}+\bullet\frac{1}{2}\right) = 0$	0
	$K_o - \theta$	$+\frac{2}{3}$	$+\frac{1}{\sqrt{3}}$	$+\frac{1}{\sqrt{3}}$	0	$\circ\frac{1}{\sqrt{3}}$	$\circ\frac{1}{\sqrt{3}}$	0	
	$K_{\pi} - \theta$	$+\frac{2}{3}$	$+\frac{1}{\sqrt{3}}$	$+\frac{1}{\sqrt{3}}$	0	$\bullet\frac{1}{\sqrt{3}}$	$\bullet\frac{1}{\sqrt{3}}$	0	
	$K_o - \phi$	$+\frac{2}{3}$	$+\frac{1}{\sqrt{3}}$	$+\frac{1}{\sqrt{3}}$	0	$\bullet\frac{1}{\sqrt{3}}$	$\bullet\frac{1}{\sqrt{3}}$	0	
	$K_{\pi} - \phi$	$+\frac{2}{3}$	$+\frac{1}{\sqrt{3}}$	$+\frac{1}{\sqrt{3}}$	0	$\circ\frac{1}{\sqrt{3}}$	$\circ\frac{1}{\sqrt{3}}$	0	
	$+V - \phi$	0	$+\frac{1}{\sqrt{3}}$	$+\frac{1}{\sqrt{3}}$	$\bullet\frac{2}{3}$	$\bullet\frac{1}{\sqrt{3}}$	$\circ\frac{1}{\sqrt{3}}$	$\bullet\left(\frac{1}{2}+\circ\frac{1}{2}\right) = 0$	
$-V - \phi$	0	$+\frac{1}{\sqrt{3}}$	$+\frac{1}{\sqrt{3}}$	$\circ\frac{2}{3}$	$\circ\frac{1}{\sqrt{3}}$	$\bullet\frac{1}{\sqrt{3}}$	$\circ\left(\frac{1}{2}+\bullet\frac{1}{2}\right) = 0$	[0]	
<b>Diagram 5 – Anti Proton</b>	$W_{+x} - \theta$	0	$+\frac{1}{\sqrt{3}}$	$-\frac{1}{\sqrt{3}}$	$\circ\frac{2}{3}$	$\bullet\frac{1}{\sqrt{3}}$	$\bullet\frac{1}{\sqrt{3}}$	$\circ\left(\frac{1}{2}+\bullet\frac{1}{2}\right) = -1$	
	$W_{-x} - \theta$	0	$+\frac{1}{\sqrt{3}}$	$-\frac{1}{\sqrt{3}}$	$\bullet\frac{2}{3}$	$\circ\frac{1}{\sqrt{3}}$	$\circ\frac{1}{\sqrt{3}}$	$\circ\left(\frac{1}{2}+\bullet\frac{1}{2}\right) = -1$	-1
	$K_o - \theta$	$-\frac{2}{3}$	$+\frac{1}{\sqrt{3}}$	$-\frac{1}{\sqrt{3}}$	0	$\circ\frac{1}{\sqrt{3}}$	$\bullet\frac{1}{\sqrt{3}}$	0	
	$K_{\pi} - \theta$	$-\frac{2}{3}$	$+\frac{1}{\sqrt{3}}$	$-\frac{1}{\sqrt{3}}$	0	$\bullet\frac{1}{\sqrt{3}}$	$\circ\frac{1}{\sqrt{3}}$	0	
	$K_o - \phi$	$-\frac{2}{3}$	$-\frac{1}{\sqrt{3}}$	$+\frac{1}{\sqrt{3}}$	0	$\circ\frac{1}{\sqrt{3}}$	$\bullet\frac{1}{\sqrt{3}}$	0	
	$K_{\pi} - \phi$	$-\frac{2}{3}$	$-\frac{1}{\sqrt{3}}$	$+\frac{1}{\sqrt{3}}$	0	$\bullet\frac{1}{\sqrt{3}}$	$\circ\frac{1}{\sqrt{3}}$	0	
	$+V - \phi$	0	$-\frac{1}{\sqrt{3}}$	$+\frac{1}{\sqrt{3}}$	$\bullet\frac{2}{3}$	$\bullet\frac{1}{\sqrt{3}}$	$\bullet\frac{1}{\sqrt{3}}$	$\bullet\left(\frac{1}{2}+\bullet\frac{1}{2}\right) = +1$	
$-V - \phi$	0	$-\frac{1}{\sqrt{3}}$	$+\frac{1}{\sqrt{3}}$	$\circ\frac{2}{3}$	$\circ\frac{1}{\sqrt{3}}$	$\circ\frac{1}{\sqrt{3}}$	$\circ\left(\frac{1}{2}+\circ\frac{1}{2}\right) = +1$	[+1] = +i1	
<b>Diagram 6 – Positron</b>	$W_{+x} - \theta$	0	$-\frac{1}{\sqrt{3}}$	$+\frac{1}{\sqrt{3}}$	$\circ\frac{2}{3}$	$\circ\frac{1}{\sqrt{3}}$	$\circ\frac{1}{\sqrt{3}}$	$\circ\left(\frac{1}{2}+\circ\frac{1}{2}\right) = +1$	
	$W_{-x} - \theta$	0	$-\frac{1}{\sqrt{3}}$	$+\frac{1}{\sqrt{3}}$	$\bullet\frac{2}{3}$	$\bullet\frac{1}{\sqrt{3}}$	$\bullet\frac{1}{\sqrt{3}}$	$\bullet\left(\frac{1}{2}+\bullet\frac{1}{2}\right) = +1$	+1
	$K_o - \theta$	$-\frac{2}{3}$	$-\frac{1}{\sqrt{3}}$	$+\frac{1}{\sqrt{3}}$	0	$\circ\frac{1}{\sqrt{3}}$	$\bullet\frac{1}{\sqrt{3}}$	0	
	$K_{\pi} - \theta$	$-\frac{2}{3}$	$-\frac{1}{\sqrt{3}}$	$+\frac{1}{\sqrt{3}}$	0	$\bullet\frac{1}{\sqrt{3}}$	$\circ\frac{1}{\sqrt{3}}$	0	
	$K_o - \phi$	$-\frac{2}{3}$	$-\frac{1}{\sqrt{3}}$	$+\frac{1}{\sqrt{3}}$	0	$\bullet\frac{1}{\sqrt{3}}$	$\circ\frac{1}{\sqrt{3}}$	0	
	$K_{\pi} - \phi$	$-\frac{2}{3}$	$-\frac{1}{\sqrt{3}}$	$+\frac{1}{\sqrt{3}}$	0	$\circ\frac{1}{\sqrt{3}}$	$\bullet\frac{1}{\sqrt{3}}$	0	

$+V - \phi$	0	$-\frac{1}{\sqrt{3}}$	$+\frac{1}{\sqrt{3}}$	$\bullet \frac{2}{3}$	$\bullet \frac{1}{\sqrt{3}}$	$\bullet \frac{1}{\sqrt{3}}$	$\bullet \left( \frac{\frac{1}{2} + \frac{1}{2}}{2} \right) = +1$	$[+1] = +i1$
$-V - \phi$	0	$-\frac{1}{\sqrt{3}}$	$+\frac{1}{\sqrt{3}}$	$\circ \frac{2}{3}$	$\circ \frac{1}{\sqrt{3}}$	$\circ \frac{1}{\sqrt{3}}$	$\circ \left( \frac{\frac{1}{2} + \frac{1}{2}}{2} \right) = +1$	

Table 2 – Charge and Spin Table for Anti Matter for C & L =1

## 2c — Geometric Considerations of Rotational Oscillation and Beta Decay

Electrical charge (conventionally negative) is a transmission of wave momentum as will be described in the following. In the case of the neutron, the rotational oscillation sets up a wave mechanical analogy of an LC current, where the sustained maintenance of a maximum potential energy constitutes charge and the sustained maximum wave kinetic energy constitutes a current sustained within the discrete wave form of the neutron. The potential energy of this charge is therefore concentrated in the  $+/- V$  poles of the oscillation and its maximum kinetic energy at  $+/- K$  as they move around the  $\theta$  circle. Ongoing expansion of the manifold leads to a decrease in inertial density in the environment around the wave form and a transmission of the kinetic charge which is localized or focused in the transmitted wave node as a negative charge.

In order for the energy of beta decay, which is quantified as the mass of the electron, to be transmitted from the neutron waveform, the density and impedance at its boundary must decrease sufficient to permit that mass-energy to pass. The electron mass,  $m_e$ , is determined according to geometric constraints of the neutron oscillation and is approximately 0.000543867 . . . of the neutron mass,  $m_0$ .

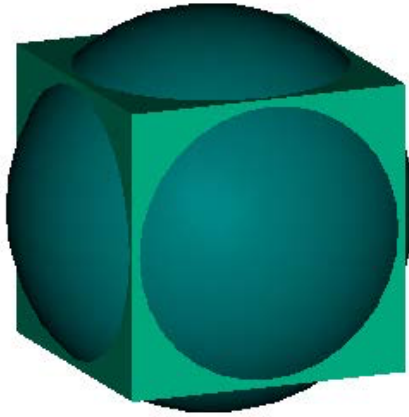


Figure 9

For an intuitive approach, the above figure shows a concentric sphere and cube which have equal individual surface areas. Assuming a sphere of radius  $r_0$  and area  $A_s$  and a corresponding cube with area  $A_c$  and edge length  $l_c$ , we have

$$\begin{aligned}
 A_s &= 4\pi r_0^2 = 4\pi = 6l_c^2 = A_c \\
 l_c / r_0 &= \sqrt{\frac{2}{3}\pi} = 1.4472\dots
 \end{aligned}
 \tag{1.34}$$

Tension stress on the surface of each would be equal, though the sphere represents isotropic stress while the cube represents a breakdown of the orthogonal components of such stress in keeping with the above development. The points midway along each cubic edge are loci of closest stress/strain equivalence between cube and sphere. They are also the points of optimal shear stress and strain in the rotational oscillation, as evidenced by the power moments,  $E$  and  $M$ . Such stress force operates in an oscillatory manner toward a leading adjacent vertex, directed by the two resultant torques,  $C$  and  $L$ , aligned with two of the cubic diagonals, toward one or the other of the two vertices beyond the leading adjacent one. These vertices also represent the rotating direction of expansion stress of  $T_0$ .



Over time the length of the moments vary as  $\delta r_0$ , in the context of an expanding spacetime, generally in an increasing direction represented by the vertices. The edge of the cube represents a limit for the increase in the moments, which is reflected by an increase in  $C$  and  $L$  and their orthogonal vector representations  $\varepsilon$  and  $\mu$  in the Spin Diagrams and Tables. The result is an increase in the cross-product along the  $W_{+x} - W_{-x}$  axis for  $\phi$ , an advance of the moments and a transmission of energy and power at that  $W_{-x}$  node as beta decay, where  $\delta r_0^2$  represents the relative energy and therefore mass of the transmitted oscillation.

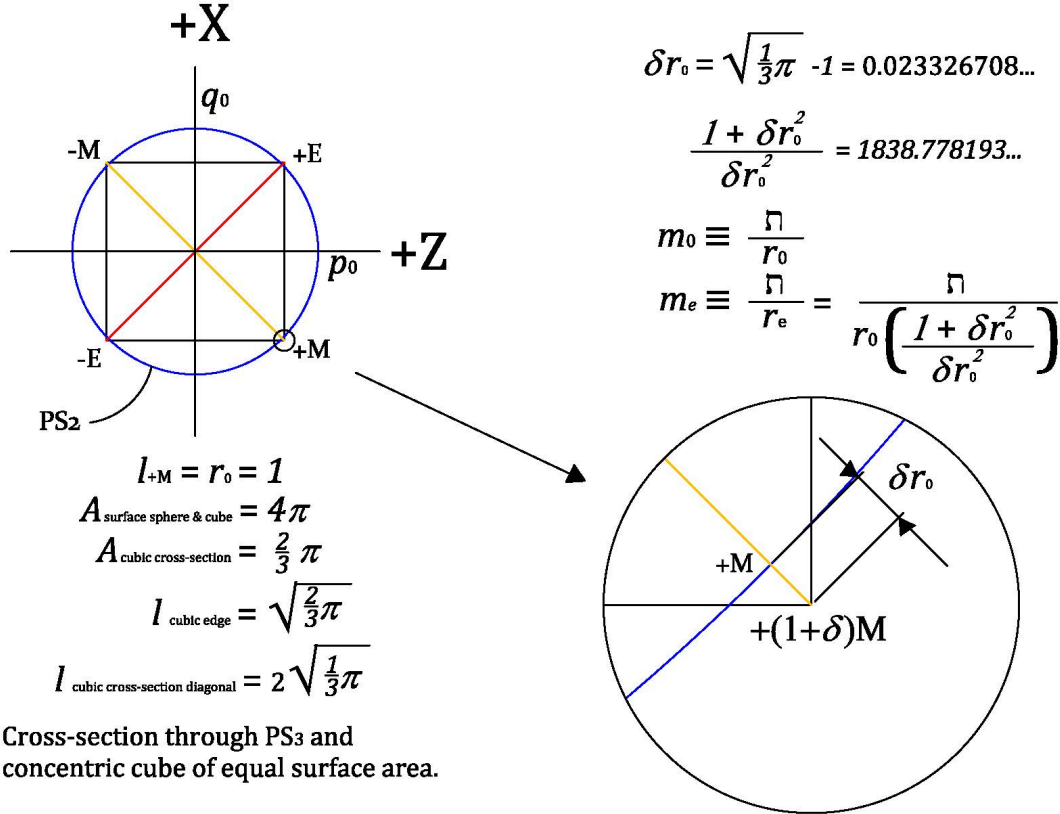


Figure 10

This figure shows a cross-section through the developed 2-sphere structure at the X-Z plane, so that the moments  $\pm E$  and  $\pm M$  are aligned with the four half diagonals of the cubic cross-section. This indicates the moments rotating in alignment with the mid points of two of the four edges of the upper and lower cubic faces. Each half diagonal length is therefore  $\sqrt{\frac{\pi}{3}}$  to the parallel moment length (not strength) of  $r_0$  of 1.

The square of the differential  $\delta r_0$  is reflected in the cross-product of the differential values of  $\varepsilon$  and  $\mu$  as

$$\delta r_0 = \sqrt{\frac{\pi}{3}} - 1 = 0.023326708\dots \quad (1.35)$$

$$\delta r_0^2 = 0.0005441353061\dots \quad (1.36)$$

The ratio of the differential stress to the augmented total according to the resulting strain is

$$\frac{\delta r_0^2}{1 + \delta r_0^2} = 0.0005438393841\dots \quad (1.37)$$

which when inverted is

$$\frac{1 + \delta r_0^2}{\delta r_0^2} = 1838.778193... \quad (1.38)$$

The 2010 CODATA ratio of the electron to neutron mass is 0.00054386734461(32) or inverted 1838.6836605(11). While outside the stated standard uncertainty shown here, the ratio derived here is within  $2.8... \times 10^{-8}$  of the CODATA ratio. Since mass computation presumably uses Newton's gravitational constant somewhere in the standardization of mass and weight, and given that the relative standard uncertainty of that constant at  $1.2 \times 10^{-4}$  is relatively large, it appears that (1.37) and (1.38) are within the relative standard uncertainty of the neutron-electron mass ratio.

## 2d — Derivation of Beta Decay as a Function of the Hubble Rate

Conventionally, the reduced Compton wavelength of the electron is related to the electron mass and as indicated as a portion of the neutron mass by (1.37) as

$$\tilde{\lambda}_{C,e} = r_e = \frac{\hbar}{cm_e} = \frac{\hbar}{m_e} = \frac{m_0 r_0}{m_e} \quad (1.39)$$

According to this modeling, the mass density within the boundary of the fundamental rotational oscillation is constrained by that oscillation while the region outside the boundary that starts as the interstitial areas between oscillation boundaries decreases with manifold expansion. The rotational oscillation as defined in (1.20) is then responsible for the particle interactions that result in the large aggregations of stellar and galactic matter, while the interstitial areas span the space between particles and define the large voids between the webs of galactic matter. At a minimum the differential change in inertial density of the manifold required for beta-decay represents a loss of potential mass-energy from the region exterior to the neutron oscillation nodes equal to and eventually replaced by that of the transmitted electron by beta-decay from the neutron mass or

$$d\lambda_0 = \frac{\hbar}{cr_e^2} = \frac{\hbar}{r_e^2} = \frac{1}{c^2} \hbar \omega_e^2 = \frac{1}{c^2} \tau_e, \quad (1.40)$$

where  $\omega_e$  is the rest mass oscillatory frequency of the electron given by

$$\omega_e = \frac{\theta_e}{t_e} = \frac{c}{r_e} = \frac{c}{\tilde{\lambda}_{C,e}} \quad (1.41)$$

and  $\tau_e$  is the characteristic wave force of that oscillation. The subscript  $e$  in this regard can be thought of as representing the electron, but as a differential value can also stand for the effect of ‘expansion’ or an ‘emergent’ condition.

The differential density in the second term of (1.40) represents the decrease in inertia over the distance of a wavelength required to generate a waveform of such mass; the mass of an electron as a differential value distributed over a characteristic differential angular wavelength which we can think of as the initial ground state orbital of an electron in a hydrogen atom; it is stated without further analysis that this value divided by the fine structure constant gives the Bohr radius of the hydrogen atom. For the wave speed to be invariant, the differentials in (1.41) must be equally contravariant, which means that the differential length and time must vary proportionally so that with expansion the wave speed,  $c_e$ , is invariant as

$$c_0 = r_e \omega_e = r_e \frac{\theta_0}{t_e} = \frac{r_e}{t_e} = \frac{dr_0}{dt_0} = c_e. \quad (1.42)$$

For the wave speed to remain invariant with expansion, the unit time standard, with the addition of the differential time standard, must strain as well as

$$c_0 = \frac{r_0}{t_0} = \frac{r_0 + dr_0}{t_0 + dt_0} = \frac{r_e}{t_e} = c_e. \quad (1.43)$$

This simply says that the wave speed over the distance  $dr_0$  is the same as it is over the distance  $r_0$ , and takes a proportional amount of time, whether  $dr_0$  is much less than or much greater than  $r_0$ , and whether  $r_e = dr_0$  or  $r_e = r_0 + dr_0$ . Thus, if a unit of distance, natural or arbitrary, increases with expansion of the manifold,

say where a new unit of distance  $r_{0e} = r_0 + dr_0$ , any corresponding unit of time,  $t_{0e}$ , must increase proportionally, so that the frequency proportionally decreases, and

$$c = r_0 \omega_0 = r_{0e} \omega_{0e}$$

$$\frac{r_{0e}}{r_0} = \frac{\omega_0}{\omega_{0e}} = \frac{t_{0e}}{t_0} \quad (1.44)$$

With separation of one of the wave speed components,  $c$ , in (1.40), which can be expressed as differentials, a change in inertial density over time is equal to a change in the mechanical impedance over distance as

$$\frac{d\lambda_0}{dt} = \frac{\tau_e}{c} \frac{1}{dr} = \frac{dZ_0}{dr} \quad (1.45)$$

We can rearrange this in keeping with (1.15) to show that the wave speed is given by the quotient of the change in impedance over the change in inertial density as

$$c_e = \frac{dr}{dt} = \frac{dZ_0}{d\lambda_0} = \frac{dm/dt_0}{dm/dr_0} = c_0 \quad (1.46)$$

Note that we are not using partial derivatives in this case, as  $dr_0$  and  $dt_0$  are dual functions of the expansion of the manifold as with the dual functions of wave number and wave frequency. In the next to last term of (1.46) the dimensional analysis indicates that mechanical impedance is a function of mass over time as inertial density is a function of mass over distance. While  $dm$  is a property of the manifold and should be the same for both the impedance and the density terms, and while it may be tempting to think so, it does not follow that  $dt = dt_0$  or that  $dr = dr_0$ , since the first of the differentials in each case represent properties of the manifold to be integrated to unit values  $t_0$  and  $r_0$ , while the second in each case are differentials of the unit standard or coefficients of unit strain, and are effectively second order differentials.

Since the values of the inertial constant as Planck's constant over the speed of light and the electron reduced Compton are well determined, we can solve for  $d\lambda_0$  in (1.40) and get

$$\frac{\Delta\lambda_0}{t_{0SI}} = 2.358970395\dots \times 10^{-18} \frac{kg/m}{s} \quad (1.47)$$

The change in density is due to a stretching of the spacetime manifold and not to a loss of energy/inertia within an arbitrary boundary of an expanding region, which is conserved, so this value represents a rate of change of the manifold strain, a dimensionless number, per second. This is essentially what the Hubble rate is, as a measure of spatial expansion, a dimensionless number, per second,  $H_0$ , experimentally calculated as roughly 72 to 76 km,  $\Delta R$ , per megaparsec per second. A megaparsec is  $3.0857\dots \times 10^{19}$  kilometers,  $R$ , so that the spacetime strain per second is given as a Hubble rate, customarily expressed as an expansion velocity per second per megaparsec,

$$H_0 = \frac{\Delta R}{t_{0SI} R} = \frac{\Delta R}{R} \Big/ t_{0SI} = \frac{73km}{3.0857\dots \times 10^{19} km} \Big/ s \cong 2.3657\dots \times 10^{-18} s^{-1} \quad (1.48)$$

This indicates that the Hubble rate as a spatial strain is capable of generating the force required for beta-decay. However, we would like something more precise, dimensionally correct, and analytically pleasing.

Returning to (1.45), we can transpose the time and length standard differentials as follows, where integrating the equation for the expansion change in length and time should give the resulting mass change in inertial density-impedance of the manifold

$$d\lambda_0 \int_{\text{unit-length}=0}^1 dr \equiv dZ_0 \int_{\text{unit-time}=0}^1 dt \quad (1.49)$$

$$\frac{\nabla}{r_e^2} dr_0 \equiv \frac{\nabla \omega_e^2}{r_e \omega_e} dt_0 = \frac{\nabla \omega_e}{r_e} dt_0$$

$$\frac{\nabla}{r_e^2} \left( \frac{t_e}{t_0} r_e \right) \equiv \frac{\nabla \omega_e}{r_e} \left( \frac{r_e}{r_0} t_e \right) \quad (1.50)$$

where the change in wavelength,  $r_e$ , due to expansion is modified by the time strain as

$$dr_0 = \frac{t_e}{t_0} r_e \quad (1.51)$$

and the change in corresponding time standard,  $t_e$ , due to expansion is modified by the length strain as

$$dt_0 = \frac{r_e}{r_0} t_e . \quad (1.52)$$

Both of these strains represent the Hubble rate,  $H_0$ , which we can see in this analysis is an acceleration and not a velocity, since it represents a continuous augmentation of a length or time unit standard. Using the CODATA SI values for the electron and neutron reduced Compton wavelength converted conceptually to rotational wave form radii,  $r_e$  and  $r_0$ , and related value from the electron angular frequency for time,  $t_e$ , we can solve for the change in time standard, which we will call the Hubble time standard,  $H_t$ , as

$$dt_0 = \frac{r_e}{r_0 \omega_e} = \frac{r_e}{r_0} \frac{t_0}{\theta_e} = \frac{r_e}{r_0} \frac{t_e}{\theta_0} = 2.36838769...x10^{-18} s = H_t \quad (1.53)$$

and for the change in the length standard, which we will call the Hubble length standard,  $H_r$ , as

$$dr_0 = \frac{\omega_0}{\omega_e} r_e = \frac{t_e}{t_0} r_e = 7.100247672...x10^{-10} m = H_r . \quad (1.54)$$

The length standard change must be normalized to the time standard by the distance of propagation at wave speed if we want to evaluate in the familiar SI time terms so that in keeping with (1.43) the dimensionless length strain per second is equal to the time strain per second which is equal to the Hubble rate as

$$H_0 = \frac{dr_0}{299,792,458m} / s = \frac{dt_0}{1s} / s = 2.36838769...x10^{-18} / s \quad (1.55)$$

Given the constraints of (1.45) , (1.46) and (1.49) we find that the product of (1.47) and the Hubble length integral of (1.54) gives the fundamental mass of the system,  $dm$ , that of the neutron, which is the product of the Hubble time integral and the change in the mechanical impedance,  $dZ_0$ , or

$$d\lambda_0 \int_{H_r=0}^1 dr_0 \equiv dZ_0 \int_{H_t=0}^1 dt_0 = dm = m_0 \quad (1.56)$$

This is the threshold rate of expansion required to drive and sustain the condensed matter quantum system, that of the proton, the electron, and the “missing” mass of beta decay, equal to the mass of the neutron or

$$m_0 = m_n = m_p + m_e + \Delta m_{n-(p+e)} . \quad (1.57)$$

In natural units of mass the three values on the right hand side of the equation are simply the ratios of the particle mass or difference with respect to that of the neutron or

$$1.0 = 0.998623471\dots + 0.000543867\dots + 0.000832661\dots \quad (1.58)$$

The following table gives this model’s analytical view of this condition. The top row states the value of the density and impedance differentials due to expansion based on the wave properties of the electron as stated above in (1.49) and whose quotient is the wave speed,  $c$ . This is relative to an initial condition at neutron density of

$$\left( c_0 = \frac{Z_0}{\lambda_0} = \frac{2.3908\dots \times 10^{-3} \text{ kg/s}}{7.9751\dots \times 10^{-12} \text{ kg/m}} \right) = \left( c_e = \frac{dZ_0}{d\lambda_0} = \frac{7.0720\dots \times 10^{-10} \text{ kg/s}}{2.3589\dots \times 10^{-18} \text{ kg/m}} \right) \quad (1.59)$$

The strain rates for a natural length and time scale in the second and third columns,  $H_r$  and  $H_t$ , are required to drive the equivalent integral mass values in the first column, given the stated differential density and impedance values. The corresponding Hubble rates,  $H_0$ , (1.55), expressed in conventional terms as kilometers per second per megaparsec, are tabulated in the fourth column. The fifth column gives the identity of the ratio between the differential density and  $H_t$  and the differential impedance and  $H_r$  for the pertinent strain rates. The sixth column gives the ratio of the product of the strains and the resulting mass integrals in accordance with the inverse of the following differential equation

$$\frac{d\lambda_0}{dt_0} = \frac{dZ_0}{dr_0} = \frac{dm_0}{dr_0 dt_0} . \quad (1.60)$$

The relationship of these strains represents an acceleration of  $H_0$  over time, rather it indicates that the Hubble rate is in fact an acceleration and not a velocity. In the context of a model of physical particles as ontologically wave forms with an inherent coupling to cosmic spacetime, as seems required by general relativity, an accelerating spacetime expansion strain implies a differential force on the waveforms, as developed previously. From the perspective of dimensional analysis in column 5, any value greater than 1 indicates a predominance of inertia over changes in space and time and a lack of sufficient force to effect beta decay, much less drive the fundamental,  $m_0$ , while values less than 1 indicate a capacity for those spacetime variables to produce changes in the inertial state. With respect to column 6, anything less than 1 is insufficient to drive the whole system as indicated by (1.57) and (1.58). This means that a Hubble rate of 73.0813 km is the threshold required, not just for beta decay, but to drive the cosmos. A recent study by Riess et al determined the most accurate Hubble to date at  $H_0 = 74.03 \pm 1.42 \text{ km s}^{-1} \text{ Mpc}^{-1}$ .

The row marked ‘*Planck*’ is generated based on a Hubble rate of  $67.74 \pm 0.46 \text{ km s}^{-1} \text{ Mpc}^{-1}$  from a revised report by the European Space Agency Planck space telescope mission in 2015.

The final two rows show the two theoretical extremes that we might imagine, both evoked by the application of the Planck scale to the analysis. The first of these uses the Planck length and time as the differential values for the Hubble length and time as the smallest conceivable strain based on current theoretical thinking. The result is an inertia/spacetime ratio 25 orders of magnitude above that of unity, indicating an astronomical predominance of inertia over observed spacetime kinematics. The corresponding Hubble rate is the equivalent of  $1/10,000^{\text{th}}$  the neutron Compton wavelength per megaparsec per second and would be capable of moving only  $3.7e^{-53}$  kilograms. At the other extreme, to drive the Planck mass would require an expansion rate of approximately 30 megaparsecs per megaparsec per second, which is in the inflationary regime, but is not consistent with current observation.

	$d\lambda_0 = dm/dr$	$2.358970395 e^{-18} \text{ kg/m}$			
	$dZ_0 = dm/dt$	$7.072015331 e^{-10} \text{ kg/s}$			
Mass integrals with integration of $dr_0$ & $dt_0$	Strain values due to cosmic expansion needed to produce wave particle mass integrals shown		Effective Hubble rate (conventional) km/s/mps	Ratio of $\Delta$ Inertia to $\Delta$ Spacetime strain	Ratio of mass integral to $m_0$ $dr_0 dt_0 / dm_0$
	$H_r = dr_0$	$H_t = dt_0$	$H_0 = H_t$	$d\lambda_0 / H_t = dZ_0 / H_r$	$(d\lambda_0 * H_r) / m_0$
$m_0$	$7.10025 e^{-10}$	$2.36839 e^{-18}$	73.0813	0.996024	1.000000
$m_0 - m_e$	$7.09638 e^{-10}$	$2.36709 e^{-18}$	73.0413	0.996570	0.999456
$m_0 - \Delta m$	$7.09432 e^{-10}$	$2.36641 e^{-18}$	73.0203	0.996856	0.999167
$m_p = m_0 - (m_e + \Delta m)$	$7.09045 e^{-10}$	$2.36512 e^{-18}$	72.9805	0.997400	0.998623
<i>Eq. (1.47)</i>	$7.07202 e^{-10}$	$2.35897 e^{-18}$	72.7907	1.000000	0.996018
<i>Planck</i>	$6.58131 e^{-10}$	$2.19529 e^{-18}$	67.74	1.074560	0.926912
$\Delta m + m_e$	$9.77368 e^{-13}$	$3.26015 e^{-21}$	0.1006	723.5773	0.001376
$\Delta m$	$5.91209 e^{-13}$	$1.97206 e^{-21}$	0.0609	1196.1961	0.000832
$m_e$	$3.86157 e^{-13}$	$1.28808 e^{-21}$	0.0397	1831.3850	0.000543
		Mega Parsec = $3.08570 e^{19} \text{ km}$			
<i>Planck scale</i>					
$3.7 e^{-53}$	$1.61612 e^{-35}$	$5.3908 e^{-44}$	$1.66 e^{-24}$	$4.38 e^{25}$	$2.29 e^{-26}$
$m_{PL} = 2.17 e^{-8}$	$9.22696...e^9$	30.77784	$9.50 e^{20}$	$7.66 e^{-20}$	$1.30 e^{19}$

Table 3 — Relationship of Hubble rate and particle mass/energy

This modeling suggests a Hubble exponential strain rate of 73.0813 kilometers per megaparsec per second. That is, a unit of space and co-variant time are currently extended/dilated at this rate. The implication is that space and time are currently expanding exponentially, and such expansion drives the natural frequency as indicated by the conjugate of the frequency, wave number hence mass, as

$$m_0 = \hbar \kappa_0 = dZ_0 H_0 = d\lambda_0 c_0 H_0 \quad (1.61)$$

Thus, if the Hubble threshold rate of expansion is roughly 73 kilometers per second per mpc, this indicates that every local section of space is moving away from every other at approximately  $2.37 \times 10^{-18}$  meters per second per meter of separation. However, we would expect this expansion to show up primarily in the large voids between galactic filaments and clusters and not in the galactic environs or filaments of baryonic matter due to the counter effects of gravity and electromagnetism. It follows conventionally that inversion of this number would give us the approximate time since all the matter was at the same locale, though by no means a singularity, and that the universe has been expanding for  $4.22 \times 10^{17}$  seconds, which is roughly 13.4 billion years.

While this is generally portrayed as an absolute time, it is the position of this model that this figure represents the mean lifetime in the expansion process of the cosmos in a manner analogous to the inverse of a decay function, so that we can look backwards in time since the beginning of such expansion as if it were a decay function. As such, this number represents an expansion via a compounded augmentation of the scale of spacetime itself, as  $2.37 \times 10^{-18}$  meters per second per meter of separation, and not simply an extension of matter within that spacetime, and the following equation for the doubling of spacetime applies, in which: the Hubble rate,  $H_0$ , is the eigenvalue of the expansion process analogous in the inverse for past time as a decay rate;  $H_{mt}$  is the Hubble mean lifetime given by the inverse of  $H_0$ ; giving us the Hubble time or half-life,  $\tau_H$  as

$$\tau_H = \frac{\ln 2}{H_0} = H_{mt} \ln 2 = 2.92666... \times 10^{17} s \quad (1.62)$$

This indicates that space is doubling at a current rate of every 9.274 billion years, measured in terms of today's seconds. If we assume that the wavelength of the cosmic background radiation at approximately 5mm embodies that augmentation, while harkening back to a period of primal beta decay as indicated by the reduced Compton wavelength over  $2\pi$  of an electron, this represents a doubling of some 31 times, or

$$\frac{\ln\left(\frac{.005}{2\pi r_e}\right)}{\ln 2} = \frac{\ln 2.060... \times 10^9}{\ln 2} = 30.94... \text{ doublings} \quad (1.63)$$

a lifetime in terms of today's measure of time of roughly 287 billion years. If we extrapolate back on the same basis for the expansion over the scale of  $r_0$  to  $r_e$ , prior to beta-decay where it may or may not be applicable, we have an additional doubling of 10.84 times or

$$\frac{\ln(1838.6836...)}{\ln 2} = 10.84... \quad (1.64)$$

or a total number of instances of the Hubble time of 41.78 or 393.47 billion years in current time as

$$(2.927... \times 10^{17})(41.78...) = 1.2227... \times 10^{19} s \quad (1.65)$$

Finally, if we envision that a current expansion extent or factor,  $\kappa_{exp}$ , can be derived by a comparison of the Planck length and the neutron reduced Compton wavelength, to get the quotient as a dimensionless coefficient of expansion stress as with (1.33) which we can apply to an appropriate linear dimensional property, where we can use it for time in seconds or length in a normalized form as light-seconds

$$\kappa_{exp} = \frac{r_0}{l_p} = \sqrt{\frac{T_0}{dT_0}} = \sqrt{(d \ln T_0)^{-1}} = \frac{2.10019... \times 10^{-16} m}{1.61612... \times 10^{-35} m} = 1.29952... \times 10^{19} s \text{ or } ls \quad (1.66)$$

which is equivalent to 412 years or light years respectively, we have a close agreement with (1.65). Based on the assumption of  $\kappa_{exp}$  as a coefficient for length, which is doubling for every instance of the Hubble time, we can divide this figure in half, to get a cosmic extension,  $C_x$ , of the most recent Hubble time as 206 billion light years or in light seconds

$$C_x = 0.5(\kappa_{exp}) = 6.49763... \times 10^{18} ls \quad (1.67)$$

Dividing  $C_x$  by the Hubble time we get the rate of expansion across an extent of the cosmos over the most recent Hubble time. This indicates that the extremes of the cosmos are "receding" from each other at 22.20 times the speed of light as



$$\frac{C_x}{\tau_H} = \frac{6.49763... \times 10^{18} \text{ } l_s}{2.92666... \times 10^{17} \text{ } s} = 22.20c = \frac{(0.5)\kappa_{\text{exp}} H_0}{\ln 2} . \quad (1.68)$$

With respect to the Hubble time before the most recent period, the value of (1.67) would be halved with the Hubble time remaining the same and the expansion rate over that period would be  $11.10c$ , pointing to the observed acceleration of cosmic expansion.

However, if the speed of light is not invariant over time, but rather is continually being renormalized with expansion, so that time as determined by  $\tau_H$  is also halved, then  $22.20c$  is an invariant of the system. In such a case the Hubble mean lifetime of this interpretation is the comoving or cosmological age of the universe, where the units of time are scaled to the expansion extent of the universe. When the Hubble mean lifetime is interpreted as an inverse of a decay rate, then the cosmological or comoving time is represented as being of the order of (1.65) as the number of instances of doubling of scale times the Hubble time and the universe is best represented as a type of de Sitter universe which emerges from an initial locus of maximum density.

With respect to the period before beta-decay or the last scattering of the standard model cosmology, it is not clear from this extant modeling that rest mass quanta emerged from an initial big bang. Rather it appears likely that such matter emerges in an ongoing manner from a condition of maximum density, including from active galactic inertial centers, i.e. black holes which can be gravitational field sources as well as sinks, and their connecting filaments, in response to the tension stress of expansion, as evidenced by the observance of episodic gamma ray bursts of unknown origin, but attributable by some to active galactic nuclei. In this model, black holes are entities of maximum inertial density and not singularities and the event horizon as defined by an extreme Kerr metric represents a two dimensional locus at which the trajectory of all infalling particles becomes tangential as it approaches the speed of light, and the centripetal motion of the particles vanishes. At this point the inertial density of a particle can be absorbed into the mass of the black hole operating as a sink with the wave form smeared across the surface and/or recycled in its operation as a source by being spun up and ejected into one of the collimated jets as baryonic, and with beta decay, leptonic matter.

From this perspective, if we return to our original 2-D sphere heuristic, at the beginning of cosmic evolution once a threshold differential stress is reached radially across the manifold, the surface of the 2-sphere begins to move radially and to strain with attendant loss of density between macro-sections. These intervening areas, in a 3-D extrapolation, become the voids between galactic clusters and gas webbing that we find today. Spalling and instances of quantum oscillation occur at the peripheries of these voids. Given the preponderance of hydrogen and helium in the present-day universe it appears that such spalling is responsible for most free baryonic and leptonic matter which then circulates to form stars and galactic spaces around center points of gravitational mass, such centers being both without and with remaining inertial sources as active galactic nuclei. The voids continue to expand according to the Hubble rate, while the areas of congregated rest mass, of baryonic/leptonic matter, are not subject to this expansion due to the greater strength of the various quantum wave forces.

## 2e — The Missing Mass of Beta Decay

We are not quite through with our investigation. While the ratio of neutron-electron mass as developed here is compelling, there is still a matter of the missing mass of beta decay. According to the CODATA ratios, the difference between the neutron-electron mass ratio and proton-electron mass ratio is

$$\frac{m_n}{m_e} - \frac{m_p}{m_e} = 1838.6836\dots - 1836.1526\dots = 2.5310\dots \quad (1.69)$$

Since the relative mass of the electron in this case is 1, there is a relative mass or equivalent energy of 1.530... that is unaccounted for and sometimes referred to as the missing mass of beta decay. If it is assumed that mass is a property that is somehow bound up in the confines of a discrete particle, this is a puzzlement. However, if it is understood to be a measure of the resistance of stress to a straight-line force, therefore a measure of redirection of energy as wave action and of curvature of spacetime strain, the problem vanishes.

The entire waveform of a neutron and proton is confined within the nucleus of an atom in condensed matter and the particle wavelength, as represented by the reduced Compton wavelength, is bound by rotation of the oscillation as developed previously, so that the wave energy is bound to the transverse or anti symmetric component of the wave tensor, except for the relatively minor symmetric components of quantum gravity. The electron wave form has both rotational and translational components, particularly at the time of beta decay, so that the differential changes of exponential expansion stress which generate the decay and the beta particle or electron have both of these components. We can restate the last equation with a little more detail, where the inertial constant as developed previously is used to define mass,

$$\frac{\eta}{\tilde{\lambda}_{C,n}} - \frac{\eta}{\tilde{\lambda}_{C,p}} - \frac{\eta}{\tilde{\lambda}_{C,e_{ij}}} = 0 \quad (1.70)$$

The reduced Compton wavelength of the electron is written with subscripts,  $ij$ , to indicate the symmetric and antisymmetric components of the wave form.

Now consider the function

$$W(n) = \ln_0 e_n^n, \text{ where } \ln_n e_n^n = n \quad (1.71)$$

which is related to the Lambert  $W$  function, where  $n$  can be any real number, though we will only be considering the integers. The significant feature of this function is that it generates a system of natural logs,  $\ln_n$ , and corresponding exponential bases,  $e_n$ , that can be used as normalizing factors, so that

$$\ln_n e_n = 1, \quad \ln_n e_{-n} = -1 \quad (1.72)$$

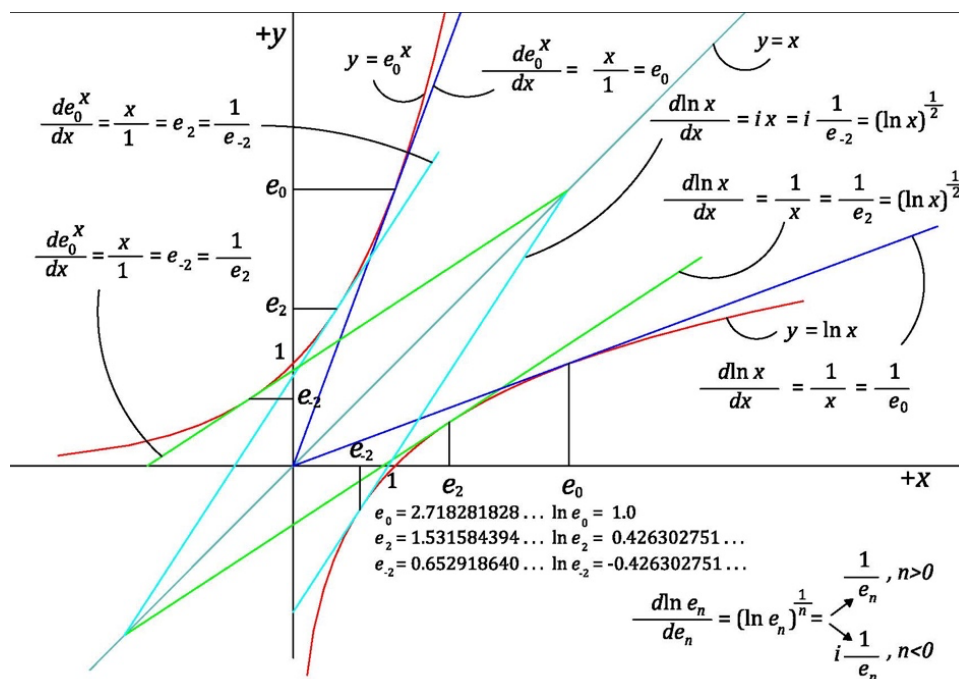
At  $n(0)$ , this is simply the natural log and exponential base, and

$$W(0) = \ln_0 e_0^0 = 0 \quad (1.73)$$

In the following Figure 11 we have graphed the significant portion of the natural log and exponential functions. Note the functions mirror each other along the line  $y = x$ , as do their derivatives. We can define the exponential base,  $e_0$ , on both  $x$  and  $y$  axes by the point on each function at which the lines (blue) whose slopes represent the derivatives intersect each other and the origin of the system. The only other instances of such intersection would be when the functions reach negative infinity along both axes, which of course they never do in the context of Euclidean space. They do on the Riemannian complex sphere, however.

The whole system of  $e_n$ , for  $n > 0$ , occurs in the range  $1 < x$  and  $y < e_0$ , and as  $n$  increases, the slope values converge while their intersection moves toward the negative infinities of both  $x$  and  $y$ . At the points on the curves corresponding to  $x = 1$  for the logarithmic and  $y = 1$  for the exponential, the derivatives of both

functions equal 1 and their slopes are parallel. (In terms of the Riemannian sphere, the slope lines for these derivatives (not shown here) actually form two ellipses about the spherical great circle  $x = y$ , tangent to a circle centered on the origin of radius  $r = 0.707\dots$  at  $(-0.5, +0.5)$  and  $(+0.5, -0.5)$  and approaching the  $\pm/\infty$  and  $\pm/\infty$  infinity intersection asymptotically.) As  $n$  decreases the slope intersections shift from negative to positive infinity at their  $x$  and  $y$  axis asymptotes. Thus  $n < 0$  occurs in the range  $0 < x$  and  $y < 1$ .



System of exponent bases  $e_n$ , shown for  $e_0$  and  $e_{\pm 2}$  where  $e_{-2} = e_2^{-1}$

Figure 11

$f(n)$	$n$	0	1	2	3	...	$\infty$
$e_n$		2.718281828..	1.763222834..	1.531584394..	1.419024454..		1
$e_{-n} = e_n^{-1}$		0.367879441..	0.567143291..	0.652918640..	0.704709490..		1
$e_n^n$		1	1.763222834..	2.345750756..	2.857390779..		$\infty$
$e_{-n}^n = e_n^{-n}$		1	0.567143291..	0.426302751..	0.349969632..		0
$\ln_0 e_n$		1	0.567143291..	0.426302751..	0.349969632..		0
$\ln_0 e_{-n}$		-1	-0.567143291..	-0.426302751..	-0.349969632..		0
$\ln_n e_n$		1	1	1	1		1
$\ln_n e_{-n}$		-1	-1	-1	-1		-1
$\ln_0 e_n^n$ $= W(n)$		0	0.567143291..	0.852605502..	1.049908893..		$\infty$
$\ln_0 e_{-n}^n$ $= W(-n)$		0	-0.567143291..	-0.852605502..	-1.049908893..		$-\infty$
$\ln_n e_n^n$		0	1	2	3		$\infty$
$\ln_n e_{-n}^n$		0	-1	-2	-3		$-\infty$

Table 4

For the range  $e_0 < x$  and  $y < +\infty$ , the slopes of the two derivatives diverge as  $x$  increases, and there are no real subscript functions of  $e_n$ . Note that for the range  $n < 0$ , however, according to the derivative of the natural log with respect to a change in  $x$ , the slope has imaginary sense, which generally indicates a rotation of some manner. The table above shows the results of this function for the first three integers, and an assumption of results carried to infinity. The table below shows related results with the introduction of imaginary sense to the various function.

$n$	$f(n)$	$n \ln_0 e_n$	$in \ln_0 e_n$	$n \ln_0 ie_n$	$in \ln_0 ie_n$
1		0.5671...	i0.5671...	0.5671...+i $\pi/2$ (=+1 i $\pi/2$ )	- $\pi/2$ + i0.5671...
2		0.8526...	i0.8526...	0.8526...+i $\pi$ (=+2 i $\pi/2$ )	- $\pi$ + i0.8526...
3		1.0499...	i1.0499...	1.0499...+i3 $\pi/2$ (=+3 i $\pi/2$ )	- 3 $\pi/2$ + i1.0499...
4		1.2021...	i1.2021...	1.2021...+i 2 $\pi$ (=+4 i $\pi/2$ )	-2 $\pi$ + i1.2021...
5		1.3067...	i1.3067...	1.3067...+i5 $\pi/2$ (=+5 i $\pi/2$ )	- 5 $\pi/2$ + i1.3067...
6		1.4324...	i1.4324...	1.4324...+i 3 $\pi$ (=+6 i $\pi/2$ )	-3 $\pi$ + i1.4324...

Table 5

In the final table, it is clear that the integers,  $n$ , are the count of the rotations of  $\frac{1}{2} \pi$  and of the powers and hence the number of orders of  $i$ , both indications of a degree of orthogonal structure as in Euler, Section 0a. We are interested here specifically in the factor  $e_2$ . As a review of the above Figures hopefully makes clear, the value in the subscript exponential bases is in determining a coefficient of proportionality between two related differentials, one of which is a function of the  $n$ th-root of the logarithm to the others linear function.

The function in (1.71) finds form in the following equation, where the negative sense in the subscript has the same meaning it does in the superscript exponent, that is it represents inversion.

$$\ln_0 e_n = e_n^{-n} = e_{-n}^n \quad (1.74)$$

Thus for  $n = 2$ , we have the following, where it is understood that  $e_2$  is a normalizing coefficient for any independent variable dimensional property,  $x$ ,

$$\ln_0 e_2 (e_2)^2 = 1, \ln_0 e_{-2} (e_{-2})^{-2} = -1 \quad (1.75)$$

and with a unit of property,  $x_0$ , and some mathematical operation and rearrangement we can state

$$(\ln_0 e_2)^{\frac{1}{2}} x_0 = e_2^{-1} x_0 = \frac{d \ln_2 e_2 x_0}{d e_2 x_0} = \frac{1}{1.53158...} \quad (1.76)$$

$$(\ln_0 e_{-2})^{\frac{1}{2}} x_0 = i e_{-2} x_0 = \frac{-d e_{-2} x_0}{i d \ln_2 e_{-2} x_0} = \frac{-0.65291...}{i1.0} = \frac{-1}{i1.53158...} \quad (1.77)$$

In the above development of the neutron scale for quantum gravity (1.33) and at (1.66) we have an expression of the change in the linear scale of  $r_0$  as the square root of the change in the natural log of the expansion stress scale,  $T_0$ . We have modeled quantum mass as a linear function of space,  $r_0$ , by the reduced angular wavelength or time by the frequency,  $\omega_0$ . As developed above in connection with the Hubble rate, using the inertial constant and/or the speed of light we have

$$m_0 = f(H_0) = f(dr_0, dt_0) \quad (1.78)$$

Stress is modeled as a function of the square of both of these,

$$f_0 = f(dr_0^2, dt_0^2) = \tau \omega_0^2 / r_0^2 = \tau \theta / t_0^2 r_0^2 = \frac{h}{c} \theta / t_0^2 r_0^2 \quad (1.79)$$

but as time and distance are dual values as defined by an invariant  $c$ , we can treat stress as a functional, where time is a measure, therefore a function of the change in  $r_0$ , (we could also use displacement as a measure, therefore a function of a change in  $t_0$ ), as

$$f_0 = f(dr_0^2, c^2(dr_0^2)) \quad (1.80)$$

Thus, a change in stress with expansion leads to an increase in  $r_0$ , where a preliminary decrease in mass of the fundamental oscillation, the neutron, is equal to the mass of the emitted electron as developed above or

$$m_e = \Delta m_n = m_n \left( \frac{\delta r_0^2}{1 + \delta r_0^2} \right) \quad (1.81)$$

The change in stress/energy density of the oscillation is

$$dE_1 = df_0 = f'(A_0^{-2}) = -\frac{\tau \omega_0^2}{A_0^2} dA_0 = -\frac{\tau_0}{A_0^2} dA_0 = -\frac{f_0}{A_0} dA_0 \quad (1.82)$$

where it is clear that a change in the log of the stress is inversely equal to a change in the log of the cross-section,

$$d \ln f_0 = \frac{df_0}{f_0} = -\frac{dA_0}{A_0} = -d \ln A_0 \quad (1.83)$$

Obviously, since both stress and cross-section are unit values

$$\ln f_0 = \ln A_0 \quad (1.84)$$

Thus for an exponential expansion of the cosmos, in accordance with (1.83) and using (1.77), we substitute  $f_0$  for  $A_0$  which is the square of  $r_0 = x_0$  and get the following where  $ii$  indicates the symmetric and  $ij$  the anti symmetric or transverse components of the electron wave form

$$(\ln f_0)^{\frac{1}{2}} = i e_{-2} f_0 = \frac{-df_0}{id \ln f_0} = \frac{-de_{-2} f_{ii}}{id \ln_2 e_{-2} f_{ij}} = \frac{-0.65291... f_{ii}}{i 1.0 f_{ij}} = \frac{-1.0 f_{ii}}{i 1.53158... f_{ij}} \quad (1.85)$$

The imaginary sense assigned to the natural log differential is an indication of transverse motion and other energy associated with the change in stress, resulting in the change to that of the reduced Compton wavelength of the proton.

The Hamiltonian or total energy of the system resulting from beta decay is therefore the energy of the neutron, which is equal to the energy of the proton plus the energy differential of the electron wave components due to the change in stress of expansion.

$$E_0 - E_p - [E_e(df_0) + E_0(id \ln f_0)] = 0 \quad (1.86)$$

In terms of mass, as in (1.70) this is accurate to a factor of  $2.16 \times 10^{-7}$ .

$$m_n - m_p - [1.0 m_e - 1.53158... m_e] = 0 \quad (1.87)$$

## 2f — Evaluation of Elementary Charge

We turn now to the nature of charge. As discussed previously, it is a function of the fundamental quantum oscillation of the neutron, as both the sustained level of maximum potential energy and the simultaneous sustained level of maximum kinetic, transverse wave energy which produces spin and the related quantum magnetic field. We can think of the potential energy as the capacity of positive charge and the induced kinetic energy as negative charge, though the senses are reversed in the case of anti-matter. In terms of phase space, potential energy indicates maximum wave displacement and kinetic energy represents maximum wave momentum.

With beta decay the wave momentum is externalized or transmitted in part from the constrained boundaries of the neutron to form the electron waveform in keeping with the mechanics of the above spin diagrams. While the electron waveform has its own quantization dynamics, for example the maximum wave momentum, along with mass-spin energy, wave force, etc., which are much reduced differential portions of the fundamental system, in total they are the effect of the fundamental wave momentum/charge of the neutron. We will go in to this in detail in a moment.

The SI fundamental charge is the coulomb, C. The coulomb, or ampere per second, is equivalent in mechanical dimensions to one kilogram-meter per second, a measure of momentum. A fundamental unit or elementary charge,  $e_0$ , is established as

$$e_0 = 1.60217653(14) \times 10^{-19} \text{Coulomb} \quad (1.88)$$

As a measure of momentum, in connection with this development and the transmission of momentum with beta decay at  $W_{-x}$ , in the spin diagram for the proton, the fundamental unit of conjugate momentum, using angular frequency, is reasonably close to this value at

$$p_0 = \hbar \omega_0 = 5.02130... \times 10^{-19} \text{kg} \cdot \text{m} / \text{s} \quad (1.89)$$

Charge is related to each of the two rotational nodes,  $W_{-x}$  and  $W_{+x}$ , indicating the need to apply semi-periodic frequency, which we can do by dividing (1.89), which is expressed in angular frequency, by  $\pi$ . In addition, the charge generation is conditioned by the product of the momentum and the mechanical impedance of the manifold from (1.59) (not to be confused with the electro-magnetically derived characteristic impedance of the vacuum), which is

$$\begin{aligned} Z_0 &= \hbar \omega_0 r_0^{-1} = 0.002390877... \text{kg} / \text{s} \\ \zeta &= \left( \frac{1 + Z_0}{\pi} \right) = 0.319070926... \\ \zeta^2 &= \left( \frac{1 + Z_0}{\pi} \right)^2 = 0.101806256... \end{aligned} \quad (1.90)$$

where we define the total factor,  $\zeta$ , and its square for later use. Thus, we would anticipate an elementary charge of

$$e_0 = p_0 \zeta = \hbar \omega_0 \zeta = 1.602152647... \times 10^{-19} \text{kg} \cdot \text{m} / \text{s} \quad (1.91)$$

This varies from the established value by a factor of 1.000015... which is in the same order of magnitude as the relative uncertainty for the gravitational constant.

Further development, using the familiar identity for the inverse of the fine structure constant,  $\alpha$ , a dimensionless number and therefore the ratio of two like-property magnitudes, as

$$\alpha^{-1} \equiv \hbar c \frac{4\pi\epsilon_0}{e_0^2} = 137.0359989... \quad (1.92)$$

and the permeability,  $\mu_0$ , and permittivity,  $\epsilon_0$ , relationship, where  $\mu_0$  is in units of inductance per meter or henrys per meter which reduces to units of force per current squared or newton's per ampere squared, and  $\epsilon_0$  is in units of capacitance per meter or farads per meter which reduces to ampere squared per newton over the speed of light in vacuo squared, so that

$$\epsilon_0 = \frac{1}{c^2 \mu_0} \quad (1.93)$$

and with rearrangement in (1.92) gives the following

$$e_0^2 = -\hbar c^2 (\alpha 4\pi\epsilon_0) = -\hbar \frac{\alpha 4\pi}{\mu_0} = -\hbar \frac{\alpha}{10^{-7}} = -\hbar (\hbar \omega_0^2) \zeta^2 \quad (1.94)$$

It is noted that the value of  $\mu_0$  is set by convention in relating charge,  $q$ , (of which elementary charge,  $e_0$ , is an effective quantum) and current,  $i = dq/dt$ , resulting in the exactness of the denominator of the next to last term. Since the negative sense of the right terms above can be attributed to the current, therefore charge, squared, it can be incorporated therein, canceling such sense in the charge squared term. This suggests the transparent presence of a current squared argument in (1.94), for which the fine structure constant is a coefficient, since from Ampere's Law for one ampere<sup>2</sup> of current, where the denominator on the right is in newton, we have

$$\mu_0 = 2\pi (2 \times 10^{-7} \text{ N}) \frac{d}{L} i_0^{-2} = 4\pi \times 10^{-7} \text{ newton} / \text{ampere}^2 \quad (1.95)$$

$2 \times 10^{-7}$  newton is the force generated for each meter length,  $L$ , of two conductors of infinite length and negligible cross-section and one meter apart,  $d$ , in a vacuum with one ampere of constant current flowing in each conductor. The  $d$  and  $L$  obviously cancel and the  $i_0^2$  component and therefore the force is positive or negative depending on whether the currents are parallel and attractive or antiparallel and repulsive.

Inserting this into (1.94) with some rearrangement gives the ratio of elementary charge squared to current squared as the product of the modified fine structure constant,  $\alpha'$  as shown, and the inertial constant. If the fine structure constant is dimensionless and its denominator is a force from the above, then  $\alpha'$  is an inverse force, which in terms of this development is the inertial constant times a frequency squared and  $k$  is an unknown proportionality factor for the frequency as

$$\frac{e_0^2}{i_0^2} = \frac{\alpha}{10^{-7} \hbar} = \alpha' \hbar = \frac{k^2}{\hbar \omega_e^2} \hbar = \frac{k^2}{\omega_e^2} \quad (1.96)$$

If the force in the last term is the base transverse wave force of the electron as in the above development, then  $k$  is an angular measure per unit of elementary charge as,

$$k = \omega_e \frac{e_0}{i_0} = \left( \frac{\theta_e}{s} \right) \frac{e_0}{ne_0} = 124.3840198... \frac{\theta_e}{e_0} \quad (1.97)$$

Using this value with (1.96) gives

$$\alpha = \frac{k^2(10^{-7})}{\hbar\omega_e^2} = \frac{k^2(10^{-7}N)}{0.212013671...N} = 0.007297352... \frac{\theta^2}{e_0^2} \quad (1.98)$$

With another look at (1.94), we get the following relationships between the fundamental wave force and  $\alpha'$

$$\alpha' = \tau_0 \zeta^2 = \hbar\omega_0^2 \zeta^2 = \zeta\omega_0 e_0 \quad (1.99)$$

Using our derived value for elementary charge in (1.91) in the first two terms of (1.96) we get the following derived value for the fine structure constant of

$$\alpha_{derived} = .007297134... \quad (1.100)$$

Comparing with (1.98) once again, in line with our missing mass derivation, this is accurate to a factor of  $2.17 \times 10^{-7}$ .



## 2g — Special Relativity and Muon & Tau Families

Concerning the compatibility of this model and special relativity, I have written about this extensively elsewhere. Suffice it to say that this model is one of constrained stress/strain in the spacetime manifold, which acts as discrete units of rest mass with derived properties. Each discrete state remains a wave form and in response to interaction with other states is free to translate and rotate in space according to the ambient energies. It will therefore contract its characteristic strain radius in response to acceleration in keeping with the Fitzgerald-Lorentz length contraction, resulting in an increase in spin energy/mass according to the definition of the inertial constant,  $\eta$ .

As to the two other families of leptons, the muon and tau, and their theoretical related hadrons, based on their short lifetime and granted my limited knowledge of the experimental background for their theoretical introduction, it is my perception that they are simply the basic states we have discussed, altered by relativistic dynamics and collision interaction. We would expect these states to behave in a generally ordered fashion under constraints of high energy collision and those defined by geometry and mathematics. The evolution of a catalogue of such short-lived phenomenology, while useful, does not indicate the need or wisdom of elevating that phenomenology to ontology. I would grant the status of “fundamental rest mass particle” only to common, stable, relatively long-lived states, of the proton, electron, and including the neutron in nuclear confinement, of course, in keeping with the general conditions of condensed matter physics.

Update 9/6/2021 concerning the Muon and Tau

### 3 — Condensed Matter Application of this Model

The above model development represents rest mass particles as localized torsional oscillations of an expanding spacetime manifold with an inherent elastic potential energy density. From a topological perspective, the spatial 3-sphere or 3-manifold without boundary is itself a boundary within a spacetime 4-manifold in which the time dimension is orthonormal to the 3-dimensional space component. The 3-dimensional analogy is the 2-sphere surface of a rupture-free balloon that expands or contracts radially over time in response to a pressure gradient at its surface and in which the dimension and direction of time is registered by the radial sense of the change. In an expansion phase, the interior of the balloon represents the past and the exterior of the balloon represents the future, while in a contraction phase, the past and future senses are reversed. For an ongoing oscillation there is no absolute time sense indicated, rather only a phase direction of the instant or current state. As the  $n$ -sphere boundary of an  $n+1$ -manifold can never be reduced to an  $n-1$ -dimensional state, any inherent density of the  $n$ -sphere must be finite; it can never be infinite or zero. Failure to understand this axiomatic, topical truth is the source of much misunderstanding in current physical theory.

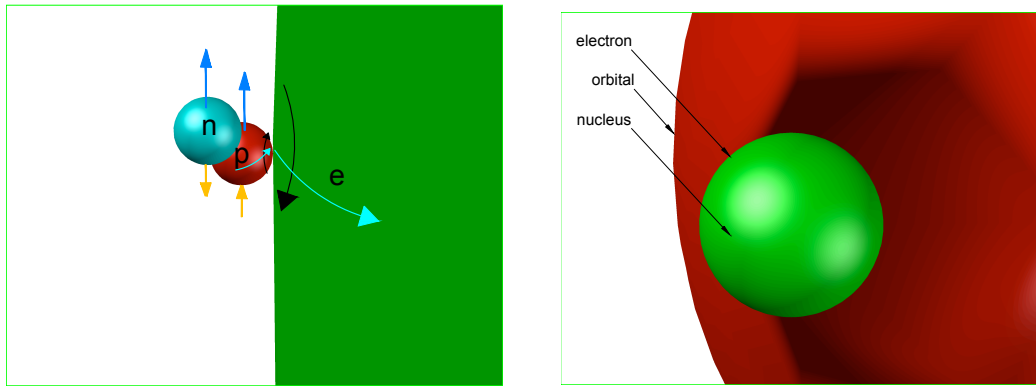
The rest mass particles generated from such change in energy density ultimately produce plasma conditions when congregated by gravitational interaction at a stellar scale, but this is not necessarily the only precursor to condensed matter states. Heat and its measure, temperature, is a convenient analogy for potential energy density, but it bears remembering that heat is a relative condition of particle translational velocity and collision interaction, which itself is an interaction of electromagnetic wave fields of the quantum electron or of the neutron/proton fundamental.

In this model under discussion, quarks are not a separable constituent of such matter states but are rather the signature of oscillatory nodes, antinodes and moments in particle collisions as registered in electronic accelerator recording systems. The fundamental physical structure in this model is the baryon, specifically the neutron, which with ongoing expansion decays into the proton, both of which are ontologically wave forms, but with a particle phenomenology when viewed from the scale of human interaction; mesons, neutrinos, and all leptons and gauge bosons are the transitional result of baryonic decay, of which the electron and photons, and perhaps the neutrino, have longevity.

In the interactions between condensed matter nucleons, i.e. protons and neutrons, it is the nodes and antinodes along with the capacitive and inductive moments that chart their configurations, so in that sense an accounting of nodal/moment “quarks” may be in order, though probably not in the manner of established quantum chromodynamics. As detailed above, sustained quantum rotational strain provides an alignment constraint and mechanism for the congregation of nucleons, and we would anticipate a geometric configuration of nucleons to form an atomic nucleus in the manner of the work of Norman Cook and others, as opposed to a liquid drop or other concepts of the nucleus. We would anticipate these configurations to mimic the constraints of the cuboctahedral lattice of our opening development just as do the crystal structures of many metals such as palladium.

In the referenced graphic representations of this paper it is easy to depict the fundamental oscillations as spheroidal objects due to their inherent rotational dynamics about the  $\theta$  and  $\phi$  axes, so it is important to emphasize that in this modeling they are not conceptualized as separate objects detached from the space around them; rather they are foci of expansion stress that results in torsion and its eventual axial rotation and the surfaces of the spheroidal graphic images represent the characteristic radii of these rotational stresses and strains.

The spin vectors as represented in the spin diagrams for the neutron and proton are parallel, as shown in Figure 12 as they might be for the deuteron, giving the nuclear system a spin of 1. Their magnetic induction vectors or dipole moments are anti-parallel and therefore have a 0 state. As they have different rotational frequencies, we would anticipate a degree of angular momentum of the system. Finally, we anticipate a torsion connection for transmission of the electron waveform anti-parallel to the  $\phi$  rotation vector of the proton.



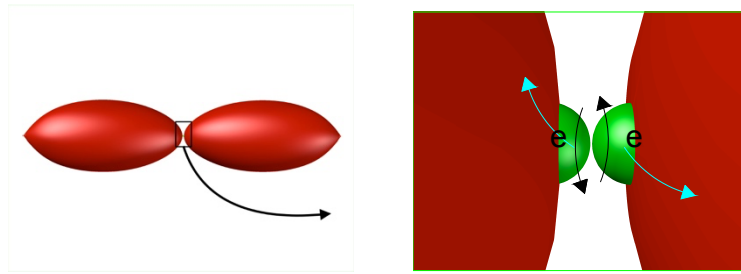
Nucleon, Electron, and Orbital relative spatial relationships. The nucleon and electron figures use the corresponding Compton reduced wavelength as a gauge of torsional wavelength in the drawings. The electron “surface” shown on the left is shown in its entirety on the right in which the nucleons are just a speck at the end of the designated arrow smaller than the period at the end of this sentence. The orbital size is correspondingly larger as seen in the next graphic and is an electromagnetic field effect of the moving electron.

Figure 12

The electron waveform in Figure 12 has been represented here in a general spherical form on the right in green, and in the absence of transient stress, that might be accurate, however, we would anticipate a tendency for elongation as an orbital in the form of a prolate ellipsoid as indicated by the large red graphic here and below, particularly in multi-nucleon atomic structures and within the context of molecular structures. The electron modeled here is not a cloud, though it would resemble the orbital configurations shown in quantum mechanics sources. Such an electron wave mechanism is essentially tethered to the nucleus, short of ionization, free to revolve about the nucleus in the absence of other electrons; in the presence of other electrons in multiple nucleon elements any given electron is constrained to the valence specific orbital arrangement.

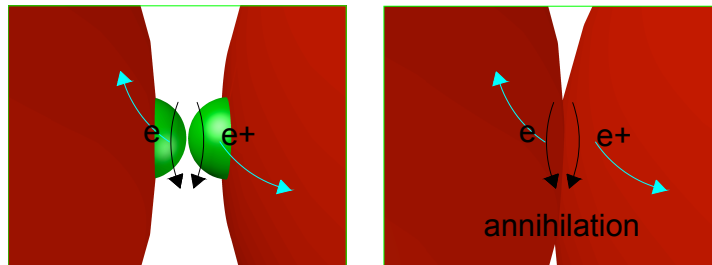
The significant thing to focus on within the context of condensed matter is that the coulomb force on a quantum level is not modeled herein as an instant isotropic symmetrical charge field, i.e. over  $4\pi$  steradians, between a positively charged proton and a negatively charged electron cloud, but rather as a transmission of potential energy and fundamental wave momentum from a “positively charged” capacitive source within the proton waveform as the propagated wave kinetic energy and momentum of the electron in a form of induced “negatively charged” electromagnetic current. The point-like charge of the electron wave form is represented by the twisting node of the positive end of the  $\phi$  rotation vector of the electron which can extend indefinitely and in fact be separated from its source through ionization. In addition to the ongoing transmission of transverse wave momentum that is responsible for the electron waveform, upon initial emission of that electron, at the leading edge of the wave propagation we can anticipate a longitudinal component of the momentum that continues on beyond the boundary of the orbital and is responsible for the phenomena of the neutrino.

In the context of molecular bonding, as in Figure 13, when two  $\phi$  rotational nodes meet, being of the same axial twist, but antiparallel, and therefore of opposite spin state, they reinforce and strengthen the nodal point and form a stabilizing bond. If a positron and electron meet, as in Figure 14, being of opposite twist and antiparallel, the rotational stress opens the nodal structure and destroys the characteristic wave forms with a release of wave energy.



Bonding of two orbitals at point of maximum torsional interaction between electrons as shown in inset enlargement.

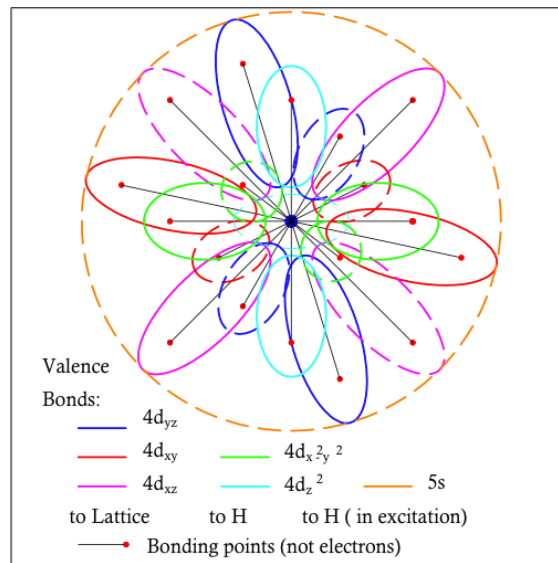
Figure 13



Interaction between electron and anti-electron which is of opposite nodal twist, destroying the nodal structure and releasing the wave energy as antiparallel gamma rays.

Figure 14

The same inherent cuboctahedral stress and strain constraints that produce the neutron, and eventually thereafter the proton, and then nuclear configuration, is found in molecular bonding of metals like palladium that exhibit the face centered cubic crystal structure as seen in the following graphic.



Palladium Valence Electron Orbitals  $4d^{10}$

The brown circle represents the  $5s$  excitation that is absent in the atom's ground state.

Figure 15

The  $4d_{yz}$ ,  $4d_{xy}$ , and  $4d_{xz}$  electrons are constrained to the corresponding orbital arrangement of the  $4d$  subshell by cuboctahedral geometry and are occupied in forming the FCC lattice structure. The  $4d_{x^2-y^2}$  and  $4d_{z^2}$

electrons/orbitals center on the six nodal orientations of the octahedral chambers of the FCC lattice and are available for bonding with any hydrogen absorbed into the lattice. There is no bonding potential for the four nodal orientations within the tetrahedral chambers, however, as there are no orbitals defined in the shell geometry for these locations, EXCEPT in the case of the excitation of one of the deeper (as 4s) electrons to the 5s shell. In that case the subtended solid angle represented by each of the six octahedral chambers around each FCC node, being 1.359347638 steradians(sr) for a total of 8.156085832 sr, leaving a difference from  $4\pi$  of 4.410284782 sr divided by 8 tetrahedral chambers is 0.551285598 steradians or 4.3869914% of the total  $4\pi$  sr surface giving a corresponding raw probability of a little less than 5% of such excitation resulting in a bonding potential with any hydrogen in the tetrahedral chamber as a deep electron jumps to the 5s shell. If we assume that the exclusion principle precludes the octahedral spaces from such bonding, the probability is simply 1/8 or 12.5% for any surrounding tetrahedral space.

Table 6 gives some of the parameters of the lattice and the elements involved in this catalytic system.

### Lattice and Element Parameters

Lattice statistical data		Palladium	Nickel
1	Valence shell	*[Kr]4d <sup>10</sup>	[Ar]3d <sup>8</sup> 4s <sup>2</sup> or [Ar]3d <sup>9</sup> 4s <sup>1</sup>
2	Covalent radius	139(6) pm	124(4) pm
3	d, Covalent radius x 2	278.0 pm	248.0 pm
4	a, Unit cell edge,	393.2 pm	350.7 pm
5	O Chamber width	115.2 pm	102.7 pm
6	T aperture spherical capacity	43.0 pm	38.4 pm
7	T chamber spherical capacity	62.5 pm	55.7 pm

#### Hydrogen isotopes and Helium 4

8	H covalent radius x 2	62 pm	62 pm
9	D covalent radius x 2	<62 pm	<62 pm
10	He-4 covalent radius x 2	56 pm	56 pm
11	H length as ellipsoid in T aperture	128.9 pm	162 pm

\* Unique in [Kr] for lack of 5s subshell, Electronegativity is 2.20 for both Pd and H

Table 6

We next consider the cuboctahedral perspective of the FCC lattice of palladium, in other words with twelve edge centered atoms around a central atom, instead of the 6 face and 8 vertex atoms around a central octahedral void of the FCC. We will consider the valence 4d subshell structure to present a generally spherical atomic component of the lattice. The six octahedral chambers around each center atom offer a potential for bonding with hydrogen infused or absorbed in the bulk or adsorbed in any surface octahedral chambers that are open on one face. If the crystal is faceted along the octahedral axes, as shown in the last cell of the Cuboctahedral Lattice Configuration table, there will be no octahedral opening and any diffusion will require penetration of a tetrahedral aperture and transit of the enclosed T chamber before entry into an

interior O chamber, making that diffusion difficult. If the crystal is faceted rectilinearly, surface octahedral openings will be available and will facilitate both adsorption and thereby absorption.

Palladium and hydrogen are somewhat unique in that both have the same electronegativity on the Pauling scale of 2.20, and upon molecular bonding of the electrons, the nuclei of each will seek the same distance from their corresponding nucleus. As palladium is the much more massive atom and is also in a crystal configuration, this means that upon bonding with the palladium, the hydrogen nucleus will move away from the bonded palladium atom. While the  $4d_{yz}$ ,  $4d_{xy}$ , and  $4d_{xz}$  bonds in the idealized crystal are delocalized, that between the Pd and D would be a sigma bond or localized.

In the confines of an O chamber, if it bonds to one of the  $4d_{x^2-y^2}$  and  $4d_{z^2}$  electron/orbitals of the four surface atoms and not the first interior layer atom, the H or in this case D nucleus has only one of two places to go other than exiting the crystal, and that is to the center of one of the two opposite T apertures leading to a T chamber and eventually to the interior of the bulk. The geometry is such that the D nucleus will thereby be positioned directly in the center of the aperture and in the plane of the three surrounding Pd nuclei by the fact of a common electronegativity of Pd and D.

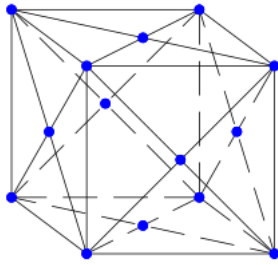
The “naked” or unshielded D nucleus will be positioned toward the center of the opening by electrostatic force, which is an extension of the wave stress in this model, where it will remain as long as the Pd-D bond is maintained. If there is an electrolytic charge or gas pressure on the crystal sufficient to break the covalent bond to the O chamber Pd atom, the D will have a potential to enter and occupy the T chamber. If the T chamber is occupied, and a pathway into the bulk by that occupant is blocked, entry of the nucleus will be blocked, but if the chamber is empty, the D atom will enter the T chamber. However, it will not be able to bond to the lattice in the absence of an available orbital.

In the case of a D atom occupying a T chamber, if one of the surrounding four Pd atoms is excited to raise one of its electrons to the 5s shell and in the area of the T chamber, the D will be induced to covalent bonding with that Pd electron, and the D nucleus will be accelerated through the T aperture opposite that Pd atom according to the common electronegativity of the two elements. An unshielded D nucleus positioned in the center of the aperture is essentially an inertially confined target for the accelerating D nucleus from the T chamber, and the two nuclei will be positioned to collide. In keeping with the above development of rest mass particles, we can expect the proton of each D nucleus to be oriented toward its bonding electron and for the neutron of each to be opposite that electron direction. This is not due to electrostatic forces as conventionally modeled, but rather is a result of the fact that the electron waveform is being generated by the proton while the neutron is essentially passive to and moved out of the way by that ongoing interaction. The fact that the neutron is on the leading edge of the accelerating D nucleus and on the proximal side of the other, target D nucleus shields the two protons from repulsive near-field coulomb interaction and increases the potential for nuclear fusion with nuclear coincidence which will occur due to wave-spin/moment alignment of the two nuclei.

$D + D > {}^4\text{He}$  is not a generally recognized fusion pathway. Because the current model of particle physics tacitly or expressly views matter as comprised of particles that under certain circumstances have wavelike properties, it tends to assume that conservation of energy and momentum in an interaction demand that the energy that is liberated in one such as nuclear fusion be carried off by the particles that are produced by the reaction. Under this thinking, even if  $D + D > {}^4\text{He}$  did occur, it would require a tremendous velocity on the part of the Helium 4, single product of reaction to be registered, and that is not observed to happen. It does not occur to such a model that if particles are essentially waves, such an interaction can release the energy to the lattice in the form of wave energy, in this case as phononic energy or vibration of the lattice.

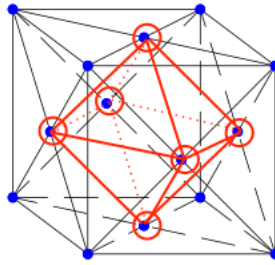
We can also expect a probability of fusion occurring when two D enter from two adjacent apertures into a T chamber that has its two other apertures blocked by occupied adjacent O chambers. In this event, there will be a lower probability of the helium escaping from the lattice.

### FCC Structure



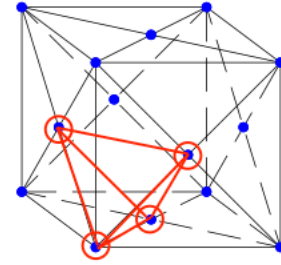
A unit of a face centered cubic lattice depicting a palladium crystal, the blue nodes representing palladium nuclei at the cubic vertices and at the center of each of the cubic faces. In the bulk lattice, 14 nodes are shared with 26 adjacent cubes. In the surface, 13 are shared by 17 cubes.

### Octahedral Chamber



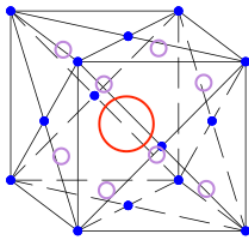
The center of the cube forms an octahedral space with the face centered nodes, but contains no lattice element. It readily absorbs hydrogen, protium and deuterium, at room temperature.

### Tetrahedral Chamber



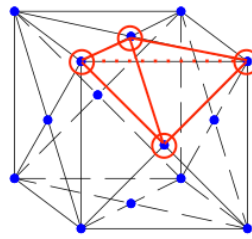
Each corner nuclei forms a smaller tetrahedral chamber with the three adjacent face centers. Any hydrogen entering the lattice bulk must pass through the T chambers.

### O & T Relationship



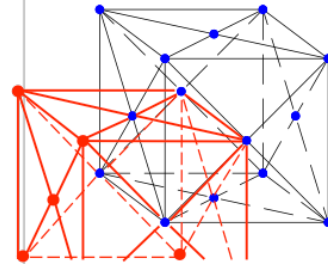
Each octahedral space or O chamber in the bulk is accessed through one of 8 adjacent and smaller tetrahedral spaces or T chambers, the chamber boundaries formed by the orbitals of lattice bonding. In the bulk, there are one O and two T chambers for each palladium atom.

### Adjacent 1/4 O Chamber



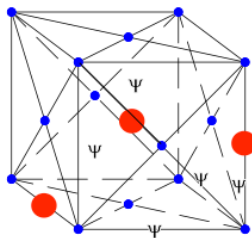
In the bulk, each edge of the cube shares the adjacent two center and two corner nodes to form one fourth of an octahedral space with three adjacent cubes with a total of 18 such cubes. Each bulk cube contains 4 O chambers in its volume. In the surface, the total number of adjacent cubes in the rectilinear configuration is 13, and the O chamber is open at the surface.

### Lattice Interlace



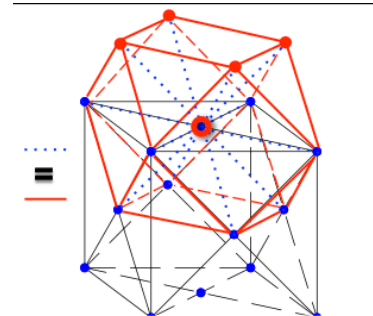
One of 12 interlaced cubes in the bulk sharing and repeating the same nodal configuration as the original cube, but offset in two dimensions by half a cubic length; these are in addition to and interlaced with the other 26.

### Coulomb Interaction



The lattice absorbs 900 times its volume of hydrogen at room temperature equivalent to 70% of the O chambers, assuming one H per chamber. Three random H are shown. The coulomb force, broadly understood to include all electromagnetic interactions and represented by the wave function, psi, is responsible for bonding of the atoms in the lattice. There is one wave function for the system.

### Cuboctahedral Form



In the bulk, all nodes serve as a face centered node for an arbitrary cube and each such node is also the center of a 14 sided cuboctahedral lattice with 12 vertices equidistant from the center and with 24 equal length edges. Significantly, each such center atom shares 6 O and 8 T chambers with adjacent atoms, the O chambers along the 3 rectilinear axes and the T chambers along the 4 cubic diagonal axes.

Chart 1 — FCC Lattice Properties

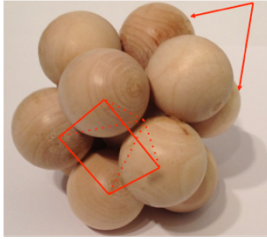
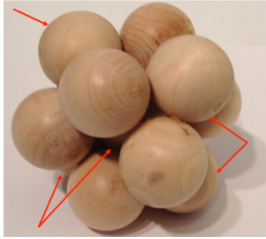
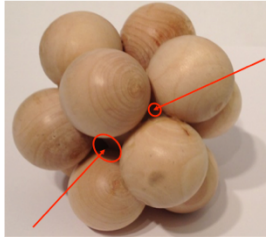
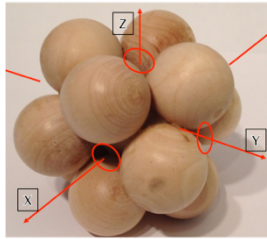
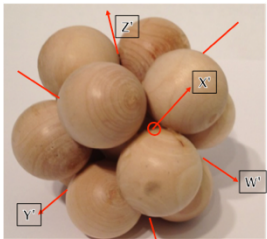
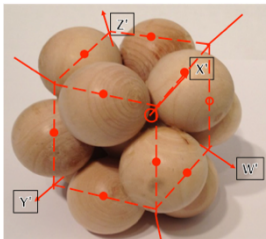




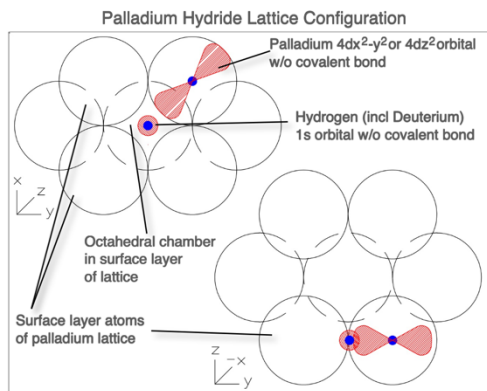
<p>Cuboctahedron Slide 1</p> 	<p>Cuboctahedron Slide 2</p> 	<p>Cuboctahedron Slide 3</p> 	<p>Cuboctahedron Slide 4</p> 
<p>The same lattice seen as cuboctahedral with spheres representing the covalent bonding extents, but with the left face of the fcc removed to reveal the center O chamber. 4 face center nodes are added to the right end, 2 shown here with arrows. This configuration shows 12 atoms around a center atom to form a cuboctahedron.</p>	<p>Arrows here point to the atoms of the right hand face of the original fcc above.</p>	<p>Apertures to surface O chamber on left and to interior T chamber on right.</p>	<p>Three orthogonal axes of the fcc and the cubic component of the cuboctahedral lattice, centered on the O apertures.</p>
<p>Cuboctahedron Slide 5</p> 	<p>Cuboctahedron Slide 6</p> 	<p>Cuboctahedron Slide 7</p> 	<p>Cuboctahedron Slide 8</p> 
<p>4 diagonal axes of symmetry centered on the T apertures for the 8 T chambers around the center palladium atom.</p>	<p>The same lattice cell as the fcc, but here centered on a lattice elemental atom so that another lattice atom is centered on each of the cubic edges.</p>	<p>Direct view of a surface O chamber showing relative size and configuration. The surface opening is 115.2 pm between Pd orbitals, readily admitting deuterium at a covalent diameter of &lt;62 pm.</p>	<p>Direct view of a T chamber aperture which will admit a spherical diameter of 43.0 pm assuming more or less spherical Pd orbital constraints, too small for free D, but adequate for tunneling of one under covalent bond extension across O chamber.</p>
<p>3 axis rectilinear surface</p> 	<p>4 axis octahedral surface</p> 		
<p>A view of the fcc lattice which gives an idea of the porosity of the surface when it is in a rectilinear configuration.</p>	<p>A view of the lattice sheared normal to the diagonal axes shows surfaces with 20% the porosity of the rectilinear configuration. All apertures are to T chambers directly and preclude covalent bonding of deuterium in an open surface O chamber and thereby the nuclear target confinement understood to facilitate fusion in this model.</p>		

Chart 2 — Cuboctahedral Lattice Configuration

The lattice is physically and geometrically the same as the FCC, but the unit perspective is centered on a nuclear node instead of on an octahedral chamber.

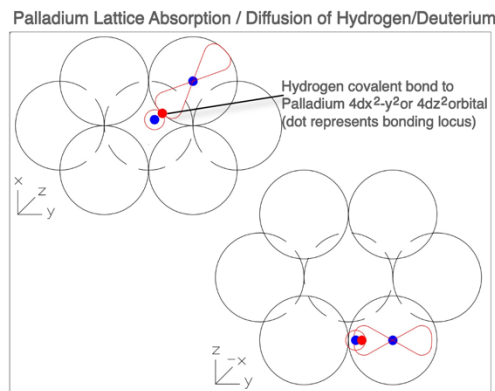


## Hydrogen (protium or deuterium) diffusion in the palladium lattice



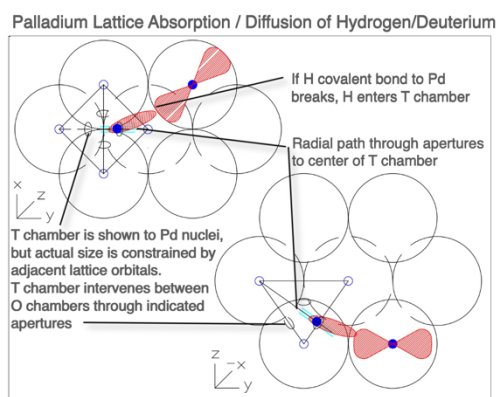
H enters surface octahedral chamber

**1A**



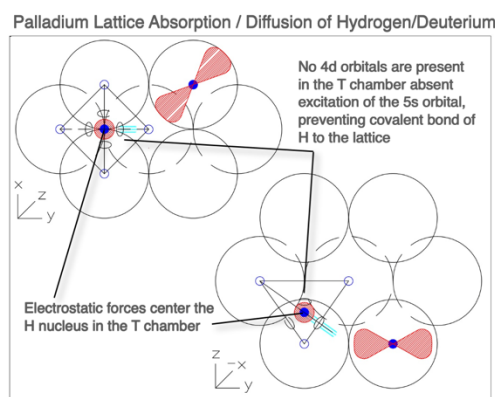
H and Pd form covalent bond

**1B**



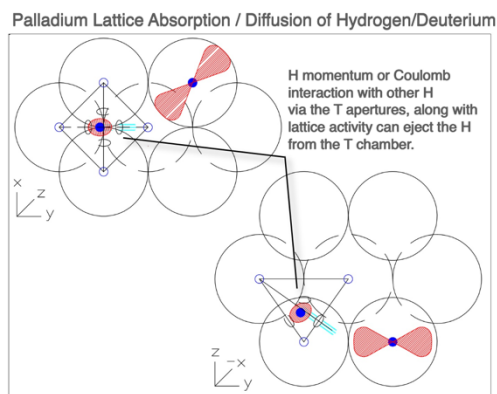
H centers in aperture to Tetrahedral chamber

**1C**



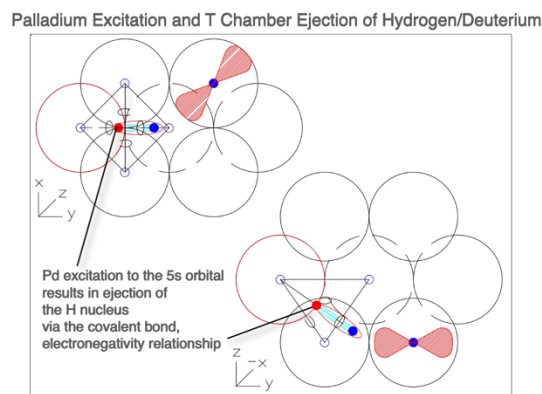
H enters connecting Tetrahedral chamber

**1D**



H exits Tetrahedral chamber to surface or adjacent bulk O chamber

**1E**

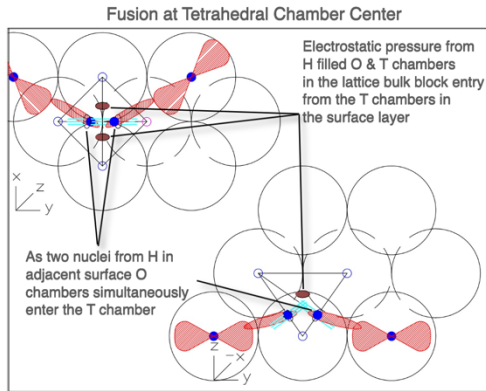


H ejected from the Tetrahedral chamber by Pd 5s excitation

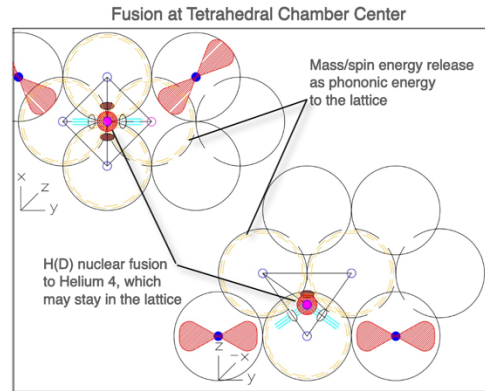
**1F**

Palladium and hydrogen both have an electronegativity of 2.20 Pauling units which indicates that in this covalent bond the respective nuclei will separate equidistant from the bond or in this case twice the Pd covalent radius. Assuming a uniform charge distribution of the orbital around the three lattice bonds at the tetrahedral aperture, such extension for the H atom projects its nucleus with a high degree of precision to the center of one of the Tetrahedral apertures. If the bond to Pd breaks in the process, the H enters the Tetrahedral chamber.

**Chart 3 — Hydrogen Diffusion**

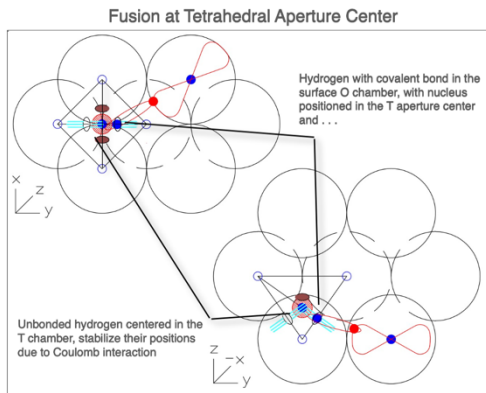


2A

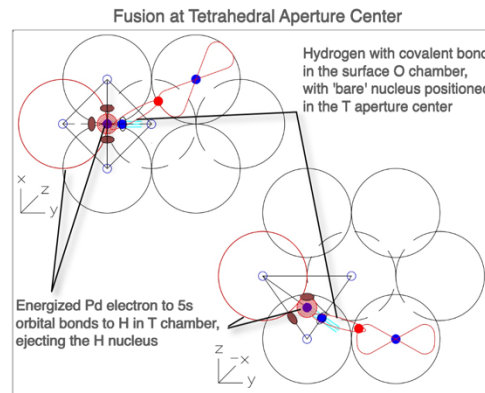


2B

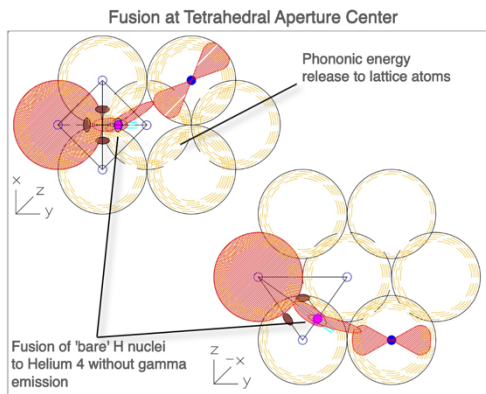
Chart 4 — Fusion path 1 in the Tetrahedral chamber  
All hydrogen are assumed to be deuterium.



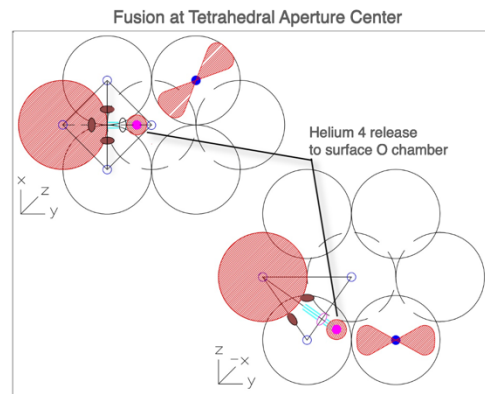
3A



3B



3C



3D

Fusion path 2 appears the most likely for controlled fusion as the common Pauling electronegativity of H and Pd provides precise inertial confinement of the deuterium nucleus in the T aperture of a surface O chamber while in the covalent bond with a surface Pd atom for targeting by another such nucleus ejected by excitation to the 5s orbital of a Pd atom, with each nucleus proton shielded by its neutron. With presumed filling of the bulk chambers, the nuclei merge in the target with a drop in rotational energy transmitted to the bulk and environment as phonic energy and the resulting helium 4 emitted from the surface without gamma emission.

Chart 5 — Fusion path 2 in the Tetrahedral aperture

## 4 — Conclusions

In 1989, chemists Martin Fleischmann and Stanley Pons reported the results of a table-top experimental electrolysis of heavy water using a palladium electrode in which the recorded heat produced exceeded the energy input plus any known molecular bonding release. They reported some measurement of nuclear byproducts and found the results suggested the possibility of nuclear fusion of hydrogen/deuterium nuclei, catalyzed by the palladium lattice. After initial interest in the announcement from within the physics community, ambiguous and null results from attempts to replicate the process, hampered by a lack of a theoretical understanding of condensed matter nuclear processes that could produce such results, led to a loss of professional interest from within the community.

Interest on the part of a few, from both a technical and business perspective, has led to reports of repeated production of excess heat and in some cases helium production from this and similar experiments, but the ongoing theoretical shortfall and denigration of the effort by various parties has continued to impede the investigation of this possible beneficial and cheap source of energy for human utilization. It is not my intention to go into the historical or technical details of this investigation here; a cursory read of the current article in Wikipedia under “Cold Fusion” appears to give a fair and invective-free overview of the state of the art.

If there is a technically and economically viable avenue to the utilization of a cold fusion process, it is worth pursuing the investigation by correcting the perceived theoretical short-comings and thereby removing one of the major obstacles to increased professional interest in the matter; this work is offered in that spirit.

As I have attempted to convey in this paper, it is my belief that the lack of theoretical understanding of this subject is grounded in the inability of current models to couple the action of the quantum level with the action of spacetime on a cosmic scale. Despite its century of success, general relativity still has no widely accepted explication of the coupling of spacetime and matter at a quantum level; that is, no explication of quantum gravity. And despite its refinement in observation and experimental control down to the nano scale and beyond, the standard model of particle interactions has no explication of this coupling and is at an impasse.

This may be because theoreticians take the results of experiment and try to fit them into the successfully established modeling; when the results fit the model in a straightforward manner, the model is bolstered, but when there is a lack of fit, the response is often to engineer a system of scaffolding and buttresses to keep the theoretical superstructure upright. Sometimes the impetus to enhance the superstructure is valid both for the model and to the satisfaction of the theoretician, but often it can become a set of blinders to a fuller understanding. The history of innovation in general consists of doing more with less, by sometimes revising the foundations and in some cases bulldozing the foundations and rebuilding from the ground up.

Development of this toy model grew out of an initial desire to understand gravity on a quantum level as a function of quantum action and therefore of  $\hbar$ . I began with a couple of assumptions, one being that gravity, despite being presented as a result of spacetime curvature by general relativity and not due to a force, still involves an interaction of basic physical particles, where interaction necessarily implies a force, but in this case a stress force and not a body force.. The other was that fundamental particles are some form of more or less stationary waves consisting of oscillating strains of the spacetime fabric that are able to congregate at nuclear density without annihilating each other, though initially I had no idea what that form might be. With respect to such wave forms,  $\hbar$  represents the spin angular momentum of the waveform. It quickly became apparent that if the speed of light and  $\hbar$  are invariant, the quotient  $\hbar$  over the speed of light must be as well, and the resulting time independent inertial constant,  $\tau(\text{tav})$ , emerged as a helpful central analytical component of a rest mass quantum model in which particle phenomenology is seen to be based on an underlying wave ontology.

I decided to see according to Newton’s gravitational law what the strength of that force might be between two neutrons, the more massive of the two condensed matter nucleons, in “contact” with each other, which

to me meant using the reduced Compton wavelength of the neutron as the distance of separation. The result was something like the development in section 2a as quantified in (1.29). Though it initially lacked the differentials and general context as a function of a change in stress, it clearly pointed to the square of the neutron Compton wavelength as the value of what had to be a fundamental interaction. I was surprised when I could find no reference to this phenomenology online, and I went in search of an explanation. I was pointed to a string theorist, the first of many, who seemed mildly perplexed and told me to investigate the relationship of this finding to Planck's constant,  $h$ -bar, which I have done.

Along the way, I have made use of certain sources, some of which are listed below. As this is a model of quantum wave phenomena emerging from a classical continuum, chief among these has been Physics of Waves, by William Elmore and Mark Heald, both for the development of the Euler formalism and the complex wave and for their treatment of the stress and strain tensors. Eventually the physical nature of the fundamental rotational oscillation as shown in Diagrams 0 to 6 became apparent, with its relationship to spin, the magnetic moment, the capacitive-inductive nature of the inherent spin energy and eventually it became apparent that something must be energizing the fundamental oscillation. In other words, the inherent spin energy and action, charge, and magnetic moment of the neutron, proton, and electron could be modeled as emergent properties of a constrained wave and not input as free parameters or inferred to some deeper level of ontology of quarks and leptons.

As the accelerating expansion of the cosmos was well publicized, it seemed probable that this acceleration serves as a source; it also explained the predominance of matter over anti-matter, the latter being a feature of a contracting region of spacetime in this model. I have not devoted a lot of study on the nature of the electron, which in this model is derived from the fundamental oscillation of the neutron. In this regard it has never made sense to me how the necessary number of electrons and protons as required to establish charge conservation were generated in a big bang, when if they are both the product of beta decay, charge conservation is straightforward. At some point, from the continuity conditions of the model it became clear that beta decay must be related to the force of expansion operating on the periphery of a free neutron, and analysis showed that it was in fact tuned to a Hubble strain rate of around 73.08 km per Mpc per second, as I prefer to view it dimensionally.

I have used a form of dimensional analysis from the first in this model, which has no extraneous parameters and is not stochastic, and as a result I have been able to avoid some of the pitfalls that I believe ensnare some cosmological investigations. For one, from this perspective neither big bang high energy or quantum mass at the Planck scale has ever held much sway as a principle factor in understanding either the quantum or cosmic system. I don't think of quantum energy in conventional terms of Mev or Joules, but rather dimensionally as angular frequency, as angular wave number times the speed of light. Using the notion of an inertial constant within the context of a quantum wave mechanism, mass is simply wavenumber, ostensibly a time free parameter; by evoking time using the invariant speed of light, energy is simply frequency. In a natural system, for the fundamental oscillation they are both equal to 1. With respect to mass, aggregations of matter are then the summation of the number of particles in a group less any nuclear, atomic, or molecular binding energies that the aggregations liberate.

Applying the inertial constant with the basic breakdown of the Euler derivatives and integrals as stated in section 0a allows a compact way of viewing the dynamic properties of a fundamental quantum wave form. The current big bang notion of having a tremendous amount of energy emerge from a singularity to cool and condense into the form in which we now live requires the addition of a fairly large number of free parameters with no understanding of their ontology to my way of thinking; the ratios of neutron, proton, and electron mass, the underlying quark and leptonic structure, the basis of fermionic half spin and bosonic integer spin, the missing mass of beta decay, the value of the fine structure constant, Newton's gravitational constant. That is not to say that it cannot happen that way; the phenomenology of particles appears to be well known and their interactions statistically well determined, but the lack of understanding of a fundamental mechanism does not mean that the phenomenology does not accurately reflect a yet to be understood ontology.

To my mind this state of affairs offers a less than compelling logic for what we currently observe in the cosmos, which can be addressed with the notion of a non-singularity, i.e. three-dimensional manifold, finite source of initial maximum inertial density that, under an off-manifold stress from a fourth-dimension, expands and is spun up over time like a cosmic flywheel to eventually generate baryonic matter to form stars and condensed matter planets and beings like us who create models. This may be a singular event, or if we are accepting of the notion of conservation of energy (and power), a phase of a current cycle of expansion and contraction that is one of an endless series of such. I believe the possibility that most baryonic matter is generated from active galactic nuclei serving as inertial sources—black holes as sources rather than sinks—and not from a big bang singularity, albeit with a rapid decay of some neutrons to hydrogen in plasma form, with some as deuterium, and then helium and some lithium, deserves study.

While I have not researched the specific computational methodology used in the determinations, dark matter of the  $\Lambda$ CDM model is reported in a 2013 ESA Planck report as 25.8 +/- 0.4% of the total mass/energy content of the cosmos or roughly 5.35 times the baryonic (and leptonic) quantity at 4.82 +/- 0.5%. This content is needed to account for the observed failure of stellar rotational velocities about the galactic centers to decrease with distance from those hubs in accordance with Newtonian dynamics. The alternative is to account for this discrepancy with a modification of Newtonian dynamics such as MOND.

From the perspective of this wave model, the initial inertial density of spacetime is captive to the individual wave action of rotational oscillation, including the symmetric components responsible for quantum gravity as developed here, in the peripheries of generated baryonic matter. In this regard, the individual wave properties of quanta as quantified in the standard model, specifically the reduced Compton wavelengths of the baryons and the electron, are the limiting stress points—nodes, antinodes, capacitive, and inductive moments—of their wave action in this model; the physical waves themselves necessarily extend beyond these local parameters. A phenomenological fact is mentioned in that regard without further analysis. The fundamental rotational oscillation modeled herein for the neutron can be defined, as has been done elsewhere, as an extreme Kerr metric for a quantum black hole. The ratio of the volume within the surface of the ergosphere including the black hole and the volume within the event horizon only of such black hole is 5.52233. It is assumed that the density within the event horizon is 1 and that the density of the region between the ergosurface and the horizon approaches but does not equal 1, therefore the ratio of inertial density between the two will be less than 5.52233, compared to the Planck report above.

In addition, there is nothing in the development of this model that suggests that the spacetime strain on a local scale responsible for baryonic oscillation precludes the occurrence of large-scale torsional strain of the spacetime fabric responsible for galactic rotation. Thus, while the expansion stress as evidenced by the Hubble rate responsible for the oscillation of baryonic matter and registered as exponentially accelerating cosmic expansion in the large voids between galactic webbing, it does not appear to be operating within galactic environments other than in maintaining those oscillations in this model. Within those environments the density of the spatial substrate is maintained by the electromagnetic and gravitational interactions of quanta, while galactic rotational rigidity as evidenced by barred spirals and non-Newtonian dynamics appears to be bolstered by large scale torsional stress and strain. In short, the occurrence of what is dubbed dark matter is indicative of large-scale density differentials between the extra-galactic voids and galactic webbing, without the need to reference another type of particulate matter.

Finally, the customary cosmological constant value normally assigned to the field equation of general relativity and reported in the ESA Planck report of 2013 as corresponding to a dark energy density of 0.693+/-0.013 and revised downward slightly in 2015 to 0.6911+/-0.0062, as a percentage of mass/energy of the total, is at or suggestively close to the natural log of 2 at 0.693147..., indicating that it speaks to the fact that the Hubble rate, instead of being a first order velocity, is an exponential measure of expansion, that is, Hubble is a second order or accelerating rate, as developed above. When it is understood that such expansion is responsible not only for the apparent expansion of the cosmos as evidenced by red shift, but also for driving of all local particle action, as herein developed, the value of the cosmological constant within the context of the field equation of general relativity is seen in a different light. The natural log of 2 as in (1.62) gives a Hubble rate in today's seconds of 9.274 billion years.

The axioms on which this model is based are few and not unreasonable to my thinking grounded in classical wave mechanics, nor do any of their developed implications or application run in the face of observation, as far as I know. This model is offered because after twenty some years of study on this matter it continues to answer many questions concerning physical understanding that I have not been able to find addressed in the extant literature, and I believe if it gets a proper vetting it will be of benefit to the discussion and understanding of cold fusion. I am recently encouraged with regard to the developments of this model of rest mass and derived photonic energy as a function of cosmic accelerating expansion by the recent announcement of the results of the study of Riess et al with respect to a determination of the Hubble rate at  $74.03 \text{ km } \pm 1.42 \text{ km } \text{ s}^{-1} \text{ Mpc}^{-1}$ . It is believed this analysis addresses the concerns in that study of the  $4.4\sigma$  between their figure and the results of the  $\Lambda$ CDM Planck study at  $67.74 \text{ km } \pm 0.46 \text{ km } \text{ s}^{-1} \text{ Mpc}^{-1}$ , while offering an acceptable alternative to  $\Lambda$ CDM.

In addition to the determination from this model of the Hubble rate, the derivation of the gravitational constant, the explication of the dynamics of rotational oscillation of baryonic matter, the ratios of fundamental condensed matter particle rest mass, the accounting for the missing mass of beta decay, the nature of elementary charge and spin, and the derivation of the fine structure constant offer reason for a thorough review of this model. All photonic energy, which in the standard particle and cosmological models is handled as a free parameter, is not actively addressed in this model as it is held to be predicated on beta decay as a function of electron/neutrino activity in keeping with the structures of quantum mechanics.

## **Bibliography, Citations, and Other Resources**

Astronomy and Astrophysics 338, 856-862 (1998), “Magnetically supported tori in active galactic nuclei”, Lovelace, Romanova, and Biermann.

Exploring Black Holes, Taylor and Wheeler, Addison Wesley Longman, Inc, New York, 2000.

The Extravagant Universe, Kirshner, Princeton University Press, Princeton, NJ, 2002.

The Feynman Lectures on Physics :Commemorative Issue, Feynman, Leighton, Sands, Volume I, Addison-Wesley Publishing Company, Inc., Reading, Massachusetts 1963.

Fundamentals of Physics, Fifth Edition, Halliday, Resnick, Walker, John Wiley & Sons, Inc. New York, 1997.

Gravitation, Misner, Thorne, and Wheeler, W.H. Freeman and Company, New York, 1973.

Mathematical Methods for Physicists, Fifth Edition, Arfken and Weber, Harcourt Academic Press, New York, 2001.

Physics of Waves, Elmore and Heald, Dover Publications, Inc., New York, 1985.

This was the primary source for wave, elasticity and tensor equations.

The Six Core Theories of Modern Physics, Stevens, The MIT Press, Cambridge, Massachusetts, 1995.

Three Roads to Quantum Gravity, Smolin, Basic Books, New York, 2001.

The Theoretical Minimum: What You Need to Know to Start Doing Physics, Susskind and Hrabovsky, Basic Books, New York, 2013

National Institute of Standards and Technology, These are the **2002 CODATA recommended values** of the fundamental physical constants, the latest CODATA values available. For additional information, including the bibliographic citation of the source article for the 1998 CODATA values, see P. J. Mohr and

B. N. Taylor, "The 2002 CODATA Recommended Values of the Fundamental Physical Constants, Web Version 4.0," available at [physics.nist.gov/constants](http://physics.nist.gov/constants). This database was developed by J. Baker, M. Douma, and S. Kotochigova. (National Institute of Standards and Technology, Gaithersburg, MD 20899, 9 December 2003).

Table of Nuclides, Nuclear Data Evaluation Lab., Korea Atomic Energy Research Institute (c) 2000-2002, <http://yoyo.cc.monash.edu.au/~simcam/ton/index.html>

R.R.Kinsey, et al., *The NUDAT/PCNUDAT Program for Nuclear Data*, paper submitted to the 9 th International Symposium of Capture-Gamma ray Spectroscopy and Related Topics, Budapest, Hungary, October 1996. Data extracted from NUDAT database (Jan. 14/1999)

Schwarzschild, Bertram, "Tiny Mirror Asymmetry in Electron Scattering Confirms the Inconstancy of the Weak Coupling Constant", *Physics Today*, September, 2005

Wapstra, A. H. and Bos, K., "The 1983 atomic-mass evaluation. I. Atomic mass table," *Nucl. Phys. A* 432, 1-54, 1985, quoted at <http://hyperphysics.phy-astr.gsu.edu/hbase/nucene/nucbin2.html>

Adam G. Riess, Stefano Casertano, Wenlong Yuan, Lucas M. Macri, and Dan Scolnic , "Large Magellanic Cloud Cepheid Standards Provide a 1% Foundation for the Determination of the Hubble Constant and Stronger Evidence for Physics Beyond  $\Lambda$ CDM", <https://arxiv.org/abs/1903.07603>

Wikipedia.com for various sources of general information.



# Isotropic Expansion Stress on a Unit Space (IESUS)

An Addendum to Section 2g — Muon & Tau Families

of

A Condensed Matter Model of Particle Genesis (CMMPG)

as a Function

of an Accelerating Cosmic Spacetime Expansion

Fundamental Rest Mass Quanta as  
Simple Harmonic Rotational Oscillations of  
the Spacetime Continuum,

Driven by Cosmic Expansion

with

Application of the Analysis to the

Experimental Field of Cold Fusion

<https://uniservent.org/pp01-condensed-matter-model-of-fundamental-particles/>

Martin Gibson

In the latter part of July 2021, through the Twitter presence of Stacy McGaugh, @DudeDarkmatter, of the Department of Astronomy at Case Western Reserve University in Cleveland, Ohio, and his paper “Testing galaxy formation and dark matter with low surface brightness galaxies”, I became aware online of the work of Robert A. Wilson from his blog website at <https://robwilson1.wordpress.com>. Dr. Wilson is Emeritus Professor of Pure Mathematics at the School of Mathematical Sciences, Queen Mary University of London. According to his website, his work has been in group and representation theories, with an interest in its application to the foundations of physics since 2007. That work appears to have intensified with his early retirement in 2016, and has led him to the conclusion that there are fundamental contradictions incorporated in the application of these theories to the physical modeling of general relativity and quantum theory that have prevented a unifying understanding of the physical phenomena on which the modeling is based.

In a monograph by Professor Wilson entitled A GROUP-THEORIST’S PERSPECTIVE ON SYMMETRY GROUPS IN PHYSICS, <https://arxiv.org/pdf/2009.14613.pdf>, page 18, equation (17) develops the following equation as exact within the standard uncertainty, in which it expresses the following relationship of the observed rest mass for fundamental particles of baryonic and leptonic matter, generally considered as being of invariant rest mass in the standard model of particles. Text communication with Professor Wilson stated that he came across the statement from other sources in his studies; based on the fact that the equation is confirmed by the CODATA 2018 stated values of particle mass as exact within standard uncertainties, we see no need for further academic study of the source of the equation, while expressing gratitude to whoever first noticed it to be the case. If the analysis extant in the downstream development of this equation has priority in a published form, I will remain grateful, though one must wonder why, if this is the case, it has not been given the attention it would logically appear to deserve.

We have inverted and restated the order of the equation from that text to facilitate a better understanding of the process of particle evolution as developed in the work from which this is a continuation, based on the insights this equation offers,

$$5m(n) = 3m(p) + m(e) + m(\tau) + m(\mu) . \quad (1.101)$$

## Astrophysical Observation

Based on recent observation and related calculations of scientific sources, there are in the neighborhood of  $10^{80}$  particles of baryonic matter in the known universe; that is, neutrons and protons with correlated electrons, bound or free, along with other rest mass particles. As far as this author is concerned, neutrinos are not rest mass particles for the simple reason that they do not rest. They constantly move at or near the speed of light unless their energy is reabsorbed in the process of interaction with a proton to produce a neutron. In a wave model, neutrinos can be understood as a type of discrete torsional compression wave resulting from the emission of a lepton. Thus, when an electron is emitted from a neutron which transforms into a proton in the process of beta decay, and the electron is stopped in its translational motion by interaction with another particle or field, the torsional compression wave of the medium continues on. The torsional or twisting nature of this compression wave, as with the torsion of rest mass particles from which they originate, are responsible for the property recognized as intrinsic spin in the standard model.

Based on the etymology of the word, a ‘particle’ is a “minute portion, piece, fragment, or amount” of some greater qualitative *thing*, often invariantly quantized in quantum physics as a discrete value, be it wavelength or its inverse wavenumber or as a proxy for wavenumber, mass, according to a variety of conditions. The standard model of particles as currently presented assumes the thermal environment of a big bang as the condition required for the quantization of various particle fields from their various field sources or perhaps a single source, followed by the secondary composite construction of baryons and eventually as composites of the baryons, the elements. In the logic of the wave model presented here, a thermal environment is a measure of the interactions of particles already created and moving at high velocity; it is not a condition of their quantization, their creation as particles. Instead, the quantization of particles as waves are conditioned by two constraints, the finite inertial density of the wave bearing medium in and of which the waves are quantized and a finite stress, being the function of an expansion stress force operating on the medium and gauged by the cross sectional area on which the force is operating over a range of angles from normal to tangential to that area.

From this perspective, there are only three stable, condensed matter particles in existence in the universe, protons, electrons, and while they remain in nuclear congregation in an atom under certain conditions, the neutron. Absent that nuclear congregation, free neutrons decay into a proton, electron, neutrino, and apparently give up some mass in the process. Understanding the nature of this small amount of ‘missing particle mass’ is the objective of this analysis.

The universe is very large. According to some cosmological modeling, it would take an observer who did not age or die almost as long as the universe has existed, traveling at the speed of light, to get as far as anyone can see with the strongest telescopes. Yet then again, the universe may be infinite in both extent and age, or better stated, limitless and ageless.

Baryons, on the other hand, are very small. If they were all of neutron size—using the Compton angular wavelength at  $2.1 \times 10^{-16}$  meters as a gauge of particle radius, disregarding any charge, spin or other dynamics—and were laid out in a Euclidean line next to each other, there would be a few more than  $10^{15}$  of them lined up in a meter. This means there would be a bit more than  $10^{46}$  of them in a cubic meter if they were packed to maximum density, after the form of an ideal cuboctahedral lattice. Oddly enough, with a radius of  $1.5 \times 10^{11}$  meters, based on a volume of approximately  $10^{34}$  cubic meters, the  $10^{80}$  known baryons would just fit inside a sphere with a circumference delineated by the earth’s orbit around the sun. We might think of such a sphere as a primordial neutron star of earth orbit size.

In such case, the rest of the universe would be a vast empty space, devoid of matter or light. There are said to be  $2 \times 10^{12}$  or two trillion galaxies in the observed universe. If the  $10^{80}$  baryons were evenly distributed among them, this would place a sphere of 10,000-kilometer radius packed with neutrons at the center of each galaxy. Again, if evenly distributed, with an estimate of  $10^{22}$  stars in the universe, this means approximately  $10^9$  or one billion stars per galaxy, which once again, if all the packed baryons were in the stars instead of the galactic centers, the individual packed stellar cores would have a radius of 10 kilometers.

Obviously, some stars and some galaxies have more mass than these figures and perhaps many more have far less. For our sun's mass, the figure would be about 1.5 kilometers.

This total mass of  $10^{80}$  baryons are anything but evenly distributed, not in the stars, not in the galaxies or galactic groups, and not throughout the extent of the cosmos itself. Virtually all the galactic matter is observed in filaments along what appear to be strands and diaphanous sheets of light transferring matter, connected perhaps by gravity, perhaps by inertia, perhaps by electromagnetic forces. This is often deemed to be supported by a form of dark matter that responds to gravity but does not emit light, separated by large regions apparently devoid of matter or of any energy other than whatever electromagnetic energy transits through these voids, thereby allowing the observation of this distribution.

According to the modeling of general relativity, the threshold size of the event horizon as a radius of an extreme Kerr black hole (KBH) is 2.9 kilometers for a star of 2 solar masses or  $3.93 \times 10^{30}$  kilograms. Conventionally in general relativity, the particles which are inside such black hole are imagined as stretching toward a single point at the center of the KBH.

2.9 kilometers is coincidentally also the radius of the same weight as  $3.93 \times 10^{30}$  kilograms or  $2.3 \times 10^{57}$  neutrons if they were packed as indicated at maximum spherical packing. If this mass of neutrons were either oscillating individually in such a manner that they did not or could not decay and give off electrons or photons or was condensed to a uniform continuous density equal to that of the stated neutron spherical packing, this aggregate sphere would give off no light or other electromagnetic radiation and would therefore be indistinguishable from a conventionally modeled KBH, where the nature of an extreme Kerr Black Hole means that it is spinning at the event horizon and the surface of our sphere, at the speed of light, in this current model either as individual neutrons or as an aggregate mass.

The same simple formula used to calculate the threshold event horizon of a black hole can be used on masses of the same maximum density but lesser quantity such as the mass of the earth, and we will find that the calculated event horizon will be smaller than the actual maximum density.

$$R_{BHH} = \frac{G}{c^2} M \quad (1.102)$$

Here  $R_{BHH}$  is the radius of the black hole horizon,  $G$  is Newton's gravitational constant,  $c$  is the speed of light and  $M$  is the mass of a celestial body. Thus, the calculated black hole radius,  $R_{BHH}$ , is linearly related to  $M$ , all other parameters being invariant. (Some sources use a coefficient of 2 for the terms on the right in calculating  $R_{BHH}$ .)

Using this calculation, the radius of the earth mass at maximum density is 36 meters; that is if all the mass of the earth was collapsed to maximum density, it would fit into a sphere 72 meters in diameter. The calculations for a KBH event horizon based on the earth's mass is 4 millimeters, considerably smaller, and apparently an indicator of the fact that the earth's mass will not collapse into a black hole.

According to the above equation, with an estimated mass for the observed universe of  $1.76 \times 10^{53}$  kilograms, the radius of the black hole horizon is  $1.24 \times 10^{26}$  meters which is 13.1 billion light years, which would indicate that the entire universe is within a black hole event horizon. It is worth noting that perhaps either due to serendipity or some unrecognized causative or computational methodology, even distribution of this quantity of baryons amounts to a density of very closely to 1 baryon per meter. From the above back of the envelope calculations, the average stellar mass is over three times the mass of a threshold black hole.

In the cosmology of general relativity, black holes are universally thought of as being gravitational sinks leading to gravitational collapse, i.e. to a singularity, yet there is nothing in these calculations to suggest that, beyond the scale of two solar masses, everything else is not already within the event horizon of a larger black hole. Clearly something is missing from this thinking.

In the absence in the standard model or general relativity of an understanding of a quantum generation of gravity, the formation of galaxies and of baryons themselves remains an unaddressed mystery. According to current thinking, both the largest and the smallest of material phenomena is modeled as emerging from a hot big bang singularity, apparently for the single simple reason that if the Hubble rate is a velocity measure of isotropic expansion, if we trace this velocity back 13 plus billion years, all  $10^{80}$  baryons must have emerged at the same time from a single point, a point necessarily outside any current understanding of time or space.

But spatial expansion appears to be accelerating, which means among other things that a scenario exists in which the expansion is understood to be logarithmic, which if gauged by the current Hubble rate as an acceleration, indicates that the expanding extent doubles every 9 plus billion years and is much older than generally conceived. Another and different scenario exists in which the Hubble rate is a registration of the force—a dynamic acceleration—of beta decay, with a redshift from energy loss based on the distance from which it is observed, which is in turn interpreted as an expansion of the cosmos.

Perhaps the greatest boost in support of the notion of a big bang is the correlation of nucleosynthesis of the fundamental elements—of hydrogen—protium, deuterium, and tritium, of helium—helium 3 and helium 4, and of lithium 7—all of which is theoretically ascribed to the intense “heat” or high energy of electrons and quarks, the latter of which were created in a theorist’s mind to explain the magical condensation of 3 of the right type in the right mix into a neutron or a proton, the latter with just the right energy to bond with an electron. We have shown earlier in the tract for which this one is an addendum, another wholistic explanation for the generation of the three mostly stable particles, explaining the quark phenomena, quantum gravity, and a few other quandaries in the process.

Many unquestioned assumptions go into making the fruit cake that is the standard model as well as those that get whipped into the hard sauce topping that is general relativity—not to mention the couple of dozen free parameters for the ingredients. One of these is Newton’s gravitational constant, which is obviously by its function a type of force differential, but a force differential with respect to what? We have shown that it is a quantum force differential with respect to differential stress, which includes in its composition a statement of a fundamental gauge for length and mass. We have shown that this gauge can be found in an inertial constant which is equal to Planck’s constant,  $h$ -bar, over the speed of light.

From (1.101) we can now get an understanding of the nature of the missing mass of beta decay in the relationship between the gravitational differential force, the strong force as the fundamental baryon wave force, and the electroweak interaction. We will get an understanding that what is generally thought of as a black hole in general relativity is a field of maximum, not infinite, inertial density that can be an inertial source as well as an inertial sink for the extended field of mass–energy potential, in which it is seen that the mass–energy equivalence of Einstein’s famous equation is a reduced form of a simple generic wave equation. We will get an understanding that the basic structure of the cosmos proceeds not from a singularity but rather from a quiescent uniform condition of maximum density as indicated above, albeit one with an inherent gauged cuboctahedral lattice potential that separates first into the cosmic filaments and membranes as areas of maximum baryonic wave bearing density and rarefies in the volumes of vast voids that provides tension stress on the filaments and membranes at galactic nodes to produce active galactic and perhaps stellar nuclei and the fundamental light elements just indicated above.

We will look next at the particle structures that result from this interaction between the voids—as they expand and move forward in space—and the galactic centers of maximum neutron density. To those who might point to the introduction of a prime mover in this scenario responsible for the cosmic expansion of the voids as a hand of God, we will only point out that it is no different in quality and far more explicative for the observed cosmic state of affairs than the prime mover that started the modeled big bang.

In free space, over a life of 14 to 15 minutes, a neutron( $n$ ) decays through a process, generally known as beta decay, into a proton( $p$ ) and an electron( $e$ ) both of which are stable in free or condensed matter space as a hydrogen atom, specifically as a protium atom which distinguishes it from the heavier atoms of

hydrogen with one or two neutrons in the nucleus as deuterium and tritium respectively. In the high temperature of plasmic space, the stability of proton and electron as discrete particles remains, however in this case as non-binding ionized cations and anions respectively. In contrast, a tau( $\tau$ ) decays over 300 femtoseconds along an assorted branching, roughly 2/3 of the time into an assortment of mesons, which is a hadron similar to a baryon, 1/6 of the time into a muon, and 1/6 of the time into an electron, with other attendant energetic interactions and particles in the form of neutrinos. A muon( $\mu$ ) decays over an average of 2 microseconds into an electron, also with the other energetic interactions. The neutrinos are generally considered to be stable as well, but that is harder to qualify or quantify as they are generally considered to travel at very close to if not at the speed of light and in a manner such that they rarely interact with other particles other than in the case of reverse beta decay, generally denoted as inverse beta decay.

It is noted that baryonic matter along with mesons are modeled as being hadronic, that is comprised of an internal structure deemed to be more fundamental than the hadrons themselves. That internal structure is comprised of the more fundamental quarks, necessarily constrained to the particle boundary by a process known as asymptotic freedom, which basically means that the more distant the quarks in a hadron are from each other, the stronger they are attracted to each other as if they were bound together by unbreakable rubber bands which increases in intensity with strain, and the less free they are to move independently with respect to each other. In the case of the generally stable baryons, there are three quarks producing the structure, while in the case of the mesons, which are extremely short lived—much less than a second—there are only two quarks, as a particle and its anti-particle. The leptonic rest mass particles, on the other hand are deemed to be free of any internal structure as comprised by quarks, and are the stable electron, and the much shorter lived, generally transitional, tau and muon. A more concise and understandable treatment of baryonic and leptonic nature is recapitulated in part from the analysis of CMMPG later. It is recommended that the reader who really wants to understand what is going on in regard to the fundamental particles of physics read the analysis both there and in the some of the other treatments of this material on this website. The reader simply cannot understand the subject of quantum rest mass unless they have digested this material. Fortunately, that material is graphically well supported and requires only an intermediate knowledge of classical wave mechanics with the attendant algebra, calculus, and topology.

## Development of the Tau–Muon Duplet to Deuterium Interaction Path

The rest mass values used in Wilson are from CODATA 2014 expressed in MeV/c<sup>2</sup>, which can be understood with equal validity as a form of spin energy since  $E = mc^2$ . We have added an additional column of the CODATA 2018 figures to indicate that there is no overall change other than perhaps a different calibration behind the calculations, once again validating Wilson’s calculation:

	CODATA 2014	CODATA 2018	
$m(e) =$	0.510 998 9461(31)	= 0.510 998 950 00(15)	
$m(\mu) =$	105.658 3745(24)	= 105.658 3755(23)	
$m(p) =$	938.272 0813(58)	= 938.272 088 16(29)	
$m(n) =$	939.565 4133(58)	= 939.565 420 52(54)	(1.103)
<i>calculated :</i>			
$m(\tau) =$	1776.84145(3)	= 1776.84146(4)	
<i>CODATA</i>			
$m(\tau) =$	1776.82(16)	= 1776.86(12)	

Wilson has calculated the value of  $\tau$ , above, from the remaining experimentally determined values, since it is known experimentally with less certainty at 1776.86(12), within the standard uncertainty. The virtual identity of the calculated value for  $\tau$  from 2014 to 2018 indicates a constraint in the overall precision of the value determinations.

This is followed by mass converted to modular ratio values by dividing all CODATA 2014 amounts above by that of each  $m(e)$ ,  $m(\mu)$ ,  $m(p)$ ,  $m(n)$ , and  $m(\tau)$  to arrive at the following modular values.

$$\begin{array}{rcccccc}
 & \begin{array}{c} * \\ / \\ e \end{array} & & \begin{array}{c} * \\ / \\ \mu \end{array} & & \begin{array}{c} * \\ / \\ p \end{array} & & \begin{array}{c} * \\ / \\ n \end{array} & & \begin{array}{c} * \\ / \\ \tau \end{array} \\
 m(e) = & 1.0 & = & 0.004836334 & = & 0.000544617 & = & 0.000543867 & = & 0.000287588 \\
 m(\mu) = & 206.76828 & = & 1.0 & = & 0.112609486 & = & 0.112454476 & = & 0.059464131 \\
 m(p) = & 1836.152674 & = & 8.88024657 & = & 1.0 & = & 0.998623472 & = & 0.528056144 \\
 m(n) = & 1838.683662 & = & 8.89248733 & = & 1.001378426 & = & 1.0 & = & 0.528784030 \\
 m(\tau) = & 3477.1920 & = & 16.81686062 & = & 1.893738026 & = & 1.891131242 & = & 1.0
 \end{array} \tag{1.104}$$

While it is understood that the various particles are discrete and invariant in their various properties as in this case of rest mass-spin energy, a comparison of these modular arrangements offers nothing to suggest that the five particles are comprised of much smaller quantum packages of some discrete invariant size of mass-energy as opposed to being constituted as a characteristic fundamental wavelength or frequency from a wave bearing continuum of variable inertial density. The fact that the five quantities of (1.103) terminate with various statements of standard uncertainty is logically unsupportive of the notion that each particle is comprised of a set quantity of known discrete units; neither does it negate that possibility. They may or they may not be so comprised while subject to the precision of measuring devices, or they may vary continuously within a range of finite extremes as given by the standard uncertainties, all while subject to the same precision of measurement. On the other hand, if discreteness indicates that the particles are essentially the nature of a wave, it gives no indication one way or the other whether the characteristic wave forms are comprised of a much smaller particulate or of a continuous substrate. We will treat them classically as non-particulate if only as an indication that the field of their observed interactions is continuously differentiable. The uncertainty formalism of (1.103) has not been extended into the modular constructions of (1.104) or latter.

This last paragraph indicates that qualitative, non-stochastic constraints exists that are responsible for the various modular distributions, especially as shown with the effective percentages in the  $*/n$  and  $*/\tau$  columns and the fact that the particles greater than  $e$  are not comprised of discrete units of  $e$  as shown in the column  $*/e$ . Such constraints can be understood analytically as discrete in terms of geometry and wave mechanics and the mathematical fundamentals applied to each of these two disciplines.

We parse these parameters of (1.101) over three lines, for reasons that should become clear, where the explicit quality being evaluated above as masses from the first column,  $*/e$ , of (1.104) is implicit in the following particle designations.

$$5n = \left\{ \begin{array}{c} n \\ 2n \\ 2n \end{array} \right\} = \left\{ \begin{array}{c} p+e \\ 2p \\ \tau+\mu \end{array} \right\} = 3p+e+\tau+\mu \tag{1.105}$$

Assuming conservation of mass-energy in a physical system involving the interactions of the five fundamental particles, the missing mass in the inequalities below of each line is placed in square brackets,

which we will think of as different types or instances of transformed or transformational energy or in some cases perhaps as operational catalyts.

$$\begin{aligned}
n > p + e &\rightarrow \Delta m = [ +1.5310 ] \\
2n > 2p &\rightarrow 2\Delta m + 2e = [ +5.0620 ] \\
2n < \mu + \tau &\rightarrow 3\Delta m + 2e = [ -6.5930 ]
\end{aligned}
\tag{1.106}$$

From equation (1.57) of CMMPG, the first line of this parsing to include the missing mass of beta decay,  $\Delta m$ , is restated as

$$n = p + e + [ \Delta m ] \tag{1.107}$$

Though the term ‘decay’ and ‘decay path’ shows up often in this treatment, it should be understood that the notion is in some sense unintentionally pejorative even for the expert in that it implies, based on common usage, a decline in some state or condition from a prior pristine or ideal status, when in fact it is simply an indication of interaction between particles or between particles and their fields. From our dimensional analysis above, using the proportional modular values of  $*/e$  we have

$$1838.6836_n = 1836.1526_p + 1.0_e + [ 1.5310_{\Delta m} ] \tag{1.108}$$

The values for missing mass,  $\Delta m$ , are computed as required to satisfy this equation and is the same for all three of the parsings, based on the comment in (1.112) below. The quantity shown is empirically based and not derived from any deeper analysis of the current standard model.

The second line of (1.106) is a straightforward conclusion of the first line of the parsing from (1.101)

$$2n = 2p + [ 2(e + \Delta m) ] \tag{1.109}$$

For the two protons of the second line of (1.106) we have

$$\begin{aligned}
2(1838.6836_n) &= 2(1836.1526_p) + [ 2(1.0_e + 1.5310_{\Delta m}) ] \\
2(1838.6836_n) &= 2(1836.1526_p) + [ 2(2.5310_{e+\Delta m}) ] \\
3677.3672_{2n} &= 3672.3052_{2p} + [ 5.0620_{2e+2\Delta m} ]
\end{aligned}
\tag{1.110}$$

Since (1.101) is empirically determined to be exact within the standard uncertainty, the 3 instances of missing mass and 2 electron rest mass in the first two parsings must be equal, but of opposite sense, to the additional mass of the tau and muon as required to balance the equation of the third line with those two neutrons.

Finally, for the third line we have the following, were we transpose the missing masses in the final line

$$\begin{aligned}
2(1838.6836_n) &= 3477.1920_\tau + 206.7682_\mu - [ 2(1.0_e) + 3(1.5310_{\Delta m}) ] \\
2(1838.6836_n) &= 3477.1920_\tau + 206.7682_\mu - [ 2(2.5310_{e+\Delta m}) + (1.5310_{\Delta m}) ] \\
3677.3672_{2n} &= 3683.9602_{\tau+\mu} - [ 6.5930_{2e+3\Delta m} ]
\end{aligned}
\tag{1.111}$$

∴

$$3677.3672_{2n} + [ 6.5930_{2e+3\Delta m} ] = 3683.9602_{\tau+\mu}$$

In classical wave mechanics, for simplicity using the model of an ideal string, the ‘mass’ of a wave is a measure of the linear inertial density of the string when subjected to a transverse force operating to displace a portion of that string. The more massive the string, given some standard unit of force, the smaller will be the section of the string that can be displaced, represented by a wavelength and inversely by a wavenumber. That same linear density measure of mass, if gauged by the same standard unit of force, will apply whether the string is at rest or has been set in motion by that force, subject to whatever differential conditions are present in that motion to change that density. Therefore, the mass value of  $3677.3672_{2n}$  is present in (1.111) in the initial conditions of neutron density–black hole source material whether it is found in wave form or in the wave substrate.

There is little reason to accept the apparent empirical validity of the value of the  $\Delta m$  without at least some attempt at analysis of the cause for and the structure of the value of 1.5310 or the ratios of the various fundamental particle mass, and we will offer two such analyses which are related to one another. The first of these is found as a mathematical analysis in CMMPG on page 36 at ‘2e – The Missing Mass of Beta Decay’. The geometric analysis is included in partial form below in this addendum, IESUS, but first the mathematical basis.

The related mathematical analysis establishes a two-dimensional natural exponential component of a three-dimensional differential form of the natural log. Both of these can be found in greater detail in my work on this website, <https://uniservent.org/pp08-4-wave-foundation-version-2-2/>, with the mathematical analysis in the Appendix D – Exponentiation. The geometric analysis can be found there starting on page 41 and is reproduced in large part later in this addendum. The quantification of 2.531... stated here includes the sum of the linear, 1, and transverse, 1.531..., components, indicated by  $e$  and  $\Delta m$  respectively, in both the mathematical analytical results and the empirical observation and establishes a verification and torsional understanding for the nature of the ‘missing’ mass, so that  $\Delta m$  is in all cases in this wave analysis understood as the twisting portion of the energy embodied in the wave node at a point of wave transmission, customarily thought of as a particle decay.

$$\begin{aligned}
 &\text{Mathematical analysis of the natural logs: } 2.531584394 \\
 &\qquad\qquad\qquad + 0.000596696 \quad \Delta 3.25e^{-7} \\
 &\text{Empirical observation: } 2.5310987698 \\
 &\qquad\qquad\qquad - 0.003449702 \quad \Delta 1.288e^{-6} \\
 &\text{Geometric analysis of expanding spacetime: } 2.527550298 \\
 &\text{Relative uncertainties are gauged with respect to the neutron rest mass at } 1838.683662.
 \end{aligned}
 \tag{1.112}$$

Of interest is the fact that although the totals on each side are exact in (1.101), each parsed line is off by a relevant, and obviously quantized amount, generally referred to as the missing mass attributed to beta decay on the first line and for similar reasons the missing mass and the electron mass for both protons on the second line. In order to balance this missing mass which has been *added* to the first two lines, we will need to *subtract* the same amounts from the tau and muon on the third line in the following or transfer it as an addition to the left hand side of (3) to arrive at (3b).

$$\begin{aligned}
 1) \quad n &= p + e + [\Delta m] \\
 2) \quad 2n &= 2p + [2e + 2\Delta m] \\
 3) \quad 2n &= \mu + \tau - [2e + 3\Delta m] \\
 3b) \quad 2n &+ [2e + 3\Delta m] = \mu + \tau
 \end{aligned}
 \tag{1.113}$$

This third line raises questions about the nature of the entire assortment of quantum particles in the standard model of particles and their interactions. The first line is well recognized as a statement of beta decay, with



the second line a statement of two instances of such decay in which the protons are ionized and the electrons along with the differential mass are missing. Both indicate the decay of unstable, perhaps free, neutrons into stable protons and electrons and as parsed appear to indicate a spontaneous process of the release of energy from the nucleon,  $n$ , as  $e + \Delta m$ , with transformation to become  $p$ . As indicated in section ‘2d — Derivation of Beta Decay as a Function of the Hubble Rate’,  $e + \Delta m$  is anything but spontaneous in the global sense, and represents in tandem a coupling/uncoupling constant in the relationship between the neutron and the protium atom and thereby the rest of composite elemental and molecular matter.

The electron, of either charge,  $e^-$  or  $e^+$ , are understood as having no internal structure in contrast to the quark structure of the neutron and proton, but what that means from this modeling, CMMPG & IESUS, is that the interaction of the inductive and capacitive torques on the nodal structures of what are essentially the same fundamental, discrete 3 dimensional wave structures of all forms of rest mass quanta behave differently under different continuity conditions associated with the Hubble stress and strain to explain the distinctions we empirically find in baryons and leptons, either as matter and anti-matter, according to the following chart.

Study of these charts and the spin diagrams from which they were taken, indicates the torsional characteristics of the process of particle wave dynamics including the twisting transformation generally referred to as beta decay. This is generally modeled as occurring in the confines of an atomic nucleus, or perhaps for a neutron in free space, but we can also view it as fundamental to the genesis of rest mass particles as part of a process of nucleo-synthesis at the event horizon of a black hole source, a process in reverse to that customarily modeled at the event horizon of an extreme Kerr black hole in general relativity.

In general, black holes are customarily treated as gravitational sinks, but in the absence of an understanding of the nature of quantum gravity, this is an unwarranted assumption of general relativity, which has led to the concept of all matter emerging from an inertial source modeled as a big bang singularity. I will not go into the various reasons that this has never made logical sense to me, but I can say that based on the notion of conservation of energy and other properties, the laws of physics have always been treated as being capable of interpretation with the arrow of time in reverse. As such, the black hole dynamics attributed to gravitational attraction as an inertial sink within the context of an inert background space or spacetime are equally valid if the active source of dynamism is an isotropically expanding space or spacetime against an otherwise inertial source or sources such as active galactic nuclei (AGN) of black hole or neutron density at maximum packing, as a uniform continuum or a gauged lattice potential, which would be my preference.

From this perspective, the third line of (1.113) indicates a more complex process for a series of different reasons. First, the tau and muon are even more unstable and extremely short-lived particles than the neutrons which decay quickly in free space, though they are capable of indefinite stability in suitable congregation with other nucleons. As the rearrangement of the missing mass and  $e$  indicates in (1.114), as a reverse decay process, the bracketed mass–energy as an expansion stress must be added to or interact with the density of 2 neutrons on the left in order to produce, apparently in simultaneous manner, the heavier tau and muon, as indicated here, where the  $e$ ’s at each end represent expansion stress sandwiching the  $3\Delta m$  on either side of the developing wave forms to produce the tau and muon

$$[e + \Delta m] + n + [\Delta m] + n + [\Delta m + e] = \tau + \mu, \quad (1.114)$$





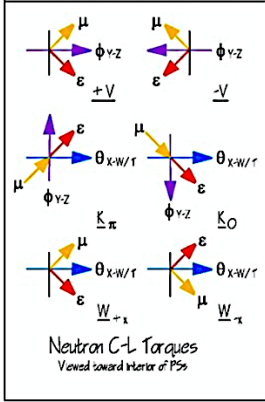
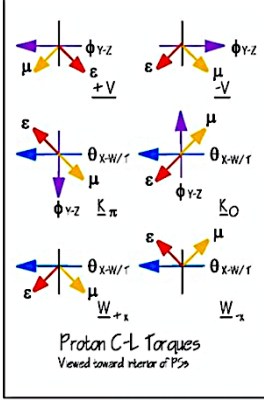
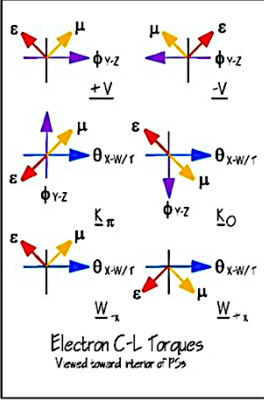
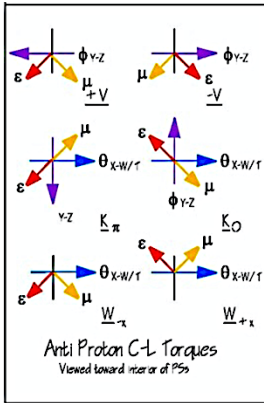
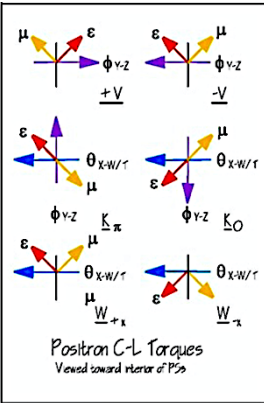
before quickly decaying into other particles, so that

$$\tau + \mu - [2e + 3\Delta m] = ? \quad (1.115)$$

If the mass of the various particles is invariant, other than at the time and conditions they are involved in a decay process, these last mathematical statements suggest that the tau and muon are necessarily produced together, as a couplet or duplet, by an energy transformation process, attributed to missing mass, interacting in a manner to redistribute the two mass equivalents of the neutrons on the left to the two transitional states on the right. In addition to (1.114) we can also combine parsing 2 and 3 of (1.113) to get

$$2p + [4e + 5\Delta m] = \tau + \mu, \text{ or} \tag{1.116}$$

$$n + p + [3e + 4\Delta m] = \tau + \mu$$

 <p>Oscillating restorative torsional wave force from initial torsional displacement</p>	 <p>Resultant rotational spin force from restorative wave oscillation</p>	 <p>Capacitive torque from moment of maximum restorative power rotating with spin</p>	 <p>Inductive torque from moment of maximum restorative action rotating with spin</p>
<p><b>Spin Diagrams</b> The diagrams from which these torque charts are taken demonstrate these five conditions in detail as found in the main paper.</p>	<p><b>Neutron</b> Neutral Baryon Resonant Mode Capacitive &amp; Inductive torques operating at maximum reinforce the nodes and antinodes of the <math>\phi</math> restorative torsion and <math>\theta</math> rotational spin which under increasing Hubble stress results in beta decay</p>	 <p>Neutron C-L Torques Viewed toward interior of PSs</p>	<p><b>Beta Decay</b> Hubble stress drives the electromagnetic force as <math>e + \Delta m</math> decouples the energy of the neutron with a spin flip from an inductive moment advance to emit the neutrino-electron and reduce the spin energy of the neutron to that of a proton</p>
<p><b>Proton</b> Charged Baryon Positive Inductive Mode With beta decay, <math>\mu</math> advances induction over capacitance as positive charge and reinforces restorative force while <math>\epsilon</math> maintains capacitance through spin</p>	 <p>Proton C-L Torques Viewed toward interior of PSs</p>	<p><b>Electron</b> Charged Lepton Negative Inductive Mode All <math>\mu</math> torques reinforce restorative and spin forces and retard capacitive torques <math>\epsilon</math> at all nodes/antinodes leading to the conclusion that leptons lack internal structure</p>	 <p>Electron C-L Torques Viewed toward interior of PSs</p>
<p><b>Anti-Proton</b> Charged Baryon Negative Capacitive Mode With anti-matter, <math>\mu</math> retards restorative force while <math>\epsilon</math> retards spin, which explains why anti-matter is not stable</p>	 <p>Anti Proton C-L Torques Viewed toward rear of PSs</p>	<p><b>Positron</b> Charged Lepton Positive Capacitive Mode All <math>\epsilon</math> &amp; <math>\mu</math> torques retard and mitigate the restorative and spin forces, explaining again why anti-matter is not stable under expansion stress.</p>	 <p>Positron C-L Torques Viewed toward rear of PSs</p>
<p><b>Chart of torques of inductive and capacitive moments on fermion particle-wave nodal structure</b></p>			

These last two equations are representative of particle interactions in the upper atmosphere in the collision of relativistic protons as cosmic rays in collision with protons and neutrons in atomic nuclei. Various other baryonic forms, all heavier than the neutron with spin 1/2, range from the lambda,  $\lambda$ , at 1.17865, to the sigma,  $\Sigma$ , 1.26001, to the xi minus,  $\Xi^-$ , at 1.39970 with respect to a neutron modular mass of 1.0. All of these are unstable with a lifetime in the sub-nanosecond range, which indicates that they do not lose their internal structure—stated in terms of their quark structure by the standard model and in terms of the stabilized nodes of rotational oscillation of this model—and revert to either a proton or neutron form at the end of that lifetime by emitting energy as a pion with decay.

The pions then decay as gamma radiation or through the weak interaction, part of the  $e + \Delta m$ , to produce the muon and then again to produce the electron. Incidentally, in the following geometric analysis, we will see a suggestion of the weak force in action with respect to the mass of the xi minus,  $\Xi^-$ , at 1.39566 and the well-known weak mixing angle of weak force decay given as

$$\sin^2\left(\frac{1}{2}\sqrt{\frac{\pi}{3}}\right) = (0.489628254)^2 = 0.239735827 \quad (1.117)$$

For a sphere of radius = 1, the surface area of the sphere is  $4\pi$ . If we portion that surface area over each of the twelve cubic edges circumscribed by that sphere, each one centered on the mid-point of each edge, dividing by twelve we have a surface area over each edge of  $\pi/3$ . The arc length of each of the four sides of each of the twelve surface areas measured along each great circle is  $\sqrt{\frac{\pi}{3}}$ , so that one half of the arc length is  $\frac{1}{2}\sqrt{\frac{\pi}{3}} = 0.511663354$ .

We will look at other options in a few minutes. If mass is conceptually thought of as a type of energy producing power as a substance of energy density, we might think that more massive particles come in larger sized packages. In fact, the inverse is the case, and the size of one of these fundamental particles, as designated by their Compton angular wavelength, is inversely related to the rest mass-energy as measured by an angular frequency of the same particle. As a result we can think of the modular mass measure of (1.104) as a measure of frequency, as in the first line of (1.111).

The energy of the tau and muon, therefore, can be understood as the product of an interaction that starts with the energy density of two neutrons. While the empirical literature is deep in the modeling of various decay paths from the baryons to the muon on the way to the generation of an electron, the information is shallow with respect to explanations of the appearance of the tau, conventionally modeled as the interaction of the energy of relativistic electrons and positrons.

Apparently, it is this conventional modeling that has resulted in the designation of the tau as a lepton, despite the fact that roughly 2/3 of the decays are hadronic and decay weakly into an assortment of pions, which are mesons. In the above torque charts and related information, the rotating restorative nodes of the torsion oscillation of  $\phi$  correspond with the mesons, comprised of a quark and an anti-quark pair in the standard model. In our wave modeling of CMMPG, following the pattern of the neutron, the nodes and antinodes of torsional oscillation are orthogonally superimposed to produce rotational oscillation and  $\frac{1}{2}$  spin, but with weak decay the superposition is broken, resulting in the realignment of the  $\mu$  and  $\varepsilon$  torques associated with either hadronic or leptonic form of the oscillation shown in the above chart.

The question of whether the tau can or should be considered a hadron, perhaps even a baryon prior to weak decay, based on (1.115), is of less interest than whether the muon and tau are created as a pair under certain conditions that give physical meaning to the exactness of (1.114) and the fact, if it represents a transformation process indicative of a deeper symmetry, in which baryonic number is conserved, a tenet of the standard model.

The notion that a proton, as a baryon comprised of 3 quarks and positive charge, and an electron, as a lepton without any internal structure but with equal negative charge, should come together in apparently equal numbers in the wake of their emergence from a big bang singularity, along with the necessary missing mass, in the absence of any deeper understanding, has never been logically compelling. The same logical challenge applies to the concept of a tau and a muon, both leptons of largely disparate energies with no internal structure in the form of the necessary quarks, coming together with a release of identical missing coupling energies to produce the six quarks of the 2 baryons of the standard model, once again in the absence of a compelling mechanism. This does not preclude their independent further decay.

A geometric analysis involves the nature of the mechanical work done by an isotropic stress differential,  $df_n$ , in a 3 and 4-dimensional manifold on a unit space as a cube and hypercube from an initial condition of a uniformly continuous inertial field with a property of an emergent lattice potential as gauged by the inertial constant,  $\eta$ , with initiation of a differential stress. This analysis establishes certain inflection points that are reached as the stress increases or decreases on the unit, or alternatively as that unit expands or contracts so that transverse stress or concomitant strain culminating in rotation is induced about such unit as an emergent phenomena. In the absence of such transverse inflection components, any stress induced strain would be an exclusively divergent and therefore curl free expansion that would amount to a scaling phenomena.

For modeling purposes, the energy embodied in a physical object is proportional to, and in some cases equal to, the work performed in moving that object or portion thereof over a distance  $a$ . This includes a force applied in stretching, compressing, expanding, bending, or twisting a portion of some object in such a manner that the portion recoils or redirects its motion as a transverse strain and/or kinetic energy when the direction of the applied force changes. For an object of uniform density, assuming a change in that density due to a change in volume in some portion of the object, the energy change can be understood to be proportionally directed according to the volume change.

As an example, we might consider a unit cube-shaped balloon with an indefinitely flexible surface that is uniformly expanding over time—that is changing in size without changing its geometric definition as a cube—due to an isotropic expansion stress at the three boundary components of the 6 (S) surfaces, 12 (E) edges, and 8 (C) corners of the cube. The expansion stress might be envisioned as inflating the cube by pumping the interior of the cube with fluid or gas, or alternately by evacuating the area uniformly around the cube. At the beginning of the expansion we can consider that it takes more energy to move the 6 faces any differential distance than it takes to move the 12 edges that same differential distance in two directions, and the 8 corners, that same distance in three directions. The work–energy done in each case is a direct function of the volume increase achieved by filling in the displaced components of the cube as they expand.

The details of this analysis are found below at ‘The Effect of Isotropic Expansion Stress on a Unit Space’. We are giving an overview of the 3-dimensional unit cube here. The 3D analysis establishes six points of inflection defined by the points at which the ratios of the increases in differential stress and/or volumes of the different components as defined by the stress or displacement,  $a$ , are unity. These six ratios are

	Component Predominance	Component Ratio = 1	Differential $dx = a$	Inflection Result
1	E+C over S	$\frac{S}{E+C}$	0.39564..., -1.89564...	Torsional symmetry break
2	E over S	$\frac{S}{E}$	0.5	Oscillation potential about S
3	C over E	$\frac{E}{C}$	0.66666...	Oscillation potential about S
4	C over S	$\frac{S}{C}$	$\pm \frac{\sqrt{3}}{2} = \pm 0.86602...$	Oscillation potential across S
5	S+C over E	$\frac{E}{S+C}$	$0.86602...e^{\pm i\frac{\pi}{6}}$	Oscillation & $\frac{1}{2}$ spin rotation
6	C over S+E	$\frac{S+E}{C}$	1.89564..., -0.39564...	Weak force decay

Table 7 – Table of IESUS Inflection Points

The modeling of these inflection points as an increase in volume is a simple heuristic device for pointing to the energy investment transitions in a unit of space as a function of expansion stress. It need not be interpreted as a local physical expansion strain for the increase in stress to be understood as an increase in energy density or mass equivalence. An increase in such density can be physically understood as an increase in frequency and corresponding decrease in wavelength of a wave particle. As a result, the interpretation of an increase of mass of the  $\tau$  should not be interpreted as an increase in physical size, but instead as an increase in frequency/decrease in Compton wavelength.

Note that the ratios are between the total stress on each type of component, so that with row 1, the total of stress–strain on 6 cubic surfaces equals the total on the 12 edges and 8 corners or vertices. In all rows, assuming a condition of increasing  $dx$ , the antecedent or numerator is decreasing relative to an increasing consequent or denominator in the ratios. The breaking of symmetry and the emergence of oscillation is apparent, at first chaotically before eventually becoming ordered with row 5, all of which have a  $dx$  less than 1, as they all indicate an isotropic stress as on a free baryon, which generally precludes the emergence of row 6. With oscillation, the totals for the consequent component stress–strain are not equally distributed across all the relevant components but are maximized and minimized sequentially in a well-ordered manner across those components as with any force oscillation.

By the time the work–energy change at the 12 edges and 8 corners rises to the level at the 6 surfaces, the first inflection point is reached as  $a$  will have increased 0.39564 (or for the sake of symmetry decreased by -1.89564) as in (1.140) in the following analysis. The tension stress at the surface of each cubic face is registered as equal to the stress at the perimeter components, the 4 edges and 4 corners, of each face, which are transverse, so that as these perimeter components begin to exceed that of the surface at the inflection point, more energy is invested in the transverse components than in the surface. As a result, the inverse of  $a$ , 2.52752, is the ratio of the initial condition to the surface differential stress, where the initial includes the total of tension and transverse stress components. This sets up a condition such that continued increase in  $a$  transfers a greater differential of stress to the transverse components and a torsional potential for a breaking of symmetry with the eventual emergence of rotation. This feature is reflected in (1.112) and again in the development of row 6.

By the time the surface has expanded as in (1.141) by a differential length,  $a$ , equals 0.5, the work–energy increased at the 6 surfaces will equal the volume increased at the 12 edges, after which the accumulated work in moving the edges will be greater than the work in moving the surfaces; we will assume that the mass difference between the three cube components, face, edge, and corner, in all cases vanishes as the work–energy is invested in the volume and not the three component surfaces.

As with (1.142) by the time the work–energy change at the 12 edges equals that at the 8 corners, differential  $a$  will have increased to  $2/3$  of the edge length.

Most significantly at (1.143), by the time the work–energy change at the 6 surfaces equals that at the 8 corners,  $a$  will have increased to  $\pm 0.86602 = \pm \frac{\sqrt{3}}{2}$ ,  $\frac{1}{2}$  spin, while at the same time with (1.144) the work–energy at the 12 edges equals the sum of both the 6 surfaces and the 8 corners, and this sets in motion an oscillation of energy flow from surface to edge to corner, with a potential for rotation of the cube.

Under conditions that mitigate free rotational oscillation as at the surface of a black hole source, with (1.145) the work–energy increase at the corners equals the sum of the increase at the faces and edges,  $a$  has increased by 1.89564 times the original edge length, and all increasing stress–strain or work–energy thereafter is concentrated in the corners, the cubic vertices. This can happen only when free rotational oscillation of  $\frac{1}{2}$  spin is restricted in some manner, as with a particle collision or in the case of emergence of that rotational oscillation from an initial condition of a stellar or galactic black hole inertial source of neutron maximum density as might be found in the galactic filaments of the cosmos. Under such conditions at the event horizon surface of such source, individual particle rotation resulting from the lattice gauge would be prevented until the inflection point of row 6 results in the emission of a tau and muon. These then quickly decay according to the various branching paths which follow.

These work–energy inflection points can be represented as angular frequency potentials in the context of a wave model, and thereby with a mass–angular wave number equivalence. The inverse of such wave number is the angular wavelength, which in the context of a rotating torsional oscillation can be represented as the particle’s radius. Thus, an energy differential inflection representing an increase of 1.89564 with respect to a base frequency of 1.0 is equivalent to a reduction in the angular wavelength from 1.0 to 0.527525232. Three relevant parameters of wave phenomena are shown here. Note the difference between the parameters for Row 1 and Row 6 is 1.5 and their inverse is 2 and that these differences are exact. This is related to the predominance of the 3-axis surface stress prior to inflection Row 1 and of its supersession by 4-axis corner stress after Row 6 is reached, reflecting the 3 to 4 axial ratio found in the cuboctahedral lattice potential, that is the three axes through the center of the 6 surfaces and the 4 axes running through the 8 corners.

$$\begin{aligned}
 \text{Row 1:} & \quad (0.395643924\dots)^{-1} = 2.527525230 \\
 \text{Row 5 (argument):} & \quad \pm i\pi / 6 = 0.523598776 = (1.909859317\dots)^{-1} \\
 \text{Row 6:} & \quad (1.895643924\dots)^{-1} = 0.527525232
 \end{aligned} \tag{1.118}$$

This last figure is significant as its representation as an inflection point for energy concentration in the vertices of the cube. Referring to the modular ratios for mass of the tau in (1.104) in the columns for  $*/p$  at 1.89373 and for  $*/n$  at 1.89113, if we assume that the figure 1.895643924 as just derived from this cubic analysis (CA) is a measure of the increase in mass/energy at the inflection point,  $\tau_{CA}$ , we can adjust this figure for the missing mass involved in the following analysis. From the column for  $*/\tau$  using the value of  $e_\tau$  as a percentage of the value of  $\tau$ , we calculate the following value for (1.114) of

$$(2 + 3\Delta m)e_\tau = (6.594753182)(0.000287588) = 0.001896572 \tag{1.119}$$

which we add to the base value of  $\tau = 1.0$  to get 1.001896572. This represents the total percentage of work–energy stress required to produce the tau, plus the ‘missing mass’ and Hubble stress related to beta decay as developed previously required for the tau and the companion muon. Dividing this into the inflection point value based on a cubic analysis to arrive at a theoretical value for the  $\tau$  with respect to the initial neutron density, we get a value in the middle of the values based on  $*/p$  and  $*/n$ .

$$\begin{aligned}
 (1.895643924)_{CA,row6} / 1.001896572 &= \tau_{CA}(1.892055505), \text{ where} \\
 \tau_p(1.893738026) &> \tau_{CA}(1.892055505) > \tau_n(1.891131242)
 \end{aligned} \tag{1.120}$$

From an alternate approach, we can compute the following difference

$$\tau_{CA}(1.895643924) - \tau_n(1.891131242) = 0.004512682 \tag{1.121}$$

which can be further unpacked as

$$\begin{aligned}
 0.004512682 \div ((2.531584394)(0.000543867)) &= 3.277552167, \text{ where} \\
 3.277552167 > (3((2.531584394)(0.000543867))) &= \{3(\Delta m + 1)e_n\} = \{3\Delta m + 3e\}
 \end{aligned} \tag{1.122}$$

This indicates that the energy represented by  $\tau_{CA}$  is sufficient to produce  $\tau_n$  and  $\mu_n$ , the tau and muon, as in (1.114) based on an excess of missing matter in (1.121) and (1.122).

$$\begin{aligned}
\tau_n, \text{ Neutron ratio:} & \quad (1.891131242\dots)^{-1} = 0.528784030 \\
& \quad \Delta(\tau_{CA-\tau_n}) = 0.000258309 < m_e(0.000543867) \\
\tau_{CA}, \text{ Cubic Analysis:} & \quad (1.892055505\dots)^{-1} = 0.528525721 \quad (1.123) \\
& \quad \Delta(\tau_{CA-\tau_p}) = 0.000469577 < m_e(0.000543867) \\
\tau_p, \text{ Proton ratio:} & \quad (1.893738026\dots)^{-1} = 0.528056144
\end{aligned}$$

With respect to this modeling, this is true whether the black hole density of the inertial field upon which the Hubble tension stress is operating to produce the tau and muon as a leptonic duplet is comprised of maximumly packed existing neutrons or a pre-emergent, gauged cuboctahedral lattice potential field of the same neutron density, both indicated by the  $2n$  of (1.114).

To answer the question of (1.115), then we have the following decay paths for a tau–muon duplet

$$2n + \{3\Delta m + 3e\}_{plus} = \tau + \mu - [3\Delta m + 2e] = -[e + \Delta m] + \tau - [\Delta m] + \mu - [\Delta m + e] = \quad (1.124)$$

A1) Molecular Hydrogen or Protium

$$\begin{aligned}
& = 2(p + [\Delta m] + e) \quad (1.125) \\
& = H_2 + [2\Delta m]
\end{aligned}$$

A2) 2 Cations and 2 Anion

$$\begin{aligned}
& = 2(p + [\Delta m + e]) \quad (1.126) \\
& = 2p^+ + 2e^- + [2\Delta m]
\end{aligned}$$

A3) Atomic Protium, a Cation and Anion

$$\begin{aligned}
& = 1(p + [\Delta m] + e) + 1(p + [\Delta m + e]) \quad (1.127) \\
& = H + p^+ + e^- + [2\Delta m]
\end{aligned}$$

B1) A Neutron and Atomic Protium

$$\begin{aligned}
& = n + (p + [\Delta m] + e) \quad (1.128) \\
& = n + H + [\Delta m]
\end{aligned}$$

B2) Atomic Deuterium

$$\begin{aligned}
& = ((n + p) + [\Delta m] + e) \quad (1.129) \\
& = D = {}^2H + [\Delta m]
\end{aligned}$$

For composite structures of 2 duplet interactions in the formation of Helium

$$2(\tau + \mu - [3\Delta m + 2e]) =$$

C1) Atomic Tritium = B1 + B2 (1.130)

$$= 2((n + p) + [\Delta m] + e)$$

$$= T + H = {}^3H + H + [2\Delta m]$$

D1) Atomic Helium 4 = 2(B2) (1.131)

$$= 2((n + p) + [\Delta m] + e)$$

$$= {}^4He + [2\Delta m]$$

D2) Atomic Helium 3 = B1 + B2 (1.132)

$$= 2((n + p) + [\Delta m] + e)$$

$$= {}^3He + n + [2\Delta m]$$

For composite structures of 3 and 4 duplet interactions in the formation of the Lithium we have

$$3(\tau + \mu - [3\Delta m + 2e]) =$$

E2) Atomic Lithium 6 = D1 + B2 (1.133)

$$= 3((n + p) + [\Delta m] + e)$$

$$= {}^6Li + [3\Delta m]$$

$$4(\tau + \mu - [3\Delta m + 2e]) =$$

E1) Atomic Lithium 7 = 2(D1) (1.134)

$$= 4((n + p) + [\Delta m] + e)$$

$$= {}^7Li + (p^+ + e^-) + [4\Delta m]$$

These path and interactions are all the result of the high energy emergence of baryonic and leptonic matter from the surface of a neutron density inertial source. In an ideal case of an extreme Kerr black hole source, the tau–muon duplets slough from the surface, generating the electromagnetic field of quasar or other active galactic nuclei along with the collimated relativistic jets comprised of the particles of these various decay paths. In this manner and by this process, the Hubble stress responsible for all quantum properties produces quantum  $\frac{1}{2}$  spin, the quantum electromagnetic field and charge, and quantum gravity and all the secondary properties of matter. Gravity plays no appreciable part in the formation of these AGN black holes. The jets then generate the clouds of gas comprised principally of the light elements, which then generate the quantum gravitational and electromagnetic interactions responsible for aggregation into stellar configurations which populate and circulate around the AGN black holes.

## Conclusion to the Addendum

Current cosmological modeling quite literally centers around the concept of a big bang singularity as a necessary foundation for the observed abundance of hydrogen and helium in the universe, based on the astrophysical observation of an apparent isotropic expansion at the Hubble rate on a universal scale of baryonic matter located in the stellar systems and interstellar gas comprising the galaxies which are congregated along filaments and across membranes of high inertial density separating vast transparent and



apparent voids but for the transiting spectra of electromagnetic energy that belies the illusion of emptiness. Such modeling embodies theoretical contradictions, some of which are unrecognized on both a quantum and cosmological level, that hamper a greater scientific understanding.

This modeling offers an amended solution to this quandary, and makes the following assumptions and development:

1. Any and all observation and activity, astronomical to quantum experimentation, is comprised of and within an extended multi-dimensional manifold of finite, variable stress–potential energy density, appearing as uniformly discrete instances of well-ordered and connected phenomena of invariant inertial properties of matter, quantized as a fundamental rest mass particle,  $m_0$ .
2. Designated as the space–time fabric (STF), the operation of such manifold can be defined using the formal structure of classical complex wave mechanics as a three-dimensional wave bearing medium with a cuboctahedral lattice potential, gauged by a time–independent inertial invariant that described by the analysis of Isotropic Expansion Stress on a Unit Space (IESUS) and recognized by the Hubble rate, results in the quantization of  $m_0$  as a discrete rotating torsional oscillation of the STF.
3. While the Hubble phenomena can be and is customarily modeled as an expansion of all ponderable matter from a single locus in such a manner as to leave the observed stochastic distribution of baryonic matter in filaments and membranes of galaxies and nebulae based on inflationary theory, that phenomena can also be modeled as a contraction of large regions of the extragalactic voids within a cosmos of indefinite if not infinite extent away from those voids and into diaphanous webs of stress–potential energy density containing loci of black hole sources sufficient to produce baryonic matter from active galactic and active stellar nuclei. Neither of these distributions is well defined; neither of them can be explained as a function of gravity as they include no quantum understanding of gravity. The second, however, offers a path for an understanding of the predominance of hydrogen and helium in the cosmos in addition to an explanation of quantum gravity that requires no explanation for the stated distribution. Other models are conceivable for the explanation of the concentration of baryonic matter in the galactic filaments and membranes separated by vast voids, that require no gravitational component; the same expansion stress represented by the Hubble rate might be indicated on a soap bubble model, for instance.
4. An alternative to big bang nucleosynthesis in the production of the lighter elements can be found in an understanding of the nature of the filaments and membranes with their entrained baryonic matter. From the above development, these web-like features can be modeled as comprised of neutron star-black hole density source material subject to the Hubble stress at the web surfaces.
5. As IESUS produces a torsion stress as a form of internal friction at the surface of these structures equivalent to that registered at the corners of the unit space equal, to  $e + \Delta m$ , the tau–muon duplets peel off the surface of the inertial source and quickly decay within a fraction of a second along one of the several paths indicated above to produce the abundance of hydrogen, helium, and lithium gas, along with the assortment of protons, electrons, neutrons, neutrons, and gamma and lower frequency photons.
  - a. This fundamental quantization,  $m_0$ , is the neutron, in which various properties can be understood as emergent qualities of simple harmonic motion as the rotating torsional oscillation, which produce
    - i. Two inductive and two capacitive moments of maximum power and action of the torsional oscillation that with rotation generate a quantum electromagnetic field and a magnetic moment and an internal neutral current, short of beta decay,
    - ii.  $\frac{1}{2}$  spin angular momentum
    - iii. A quantum of gravity as a differential centripetal force as a function of the expansion stress, which forms the basis of Newton’s gravitational constant.
  - b. The hadrons and leptons created in this process are responsible for the collimated jets and gamma ray bursts of active galactic nuclei, the aggregation of light element gas by gravitational and electromagnetic interaction into stellar formation.

This can be mathematically modeled as follows:

Initial Condition,  $M_0 \int_0^\infty df_n$ , where  $df_n = 2.53158...df_0 = \sum_{\text{symmetric}}^{1.0df_{ii}} \sum_{\text{antisymmetric}}^{i1.5318...df_{ij}}$  :

$M_n$  = Inertial-potential energy density of space

$df_n$  = Expansion stress quantized by inertial constant,  $\tau = \frac{\hbar}{c}$  where  $m(n) = \frac{\tau}{\lambda_{C,n}}$

mass-energy of Hubble tension stress ( $e$ ) =  $1.0df_{ii}$ ,

mass-energy of Hubble transverse stress ( $\Delta m$ ) =  $i1.5318...df_{ij}$

$$(\ln f_0)^{\frac{1}{2}} = ie_{-2}f_0 = \frac{-df_0}{id \ln f_0} = \frac{-de_{-2}f_{ii}}{id \ln_2 e_{-2}f_{ij}} = \frac{-0.65291...f_{ii}}{i1.0f_{ij}} = \frac{-1.0f_{ii}}{i1.53158...f_{ij}}$$

Evolution of  $M_n \int_0^a df_n$  :

Single particle beta decay:

$$n - \{df_{ij} + df_{ii}\} = p + [\Delta m] + e$$

Sum of 3 separate particles, with one bound H and 2 ionized H<sup>+</sup> :

$$3n - \sum_{1n}^{3n} \{1df_{ij} + 1df_{ii}\} = [3\Delta m + 2e] + (p + e) + 2p$$

2 neutrons at nuclear density congregation under isotropic Hubble stress, where

$$\{3df_{ij} + 2df_{ii}\} = [3\Delta m + 2e] \text{ and } (\mu + \tau) \text{ is a transitional state :}$$

Unstable state w/ expansion | Transitional state | Stable state

$$(2n) + \{3df_{ij} + 2df_{ii}\} = \mu + \tau - [3\Delta m + 2e] = n + p + e + \{\Delta m\} = D$$

↙

↘

Catalytic stress transfer

Hyper-stable State

$$2n + 2p + 2e = \text{He}_4$$

↙

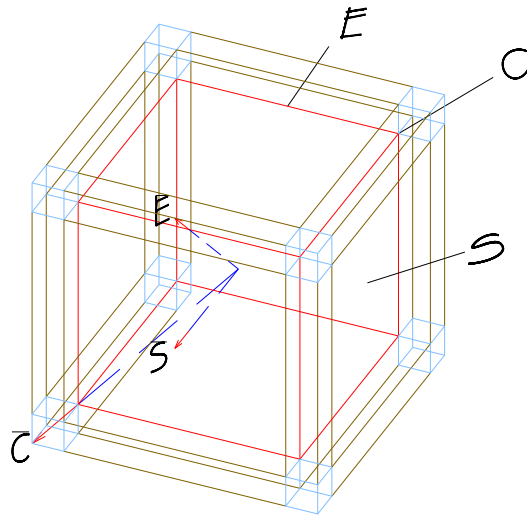
↗

$$(2n) + \{3df_{ij} + 2df_{ii}\} = \mu + \tau - [3\Delta m + 2e] = n + p + e + \{\Delta m\} = D$$

(1.135)

## Detail of the effects of Isotropic Expansion Stress on a Unit Space (IESUS)

We can imagine the center of a cube, and later hypercube, as a local center of expansion of physical space according to the Hubble rate. We will integrate the following differentials to compare the contribution made by each boundary order to the change in the corresponding core, in this case a volume. We are interested in the relative contributions of each order over time to the initial unit volume,  $V$ , and not to the changing magnitude of the volume itself. We substitute the following boundary placeholder identities for Surface, Edge and vertices (Corner),  ${}^1S = x^2$ ,  ${}^1E = x^1$ , and  ${}^1C = x^0$ , so as to maintain proper integration. It will be helpful if we assign a “normal” boundary strain vector to each of these components, which in each case will be in the direction in which the boundary is increasing. Thus



Cubic Expansion

$$|\mathbf{S}| = \left| \sqrt{\frac{1}{2}} \mathbf{E} \right| = \left| \sqrt{\frac{1}{3}} \mathbf{C} \right| \quad (1.136)$$

$$|\mathbf{E}| = \left| \sqrt{2} \mathbf{S} \right| = \left| \sqrt{\frac{2}{3}} \mathbf{C} \right| \quad (1.137)$$

$$|\mathbf{C}| = \left| \sqrt{3} \mathbf{S} \right| = \left| \sqrt{\frac{3}{2}} \mathbf{E} \right| \quad (1.138)$$

In the following, no assumption is made about the universal configuration or number of dimensions of the space in which the unit cube is embedded. We are only interested, at least initially, in the local geometry, which is assumed to be flat and therefore Euclidean. Thus, it is background independent.

The integration will be simultaneous on each order, as indicated by the pre-subscript  $n$ , in  $\int_n dx^n$  so that we have

$$\begin{aligned}
\int_V dV &= 6x^2 \int_0^a dx^1 + 12x^1 \int_0^a dx^2 + 8x^0 \int_0^a dx^3 \\
\int_V dV &= 6S \int_0^a dx + 12E \left( \int_0^a dx \right) \left( \int_0^a dx \right) + 8C \left( \int_0^a dx \right) \left( \int_0^a dx \right) \left( \int_0^a dx \right) \\
\Delta V &= 6aS + 12a^2E + 8a^3C
\end{aligned} \tag{1.139}$$

Solving for the following ratios, all at unity, where the designations S, E, and C are unit names, their dimensional quantities being absorbed in the numerical coefficients of  $a^n$ , i.e. 6 square units times  $a$ , 12 length units times  $a^2$ , 8 point units times  $a^3$ , gives the value of  $a$  for each equivalence. The ratios have been stated with the highest order in the consequent or denominator so they are decreasing from infinity as  $dx$  increases, until unity is reached as stated. We have (showing the negative for the sake of symmetry)

$$\frac{S}{E+C} = \frac{6a}{12a^2+8a^3} = \frac{1}{2a+\frac{4}{3}a^2} = 1 \therefore a = -\frac{3}{4} \pm \frac{1}{4}\sqrt{21} = 0.39564\dots, -1.89564\dots \tag{1.140}$$

$$\frac{S}{E} = \frac{6a}{12a^2} = \frac{1/2}{a} = 1 \therefore a = \frac{1}{2} = 0.5 \tag{1.141}$$

$$\frac{E}{C} = \frac{12a^2}{8a^3} = \frac{2/3}{a} = 1 \therefore a = \frac{2}{3} = 0.66666\dots \tag{1.142}$$

$$\frac{S}{C} = \frac{6a}{8a^3} = \frac{3/4}{a^2} = 1 \therefore a = \pm \frac{\sqrt{3}}{2} = \pm 0.86602\dots \tag{1.143}$$

$$\frac{E}{S+C} = \frac{12a^2}{6a+8a^3} = 1 \therefore a = \frac{3}{4} \pm i\frac{1}{4}\sqrt{3} = \frac{\sqrt{3}}{2}e^{\pm i\pi/6} = 0.86602\dots e^{\pm i\pi/6} \tag{1.144}$$

$$\frac{S+E}{C} = \frac{6a+12a^2}{8a^3} = 1 \therefore a = \frac{3}{4} \pm \frac{1}{4}\sqrt{21} = 1.89564\dots, -0.39564\dots \tag{1.145}$$

If we think of the cube as embedded in an isotropic elastic continuum, which is of some inertial density and under tension,  $dx$  represents the work done in displacing or distorting the medium, and by virtue of Gauss' theorem, the integration of that work represents the energy of the distortion. By way of reference, in an ideal elastic medium, the stress operating on the locale is a function of the strain and the elastic modulus as

$$\mathbf{F} = \frac{Y\mathbf{E} - 3\sigma\bar{P}\mathbf{1}}{1+\sigma} \tag{1.146}$$

where  $\mathbf{F}$  is the stress tensor,  $\mathbf{E}$  is the strain tensor,  $Y$  is Young's modulus of elasticity,  $\sigma$  is Poisson's ratio or the negative ratio of lateral to axial or shear to tension strain,  $\bar{P}$  is the mean pressure in the medium, and  $\mathbf{1}$  is the idemfactor or unit tensor. Assuming a value of  $\sigma$  of  $-1/3$  for an ideal isotropic 3 dimensional medium we have

$$\mathbf{F} = \frac{3}{2}(Y\mathbf{E} + \bar{P}\mathbf{1}) \tag{1.147}$$

The vector fundamental tension stress component is

$$\mathbf{f} = Y \mathbf{e} \quad (1.148)$$

and is related to the energy distribution by Gauss' theorem for the radial strain

$$E_r = \int_V \nabla \cdot \mathbf{e}_r dv = \oint_S \mathbf{e}_r \cdot d\mathbf{S} \quad (1.149)$$

and Stokes' theorem for the angular or tangential strain

$$E_t = \int_S \nabla \times \mathbf{e}_t \cdot d\mathbf{S} = \oint_r \mathbf{e}_t \cdot d\mathbf{r}_t \quad (1.150)$$

These boundary order ratios, then, are inflection points indicating the energy contributions and potential energy gradient changes over time among the boundary components. In an ideal static, kinematic case the change in the ratios with an increase in  $dx$  would have no functional effect on the components, if  $dx$  has the same magnitude for each of them as it increases. This would amount to a simple change of scale. The real solutions above would appear to reflect this static condition. However, in a dynamic condition, we understand that as each ratio decreases below unity and past the inflection point, the magnitude of the consequent exceeds and affects the antecedent or numerator, whose magnitude then becomes a partial function of the consequent. This would appear to be the case for the complex solutions in particular, which correspond with an angular gradient potential of the boundary vectors from that of the antecedent to the direction of that of the consequent.

These evaluations were done with Maple. It is significant that if we convert (1.144) to complex polar notation as in the last term, the modulus is equal to the value for  $a$  in (1.143). It is important that we understand that the ratios represent the point at which the change in volume due to the sum totals of all component orders in the antecedent and consequent are equal. It is not the point at which one single component of a given S, E, or C times its appropriate  $\int_n dx^n$  is equal to another, since this happens for all at the point where  $a = 1$ .

In these evaluations, the S component of the strain and hence of the work predominates until (1.140) is reached. At this point, the stress will begin to shift from a predominance of tension to that of shear, meaning there will be a potential for the surface and edge strains to oscillate. As the edges and vertices ring each of the surfaces, the system remains basically stable, however. At the point of (1.141) the edges assume dominance over the surfaces and a gradient is produced for the bulk strain and the tension stress in the direction of the edges and a torsional potential about each of the 3 surface axes. Once again, the 2:1 symmetry of edges to surface maintains stability. At (1.142) the vertices contribute more work than the edges and the strain gradient shifts in their direction. Thus, there is a vector potential from the surfaces to the edges to the vertices. Once more the symmetry between vertices and edges maintains stability.

Jumping to (1.145), at this point the strain contributed by the vertices dominates both of the other components combined and the related stress is greatest at these locations. This would result in a transmission and oscillation of the energy in the form of a weak interaction as a lepton in a particle context, were it not for the unusual and unique condition created by (1.143) and (1.144). The point at which the strains of the vertices come to equal those of the surfaces is also the point at which their combined strain comes to equal that of the edges, as given by the modulus of the latter's ratio. We can assume that the imaginary component of this ratio indicates a rotational component of  $\pi/6$  or  $30^\circ$ , and since the vertices are assuming a predominance over the surfaces at this point, having already exceeded the edge strain, and as there is an imbalance in the number of vertices to surfaces, a necessary break in symmetry ensues.

We can imagine a rotational potential of the surface strain in the direction of the vertices, which by virtue of the asymmetry between S and C, of 3 degrees of rotational freedom and 4 possible rotational axes, results in an eventual rotational strain about one pair of the axes. This is simultaneous with a shift of the Es in the direction of S + C and a dragging of the strains at each of the two axial C poles. This then leads to a rotation of the axial Cs in the direction of one of the three E pairs extending from those two vertices. The equation

of (1.144) gives this rotational relationship. The nature of the ambiguous sense in the argument is indicative of the equation of a rotational oscillation and its complex conjugate, when viewed from both senses of its axis, i.e. by rotating it about the real axis, where  $\pm$  means plus and minus and not plus or minus, if we adjust the Euler identity to

$$e^{\pm i\theta} = \mathbf{sin}\theta \pm i\mathbf{cos}\theta \quad (1.151)$$

One end of the axis of strain then can be shown as indicated by the “symmetry breaking” in (1.154).

$$12a^2E = (6aS + 8a^3C) \quad (1.152)$$

$$12\left(\frac{\sqrt{3}}{2}e^{\pm i\frac{\pi}{6}}\right)^2 E = 6\left(\frac{\sqrt{3}}{2}e^{\pm i\frac{\pi}{6}}\right)S + 8\left(\frac{\sqrt{3}}{2}e^{\pm i\frac{\pi}{6}}\right)^3 C \quad (1.153)$$

$$e^{-i\frac{\pi}{3}}E = \frac{1}{\sqrt{3}}\left(e^{+i\frac{\pi}{6}}S + e^{+i\frac{\pi}{2}}C\right) \quad (1.154)$$

Thus, the strain vector E, rotated in some direction  $\frac{\pi}{3}$ , is equal to  $\frac{1}{\sqrt{3}}$  of the S and C strains rotated  $\frac{2\pi}{3}$  in the opposite direction, presumably in the same plane. In fact, this states that C rotates  $\frac{\pi}{2}$  while S rotates  $\frac{\pi}{6}$ . We can see specifically how these rotations occur in Spin Diagrams 1 and 2 (of CMMPG). We can also see there how a rotation back in time of  $\frac{\pi}{3}$  equals one forward in time by  $\frac{2\pi}{3}$  and vice-versa, if their plane of rotation,  $\phi$ , is itself rotating at a constant rate with respect to an orthogonal plane,  $\theta$ , that is where the two axes intersect at the centers of rotation. However, it is shown there that this corresponds with a rotation of  $\theta$ , back  $\frac{\pi}{4}$  and forward  $\frac{3\pi}{4}$ , indicating a variability in the strain velocity.

It should be understood that this cubic structure is simply an expression of the orthogonal tendency for stress equalization and energy conservation. The condition found at (1.143) and (1.144), then becomes a stable dynamic condition of rotational oscillation or spin, within certain parameters of inertial density and mechanical impedance. If the isotropic tension in this situation was sufficient to increase the strain indefinitely, if the medium was to lose its elasticity and become plastic or even rupture, any tendency to oscillate would be overcome by the transfer of energy via strain to the vertices. Local energy would not be conserved, but be drawn away by the strain.

It is essential to extrapolate this scenario to the hypercube, H, to achieve a full understanding. We will skip the integrals but show the results for the corollary of the last line of (1.139) as

$$\begin{aligned} \Delta H &= 8aV + 24a^2S + 32a^3E + 16a^4C \\ &= 1aV + 3a^2S + 4a^3E + 2a^4C \end{aligned} \quad (1.155)$$

There are 25 combinations with corresponding non-ordered permutations or sub-combinations, for the 4-cube; 7 involving all 4 parameters, 12 permutations involving all sub-combinations of 3, and 6 one to one relationships. With the 3-Space, there are 2 single real positive solutions at (1.141) and (1.142), one instance of a complex solution at (1.144), one correspondence between a real and a complex solution at (1.143) and (1.144) where the real value of  $a$  in one is equal to the complex modulus in the other, and one instance of a correspondence of solutions with sense inversion, (1.140) and (1.145), that is their solutions have the same magnitude, but of opposite sense. As might be expected, the 4-Space of a hypercube shows significantly more of these symmetries. It should be noted that while an attempt has been made to analyze the ratios qualitatively so that all are represented as decreasing with respect to an increasing  $dx$ , they have

not all been checked quantitatively, and some may be increasing as shown. In fact, (1.168) and (1.170) are found to be increasing at the point represented by the first positive solution and decreasing at the second. For (1.165) it is worth stating that for every value of the ratio  $0.75 < \left(\frac{S}{V+E}\right) < +\infty$ , the modulus is  $\frac{1}{2}$  and the argument ranges from 0 to  $\frac{1}{2}\pi$ .

It is important to remember that a given component in the 3-cube is identical to the same component in the 4-cube, but the relationships between them are different. An edge still is bounded by 2 vertices, but there are 4 edges intersecting at each vertex of the 4-cube. A line segment in an  $x$ - $y$  plane is qualitatively no different than one in the  $z$ - $x$  or for that matter  $z$ - $w$  plane. In fact, a point in 3-space also has a location in  $n$ -space, at least in Euclidean  $n$ -space. In the following, it is also important to remember that  $a$  is not the value of the corresponding ratio, but rather the value found in both antecedent and consequent when the ratio equals 1. The evaluations are based on the following identities in (1.156)

$$V \equiv 1a, S \equiv 3a^2, E \equiv 4a^3, C = 2a^4 \quad (1.156)$$

$$\frac{V}{S}, a = \frac{1}{3} \quad (1.157)$$

$$\frac{V}{E}, a = \pm \frac{1}{2} \quad (1.158)$$

$$\frac{V}{C}, a = \frac{1}{\sqrt[3]{2}}, -\frac{1}{2}\left(\frac{1}{\sqrt[3]{2}}\right) \dots \pm i \frac{\sqrt{3}}{2}\left(\frac{1}{\sqrt[3]{2}}\right) = \frac{1}{\sqrt[3]{2}} e^{\pm i \frac{2\pi}{3}} = 0.79370 \dots e^{\pm i \frac{2\pi}{3}} \quad (1.159)$$

$$\frac{S}{E}, a = 0, \frac{3}{4} \quad (1.160)$$

$$\frac{S}{C}, a = 0, \pm \sqrt{\frac{3}{2}} \quad (1.161)$$

$$\frac{E}{C}, a = 0, 0, 2 \quad (1.162)$$

$$\frac{V}{S+E}, a = -1, \frac{1}{4} \quad (1.163)$$

$$\frac{V+S}{E}, a = -\frac{1}{4}, 1 \quad (1.164)$$

$$\frac{S}{V+E}, a = \frac{3}{8} \pm i \frac{1}{8} \sqrt{7} = \frac{1}{2} e^{\pm i 0.722734248 \dots} \quad (1.165)$$

$$\frac{V}{S+C}, a = 0.31290 \dots, -0.15645 \dots + i 1.25436 \dots = 1.26408 \dots e^{\pm i 1.694883228 \dots} \quad (1.166)$$

$$\frac{V+S}{C}, a = -1, -0.36602 \dots, 1.36602 \dots \quad (1.167)$$

$$\frac{V+C}{S}, a = -1.36602\dots, 0.36602\dots, 1 \quad (1.168)$$

$$\frac{V}{E+C}, a = -1.85463\dots, -0.59696\dots, 0.45160\dots \quad (1.169)$$

$$\frac{V+C}{E}, a = -0.45160\dots, 0.59696\dots, 1.85463\dots \quad (1.170)$$

$$\frac{V+E}{C}, a = 2.1120\dots, -0.05604\dots \pm i0.48331\dots = 0.48655\dots e^{\pm i1.686235431\dots} \quad (1.171)$$

$$\frac{S}{E+C}, a = -2.58113\dots, 0, 0.58113\dots \quad (1.172)$$

$$\frac{S+E}{C}, a = -0.58113\dots, 0, 2.58113\dots \quad (1.173)$$

$$\frac{E}{S+C}, a = 0, 1 \pm i\frac{1}{\sqrt{2}} = \sqrt{\frac{3}{2}} e^{\pm i0.615479709\dots} \quad (1.174)$$

$$\frac{V}{S+E+C}, a = 0.24415\dots, -1.12207\dots \pm i0.88817\dots = 1.43105\dots e^{\pm i2.472026458\dots} \quad (1.175)$$

$$\frac{E}{V+S+C}, a = -0.24415\dots, 1.12207\dots \pm i0.88817\dots = 1.43105\dots e^{\pm i0.669566197\dots} \quad (1.176)$$

$$\frac{V+E+C}{S}, a = -2.63993\dots, 0.31996\dots \pm i0.29498\dots = 0.43519\dots e^{\pm i0.744798022\dots} \quad (1.177)$$

$$\frac{V+S+E}{C}, a = 2.63993\dots, -0.31996\dots \pm i0.29498\dots = 0.43519\dots e^{\pm i2.396794631\dots} \quad (1.178)$$

$$\frac{V+S}{E+C}, a = -2.51702\dots, -0.25673\dots, 0.77375\dots \quad (1.179)$$

$$\frac{E+S}{V+C}, a = -0.77375\dots, 0.25673\dots, 2.51702\dots \quad (1.180)$$

$$\frac{V+E}{S+C}, a = 1, \frac{1}{2} \pm i\frac{1}{2} = \frac{1}{\sqrt{2}} e^{\pm i\frac{\pi}{4}} \quad (1.181)$$

Once again using Maple, there are a total of 10 couplings involving complex solutions, of which one is exclusively complex and one other has only a zero for the third and real solution. Only one single real positive solution is given. There are, however, 7 corresponding pairs of solutions involving sense inversion, 5 real and 2 complex. Note that all cases of sense inversion involve a combination of one or more components in either the antecedent and/or consequent and the sense change is associated with a transposition of one or two components in each pair. These do not appear to have any special relationship to the conditions of the 3-cube, at first glance, and we have not investigated them further.



There are several, however, that appear to have a direct relationship to some of the ratios of the 3-cube. Two conditions of correspondence are found between a real positive solution and the complex modulus of a complex solution with a positive real component. (1.161)  $\left(\frac{S}{C}\right)$  and (1.174)  $\left(\frac{E}{S+C}\right)$  are directly related to (1.143) and (1.144) respectively, the real solution and the modulus of the complex of the second two being equal to the product of the first and  $\sqrt{2}^{-1}$ . The argument of (1.174) is the angle at the center of a cube between a radial normal to an edge of the cube and one extended along a diagonal to a vertex. (1.158)  $\left(\frac{V}{E}\right)$  and (1.165)  $\left(\frac{S}{V+E}\right)$  are related to (1.141)  $\left(\frac{S}{E}\right)_3$  with a common value for their real solutions and the modulus of the complex one. The cosine of the argument of (1.165) is equal to the solution of (1.160)  $\left(\frac{S}{E}\right)_4$ , which is the same ratio coupling as (1.141). This pairing (1.165) in turn has a modulus equal to the real and imaginary components of an additional complex solution in (1.181)  $\left(\frac{V+E}{S+C}\right)$ . This latter solution has an argument of  $\pi/4$  or  $45^\circ$  which appears to be an extremely stable condition, as found in a sine wave model as the point of maximum power of the wave, where the product of the transverse wave force and transverse wave speed are maximum. It is also the angle of the strain vector E discussed above for the 3-cube, with respect to the plane normal to the spin angular momentum vector as shown in the spin diagrams. In the model developed here, this condition is found to be invariant and rotates about the oscillation's angular momentum vector.

Finally, (1.174)  $\left(\frac{E}{S+C}\right)$ , (1.181)  $\left(\frac{V+E}{S+C}\right)$ , and (1.159)  $\left(\frac{V}{C}\right)$  are found to be related in a most profound way in the mechanism of the oscillation herein described. The imaginary component of (1.174) equals the modulus of (1.181). Note that (1.159) represents a  $\frac{2\pi}{3}$  rotation due to the interplay between the volume and vertex components of strain and a modulus of that strain of  $\frac{1}{\sqrt[3]{2}}$ . Using the equation for (1.159) or

$$aV = 2a^4C \quad (1.182)$$

$$\frac{1}{\sqrt[3]{2}} e^{\pm i\frac{2\pi}{3}} V = 2 \left( \frac{1}{\sqrt[3]{2}} e^{\pm i\frac{2\pi}{3}} \right)^4 C \quad (1.183)$$

tells us that a rotational oscillation of the 4-volume (boundary) strain V of modulus  $\frac{1}{\sqrt[3]{2}}$  by  $\frac{2\pi}{3}$  is equal to 4 axial rotations about the vertices of the same modulus and argument, where the 2 in the consequent indicates simultaneous rotations of opposite sense at each end of an axis. The oscillation of V is fourth dimensional, and therefore beyond our direct sensory ken, however, the 4 vertices are not, and we can envision the above consequent, the expression in 3 dimension of this four dimensional rotation, as a sequence of 4,  $\frac{2\pi}{3}$  rotations about the 4 diagonals of a 3-cube. This sequence leaves the cube unchanged and avoids the entanglement condition, i.e. the continuity of Euclidean 3-coordinates of the cube are not twisted by the sequence. This condition of limits on the twistability of the continuum strain is a necessary consequence of its inertial/elastic properties. As the rotation of V is continuous, we would imagine that the sequence of 4 rotations is continuous, i.e. the strain rotates from one reference diagonal to another about one of the three surface axes of the 3-cube. We can also envision this as one diagonal axis rotating  $\frac{2\pi}{3}$ , followed by a  $2\pi$  rotation of the same sense about one of the adjacent 3-cube surface axes. We can also treat it as a sequence of 4 orthogonal permutations.

